ANALYSIS OF MALPIGHIAN TUBULE ION TRANSPORT BY MEASUREMENT OF ION CONCENTRATION GRADIENTS IN EXTRACELLULAR UNSTIRRED LAYERS

By:
KIMBERLEY ANN COLLIER, B.Sc

A Thesis
Submitted to the School of Graduate Studies
in Partial Fulfilment of the Requirements
for the Degree
Master of Science

McMaster University

ION CONCENTRATION GRADIENTS IN EXTRACELLULAR UNSTIRRED LAYERS

MASTER OF SCIENCE (1997) **McMASTER UNIVERSITY**
(biology) Hamilton, Ontario

TITLE: Analysis of Malpighian tubule Ion Transport by Measurement of Ion Concentration Gradients In Extracellular Unstirred Layers

AUTHOR: Kimberley Ann Collier, B.Sc. (McMaster University)

SUPERVISOR: Professor M.J. O'Donnell

NUMBER OF PAGES: xi, 175

ABSTRACT

The pH and concentrations of K^+ and Cl^- in the unstirred layer (USL) associated with the basolateral surfaces of Malpighian tubules of *Rhodnius prolixus* and *Drosophila melanogaster* were measured with extracellular ion-selective microelectrodes.

When stimulated with 5-hydroxytryptamine (5HT) *in vitro*, the upper Malpighian tubule of *R. prolixus* secretes Na^+, K^+, Cl^- and water at high rates; the lower Malpighian tubule reabsorbs K^+ and Cl^- but not water. Concentrations of $[K^+]$ and $[Cl^-]$ in the unstirred layer of the lower Malpighian tubule ($[K^+]_{USL}$, $[Cl^-]_{USL}$) were above those in the bathing saline, consistent with accumulation of K^+ and Cl^- in the USL during 5HT-stimulated KCl reabsorption. $[K^+]_{USL}$ exceeded $[K^+]_{BATH}$ as much as 5.3 fold. Calculations of K^+ flux based on measurements of $[K^+]_{USL}$ at various distances from the tubule surface agreed well with flux calculated from the rate of fluid secretion and the change in potassium concentration of the secreted fluid during passage through the lower tubule. Concentrations of $[K^+]$ in the unstirred layer of the upper Malpighian tubule were reduced relative

to those in the bathing saline, consistent with depletion of K^+ from the USL during 5HT-stimulated secretion of K^+ from bath to lumen. Changes in $[K^+]_{USL}$ during 5HT-stimulated K^+ secretion from single upper Malpighian tubule cells could be resolved. Although differences between $[K^+]_{USL}$ and $[K^+]_{BATH}$ were apparent for upper and lower tubules in an *in situ* preparation, they were reduced relative to the differences measured with isolated tubules. It is suggested that convective mixing of the fluids around the tubules by contractions of the midgut and hindgut reduces, but does not eliminate, differences between $[K^+]_{USL}$ and $[K^+]_{BATH}$ *in situ*. The USL was slightly acidic relative to the bath in 5HT-stimulated upper and lower tubules; contributions to USL acidification are discussed.

When stimulated with leukokinin (LKI) and cAMP *in vitro*, the main segment of the *D. melanogaster* MT secretes Na^+, K^+, and Cl^-. Concentrations of $[K^+]$ in the USL of the main segment were lower than those in the bathing saline at both stellate cell sites and principal cell sites, consistent with depletion of K^+ in the USL during LKI/cAMP-stimulated secretion. $[K^+]_{USL}$ at sites near stellate cells was significantly lower ($p<0.05$) than at sites near principal cells. Reasons for this non-uniformity are discussed. $[K^+]_{USL}$ also exceeded $[K^+]_{BATH}$ at principal cell

sites in both the proximal and distal regions of MT, consistent with LKI/cAMP-stimulated reabsorption of K^+. Studies using a Cl^--selective vibrating microelectrode were inconclusive.

The results also show that techniques described in this thesis can resolve rapid and localized changes in ion transport across different regions of Malpighian tubules in response to stimulants or inhibitors of specific membrane transporters.

ACKNOWLEDGEMENTS

I would first like to thank my supervisor Dr. Michael O'Donnell for his enthusiasm and encouragement throughout my graduate studies at McMaster. His patience in editing draft… after draft… after draft… of this thesis was greatly appreciated, especially when I was writing on "auto-pilot."

Secondly, I would like to thank my committee members: Dr. Roger Jacobs, Dr. Colin Nurse, and Dr. John Lott for the individual attention I received from each of them.

John was paramount in introducing me to research, and continued to be my motivator throughout grad studies.

Rogers' door was always open. If he couldn't answer a question at that instant, he would always have a stack of papers from pertinent journals on my desk within hours.

I could always count on Colin for a laugh over a coffee. Thanks to him, I will forever remember the difference between ion activity and ion concentration!! I still owe him a whipping on the basketball court!!

Next, I would like to thank my parents Helen and George whom though we haven't seen eye to eye the past few years,

have always supported and encouraged my academic pursuits, offering help at all times.

Lastly, I would like to thank all of the friends I have made during my stay at McMaster. Dr. Michael "hamstrings" Quinlan and his wife Nancy. Mike was the only person who truly saw me at my worst, and still managed to make me laugh. I will forever miss his quirky stories and outlook on life. Christina "karate woman" Misiaszek, the only woman I know who sprained her ankle trying to break into my bedroom window! Mary "Dancing Queen"(or perhaps kissing queen?!)Fletcher, for the great candid talks and stories. Kim Dube, Kim Barrett, Mark Rheault, and Jennifer Cowan who have all greatly added to the dynamics in the LSB 524 lab - ion transport rules!! Thomas Jacques for helping me with the preparation for grad school. Nigel "skinsuit" Waltho who taught me how much fun teaching could be. Derek "the liar" Kunsken, Robin "romeo" Battye, Sara "squash woman" Croke, Jonathan "stinky cheese and olives" Wright, Jonathon "silver tongue" Audia, Sharon Dhadallia, Deb Lorenzin, Fern Gonzales and all of the "far sliders," "gene therapists," and "abiotics." A special thanks also to Marilyn Bixby for all of the home-cooked meals, and Darren Bixby who is actually happier than myself to have this "thesis" behind me.

Dedicated to the loving memory of "Scooter" who in her 8 years taught me the innocence of nature and the fragility of life.

TABLE OF CONTENTS

CHAPTER 1: Analysis of Fluid and Ion Transport by Insect Malpighian Tubules

INTRODUCTION:

I *Insect Malpighian tubules*

Although environmental stresses promote desiccation in the terrestrial insects or dilution of the body fluids in aquatic species, most insects regulate hemolymph composition within narrow limits. This regulation is accomplished primarily by the excretory system, which consists of the Malpighian tubules (MTs) and the hindgut, including the ileum, the colon and the rectum. In most insects a nearly isoosmotic fluid is secreted by the Malpighian tubules (MT). The tubules have specific systems for active (*i.e.* ATP-dependent) ion transport. Movements of water are generally viewed to be a secondary and passive osmotic consequence of active ion transport. This primary urine is then modified in specialized segments of the tubules themselves, or, more commonly, in the hindgut. Tubules of blood feeders produce a final urine enriched in NaCl, whereas most omnivores and phytophagous insects will secrete urine in which KCl is the predominant salt. Examples of the former group include tsetse flies,

mosquitoes, and the hemipteran *Rhodnius prolixus*, each of which is discussed below. Examples of the latter group include the fruit fly *Drosophila melanogaster*, and locusts.

The Malpighian tubules are also the primary means for excretion of waste materials or xenobiotics arising from metabolism or ingestion of potentially toxic materials. The passive permeability of the tubules to a wide variety of low molecular weight solutes is relatively high. In addition, there are specific active transport systems for excretion of specific molecules, including uric acid, organic acids and bases, and alkaloids such as nicotine (O'Donnell, 1997).

II *Analysis of Malpighian tubule ion transport*

The Ramsay technique

Ramsay (1952) developed the most widely used technique for collection of fluid secreted by insect MTs. Tubules will secrete a drop of fluid if the blind end of the tubule is placed in a droplet of physiological saline under paraffin oil, and the open end is pulled out into the oil and secured by wrapping it on a pin or holding it in a slit in Sylgard. (Figure 1.1). Secreted droplets collected at intervals can then be used to determine fluid secretion rates. Droplet diameters are measured with a calibrated eyepiece micrometer and droplet volume (in nl) is calculated

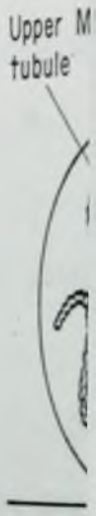

Figure 1.1 -- The Ramsay technique (1952). Isolated insect Malpighian tubules are positioned in bathing saline droplets under liquid paraffin oil. The arrangement shown here allows the upper and lower ends of the tubule to be bathed in different salines. The open-ended ampulla is pulled out of the bathing saline and anchored on a glass pin to allow secreted fluid to accumulate and be removed at intervals for ion analysis. (Taken from Maddrell and Phillips, 1976)

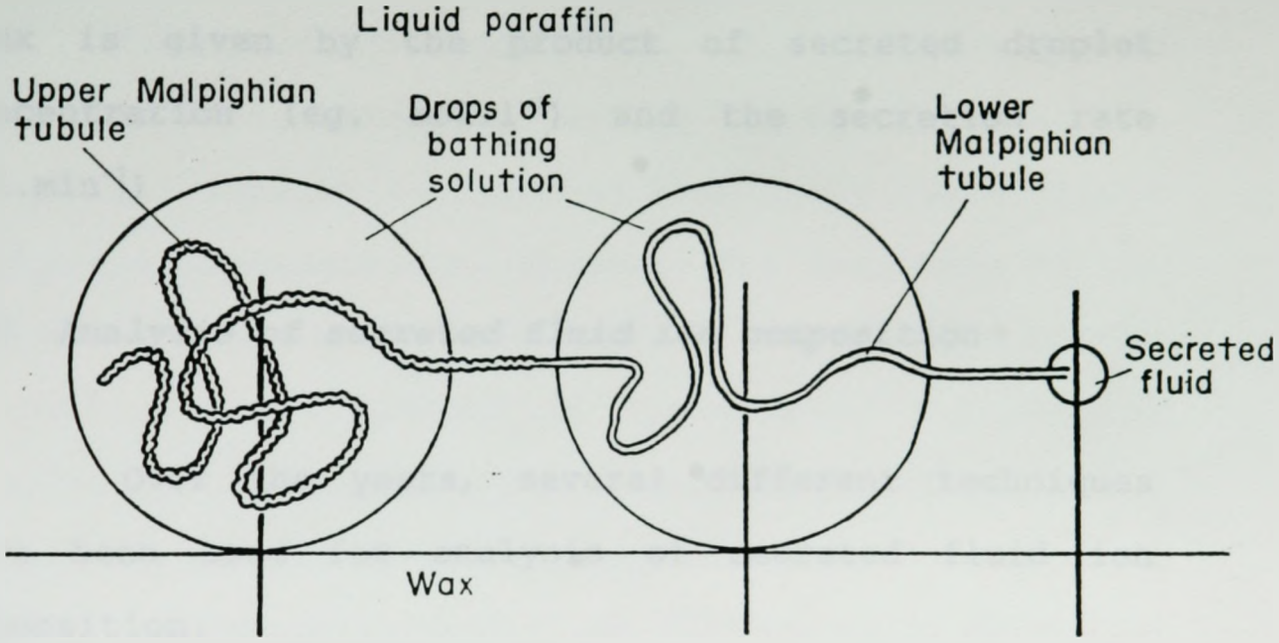
Liquid paraffin
Upper Malpighian tubule
Drops of bathing solution
Lower Malpighian tubule
Secreted fluid
Wax

using a standard formula for the volume of a sphere. Secretion rates (in $nl.min^{-1}$) are calculated by dividing droplet volume by the time over which the droplet was formed.

Ion flux (mol/min/tubule) can be calculated if the ion concentration in the droplet is known. Ion flux is given by the product of secreted droplet concentration (eg. $mol.l^{-1}$) and the secretion rate ($nl.min^{-1}$)

III *Analysis of secreted fluid ion composition*

Over the years, several different techniques have been used for analysis of secreted fluid ion composition.

A) *Flame photometry*

Flame photometry was developed to make possible the rapid and quantitative determination of the alkali metals (Na^+, K^+) in an aqueous solution. At the time there was a great need for rapid and accurate K^+ and Na^+ measurements in a large number of samples (approx. 150 samples per hour). The method involves a quantitative measurement of the characteristic light emitted when a solution of the metal is atomized as a

mist into a gas flame. The sample is atomized into the air intake of a flame under controlled conditions and the emitted light characteristic of the element in question is isolated and accurately photometered. Low flame temperatures permit only atoms of the alkali metal and alkaline earth components of the sample to emit characteristic radiation. The characteristic radiation is isolated via passage through filters. An electrical impulse is produced when the filtered light strikes a photosensitive element. The magnitude of the electrical impulse is correlated to the quantity of the respective metal present in the sample. The samples require minimum preparation; and the assembly is relatively inexpensive. Ramsay (1950), and Ramsay *et al* (1952), successfully used flame photometry to determine alkali metal concentrations in MT secreted fluid. The results were obtained in a few minutes with a mean accuracy of ± 3% (Barnes *et al*, 1945).

There are several disadvantages to this method. The rate of atomization of a sample into the instrument is of the order of 5 to 10 $ml.min^{-1}$, and therefore large volumes of sample are needed for accurate readings; the use of the instrument is limited to those samples containing elements whose flame spectra can be isolated by available filters; the presence of

foreign salts, acids, or organic molecules tend to alter the amount of light emitted; and finally, conclusive results can be found only when measuring alkali metals which emit line spectra which can be isolated by filters, and not band spectra (as with Ca^{+2}, for example).

B) *Atomic absorption*

After the development of flame photometry, several researchers developed a new use of the flame in chemical analysis -- the flame is used not as a source of excitation or emission, but as a medium for *absorbing* radiation. This new branch of flame photometry -- absorption flame photometry or more commonly, *atomic absorption* (AA), provides a mechanism for analyzing elements that are difficult (or impossible) to determine with the former conventional emission methods. Also, atomic absorption is free from interfering factors which are found in the emission methods.

Atomic absorption is an "instrumental spectroanalytical method which is based on the measurement of the absorption produced in a beam of radiation of suitable wavelength proceeding from an emitting source of constant intensity, by a medium

composed of atoms of the element to be determined"(Ramirez-Munoz, 1968). The amount of absorption increases directly with the concentration of the sample solution used when producing the absorbing medium. Atomic absorption spectroscopy is based on a system of instruments including an emitter system which produces a spectrum characteristic of the element sought; a system producing an atomic vapour (usually a flame into which an aerosol of the unknown is injected); a system of spectral selection (filters, monochromators); a photodetection system; and finally, a measurement system (for recording, or printing) (Ramirez-Munoz, 1968). Specific absorption spectra are within the range of wavelengths between 1800 to 9000 Å. The absorption of a given element must therefore be measured at the wavelength corresponding to the peak of the respective absorption line. Early use of atomic absorption in physiological study included measurement of Ca^{+2} and Mg^{+2} in serum and urine (Willis, 1960; Gimblet *et al*, 1967).

In summary, the differences in methodologies between flame photometry and atomic absorption are that the sample aerosol brought into flame utilizes emission of excited atoms in the former, whereas the aerosol brought into flame in the latter method utilizes the

absorption by atoms in the ground state.

The advantages of atomic absorption are: simplicity in operation; the absorption process is independent of the excitation potential which makes quantitative concentration limits far more acute than emission; AA is almost free of spectral interference effects which may be found in emission methods; AA is less dependent on the temperature of the flame than in emission methods; AA has a high sensitivity to elements in a sample, as elements are easily detected in the p.p.m. and p.p.b. range.

The 2 main disadvantages are: atomic absorption is less flexible than emission methods to vary instrument sensitivity to work over a wider range of concentrations of a given element; and secondly, some of the best absorption lines for some elements lie in the far ultraviolet region.

The final decision to select atomic absorption from emission or other methods is based on consideration of the elements to be determined, the type of sample, the sensitivity required, and the quantity of the sample.

C) *X-ray microanalysis*

X-rays are produced in this quantitative method

when a primary source of electrons interacts with atoms in a sample. The X-rays are characteristic of the elements in the sample. In the analysis of fluid ion secretion, the steps involved in the preparation of liquid microdroplets varied slightly with researcher, and with specimen. Van Kerkhove *et al* (1989), worked with *Formica* MT and set up the tubules following Ramsay's method (Ramsay, 1952; Ramsay, 1953). Secreted fluid was collected at predetermined time intervals with a hydrophobic glass collection pipette filled with paraffin oil. Samples of secreted fluid could then be analyzed immediately, or could be kept in the pipette between 2 layers of oil, shock frozen in liquid nitrogen and then stored until needed (Van Eekelen *et al*, 1980; Van Kerkhove *et al*, 1989). Samples could be cryofixed in liquid propane and sectioned with cryo-ultramicrotomy (Wessing *et al*, 1993; Wessing and Zierold, 1993), or placed on a dry nickel grid on a carbon support with an equal volume of glycerol and flash evaporated (Quinton, 1979; Van Kerkhove *et al*, 1989). The latter proved to be more effective at minimizing crystal formation in the sample, and background levels due to the film. Once on the grid, the oil was washed from the sample by rinsing in hexane. Once the hexane had evaporated, the samples

were mounted in a STEM or SEM system for quantitative analysis of elemental composition (Quinton, 1979).

Two different branches of microprobe X-ray analysis have been developed, and can be distinguished by the type of detector system used to collect and quantify X-rays. *Wavelength dispersive spectroscopy* (WDS), concentrates on the wave behavior of X-ray photons and uses a crystal spectrometer detector (Morgan, 1985). WDS has been used successfully by Morel and Roinel (1969). When a specimen is bombarded by primary electrons it emits X-rays with a range of wavelengths, and these X-rays leave the specimen as a whole, traveling at a certain angle. The crystal spectrometer has a specific crystal lattice spacing which allows only a narrow cone of these X-rays to be refracted and accepted by the detector. Usually, the crystal is rotated through a circle of angles until a maximum intensity of wavelength is noted by the detector and can be identified via Bragg's law (Chandler, 1977):

$$n\lambda = 2d \sin \varphi$$

where n is an integer (*i.e.* 1,2,3…), λ is the wavelength of the element, d is the interplanar space

between the crystal lattices, and φ is the angle of incidence, and of reflection of X-rays arriving at the crystal detector. The wavelength of an X-ray photon is inversely related to its energy. The major drawback to this method is that analysis is restricted to one element at a time.

The second method -- *energy dispersive spectroscopy* (EDS), concentrates on the particle behavior of X-ray photons and uses a solid state detector (Morgan, 1985). This solid state detector is more easily mounted on the electron microscope than the WDS crystal detector (Hayat, 1980). X-rays pass through a thin beryllium window to a detector made of a wafer of silicon with lithium ions "drifted" into the crystal to form a semi-conductor (Hayat, 1980). The detector crystal is kept at liquid nitrogen temperatures, under vacuum conditions, and is located between two metal electrodes across which a voltage is applied (Chandler, 1977). X-rays which enter the beryllium window to the detector, create electron-hole pairs by ionization within the detector. "The number of these pairs is proportional to the X-ray energy and is equal to the ratio of the X-ray energy and the energy required to create a pair" (Chandler, 1977). The

detector is connected to an amplifier and pulse processor to filter out background noise. Some systems can also have a multichannel analyzer which sort pulses from the amplifier based on pulse amplitude and then records the number of X-rays from a specific region of the spectrum. The great advantage of the solid state detector is that it can be placed very close to the source of X-rays and therefore can accept a larger angle of radiation when compared to the crystal spectrometer.

The disadvantages to this technique are that it is time consuming, and requires an accurate estimate of droplet volume before analysis.

D) *Microtitration of chloride*

The microtitration of chloride is based on the principle of potentiometric end-points in a titration. The first conventional method used a chloride electrode (silver wire coated with silver chloride) dipped into a titration vessel to which silver nitrate is added from a burette (Sanderson, 1952; Shaw, 1955). The Cl^- electrode is connected to a voltmeter and a reference electrode. As Cl^- precipitates out of solution to form AgCl, the potential changes. The end point is indicated by a very rapid change of potential (100 mV

or more). This method is useful with sample volumes as small as 0.2 µl and can measure 1 µg of Cl^- with an error less than ± 1%.

In a second method developed by Ramsay *et al* (1955), Ag^+ ions are added by electrolysis of the silver electrode, and not as a solution from a burette. The Ag^+ ion is added by passing a current through a silver electrode in series with a condenser. When all of the Cl^- ions have been precipitated, the potential will have fallen about 225 mV. The charge developed on the condenser correlates to the amount of Cl^- titrated. This method utilizes volumes as small as 0.5×10^{-3} µl and can measure 10^{-4} µg of chloride with an error less than ± 1% (Spring *et al*, 1975; Roinel, 1975).

The former two methods set the ground work for the development of the contemporary chloridometer or more precisely -- the *chloride titrator* which uses an amperometric method. Constant current is passed through the circuit, and the time over which current is passed provides a measure of the number of Ag^+ ions required to precipitate all the Cl^- in the sample.

The disadvantages of these microtitration methods are that the process is slow, and that the initial sample volume must be known.

E) ***Radioisotopes***

Radioisotopes decay with the emission of alpha or beta particles, or gamma rays. The maximum energy emitted by each of these rays is different and is specific for any given isotope.

Liquid scintillation counters are used to detect alpha and beta particles. An organic scintillant(eg. toluene) in close contact with a radioactive sample can absorb the radiation energy of the sample and re-emit the absorbed energy as a photon of light. The energy absorbed by the toluene is re-emitted in the UV range or in the visible region so that suitable photomultiplier tubes sensitive to these respective wavelengths can detect and quantify the photons of light. The greater the energy of the emitted radiation ray, the more photons of light arrive at the photomultiplier. As each quantum of light arrives at the photmultiplier, the electronic circuit registers an event which is continuously averaged and displayed as counts per minute.

A few disadvantages of this method are the expense of the scintillation cocktail, and the time (typically 5-15 minutes) required for analysis of each sample.

F) ***Analysis of secreted fluid ionic composition using ion- selective microelectrodes***

Ion selective microelectrodes (ISME's) can be used for measuring specific ion activity for analysis of intracellular and extracellular ion concentrations (*eg.* K^+, Cl^-: Haley and O'Donnell, 1997, Haley *et al*, 1997; pH, Ca^{+2}, Na^+, K^+: O'Donnell and Maddrell, 1995; O'Donnell *et al*, 1996; K^+: Maddrell *et al*, 1993b). Liquid membrane ISME's are made by filling the tip of borosilicate glass micropipettes with an organic cocktail containing an ionophore. Pipettes are made hydrophobic by exposure to silane vapour at moderate temperatures (approx. 200°C; Deyhimi and Coles, 1982; Munoz *et al*, 1983). Silanization makes the glass hydrophobic, thereby permitting retention of the liquid membrane when the tip is placed in aqueous solutions. In addition, the hydrophobic coat prevents short circuiting of the potential across the liquid membrane. Without silanization, electrical shunting occurs because the normal hydration of the glass provides a lower resistance electrical pathway along the inner surface of the micropipette.

In neutral carrier ionophores the carrier acts as a shuttle, transporting ions across the interface between the liquid membrane and the external solution.

A AgCl coated silver wire is placed in the electrolyte filling solution and connected to a high impedance electrometer (figure 1.2). Potential differences can then be monitored and recorded as the ion distribution across the ionophore changes (Vaughan-Jones and Aickin, 1988). Potential differences are converted into an ion concentration using the Nernst equation. Although electrodes measure ion activity, data can be expressed as concentrations if it is assumed that the activity coefficients of the calibration solutions, and the sample solution are the same. The conversion from ion activity to ion concentration is accurate to within ± 5% for a change of ionic strength differing in 60 $mmol.l^{-1}$ (Ammann, 1986).

The selectivity of an ISME for any particular ion is based on the selectivity of the ionophore used. Selectivity coefficients are usually measured using the separate solution method. The potential of the ISME (versus its reference) is measured in a solution of the test ion *"X"* and then in a solution of the interfering ion *"Y"*. The selectivity coefficient (K) is then given by:

$$K_y = a_x/a_y \cdot 10(E_y-E_x)/S$$

Figure 1.2 -- Schematic diagram representing a liquid membrane ISME filled with an organic cocktail containing an ionophore, and backfilled with an electrolyte solution (left), and a reference electrode (right) both with a AgCl coated silver wire connected to a high impedance electrometer.

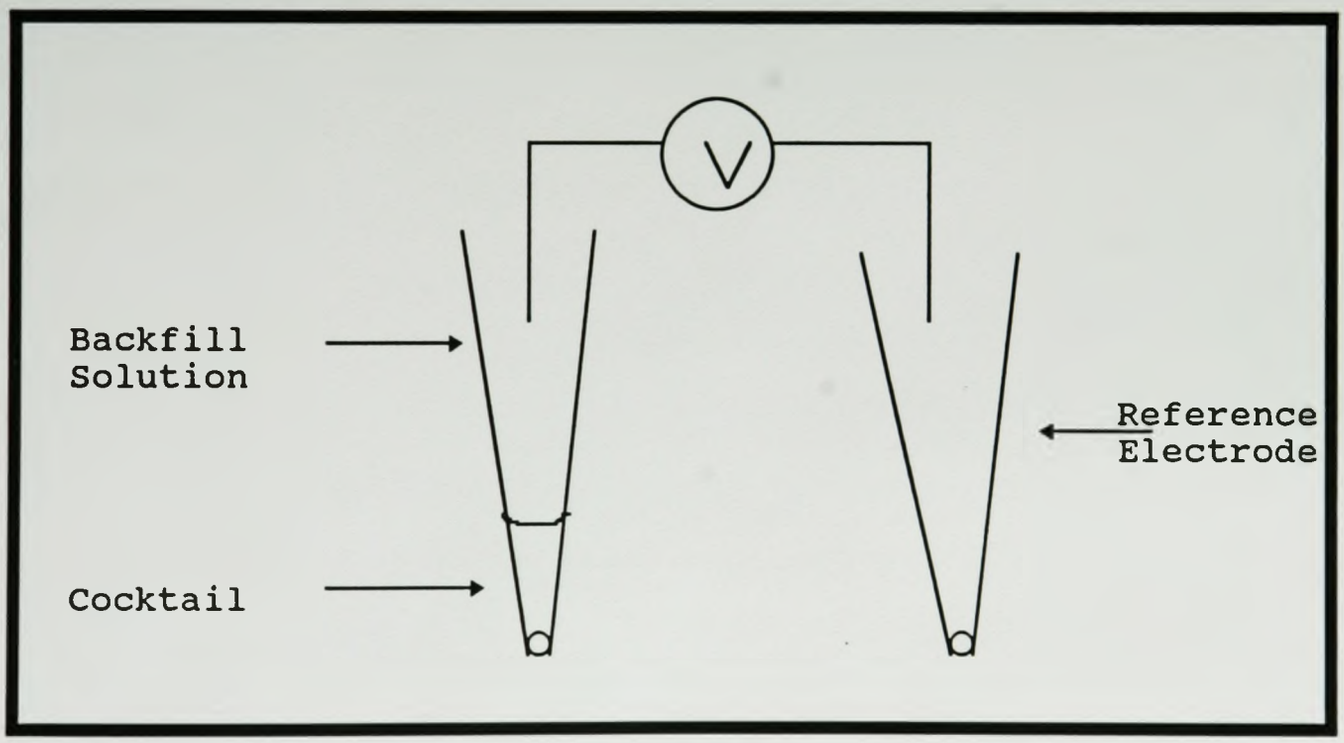
V
Backfill
Solution
Cocktail
Reference
Electrode

where E_y is potential measured in a solution containing an activity a_y of the interfering ion, E_x is the potential measured in a solution containing an activity a_x of the test ion, and S is the slope of the electrode, defined as the change in electrode potential during a 10-fold change in a_x. If an ionophore has a small selectivity constant for an ion, it is deemed more specific or selective for that particular ion, as there is less interference from other ions (Thomas, 1978).

The advantages of using ISME are as follows: rapid response times (less than 1 min., and often a few seconds); a direct measurement of ion activity; continuous measurements may be taken over many hours; fairly simple in construction and inexpensive to purchase materials; and the possibility of measuring ions *in vivo*.

The disadvantages according to Thomas (1978) are: the lack of specificity for some ions. For extracellular fluids, highly selective ionophores are available for H^+, K^+ and Ca^{+2}. Accurate measurements of Na^+ can be made providing a correction is made for interference by K^+. Chloride electrodes suffer from interference from HCO_3^-, but can provide reliable estimates of Cl^- activity in bicarbonate-free solutions. Fluid secreted by MTs, in Ramsay assays is effectively HCO_3^- free, since the loss of CO_2 to the paraffin oil depletes the droplet of CO_2 and HCO_3^-. The rank of ion

specificity from greatest to least is as follows: pH> K^+, Ca^{+2} ,Na^+> Cl^-. The latter ion needs careful attention.

Since electrodes based on chloride ion exchangers are very sensitive to interference from many organic anions (Saunders and Brown, 1977), a *solid state chloride electrode* was first developed and used on the giant squid axon in 1954 by A. Mauro. Solid state chloride electrodes are sensitive to other halides, but are excellent for use in biological fluids in which the interfering halide concentrations are presumably negligible (Wright and O'Donnell, 1992).

The method employs a silver wire coated with AgCl and acts as a perfect Cl^--sensitive electrode in chloride-containing solutions. This Cl^--sensitive microelectrode has a plug of metallic silver in the tip of a glass microelectrode and is sealed with a drop of melted paraffin wax. The electrode gives a Nernstian response to changes in Cl^- activity (Thomas, 1978).

IV *Limitations of above methods:*

All of the above methods have poor temporal resolution. All methods require the tubule to be run for typically 5-10 min to produce enough secreted fluid for analysis. This prevents experiments to follow ion transport in real time. Also, all above methods have poor spatial

resolution. Ion transport across different regions can be studied only if the tubule is long enough to permit distinct regions to be bathed in separate drops of bathing saline.

V *Hypothesis for thesis*

Rapid rates of ion transport by secretory or reabsorptive segments of insect MTs should deplete or enrich, respectively, ion concentrations in the unstirred layer bathing the basolateral surface of the tubule. These changes in ion concentration should be detectable by pH- or ion-selective microelectrodes positioned in the USL. This technique is non-invasive, and offers time resolution comparable to that of the response time of the microelectrode (a few seconds). In theory, the technique should provide spatial resolution comparable to that of the dimensions of a single MT cell.

CHAPTER 2: Analysis of Epithelial Transport by measurement of K^+, Cl^-, and pH Gradients in Extracellular Unstirred Layers: Ion Secretion and Reabsorption by Malpighian Tubules of *Rhodnius prolixus*

INTRODUCTION

Active ion secretion by insect Malpighian tubules.

Malpighian tubules of many species are capable of extraordinarily rapid rates of ion transport. Most can transport KCl under Na-free conditions or in the presence of the Na^+/K^+ ATPase inhibitor ouabain; these characteristics argue against the involvement of a Na^+/K^+ ATPase which plays a cardinal role in ion transport by most (but by no means all) epithelia. A lumen positive transepithelial potential is also a characteristic of most, but not all, insect Malpighian tubules, indicating that cation transport is against an electrical gradient. Recent evidence suggests that the active transport of alkali cations is a secondary process which is energized by a vacuolar-type (V-type) H^+-ATPase. Apical transport of alkali cations is now seen to involve the coordinated actions of two proteins; the ATP-dependent proton pump, and an Na^+/H^+ or K^+/H^+ exchanger which is driven by the

Figure 2.1 -- Proton electrochemical gradients are generated by H^+ V-ATPases across apical plasma membranes of many mitochondria-rich epithelial cells of insects and other animals. (From Harvy and Wieczorek, 1997).

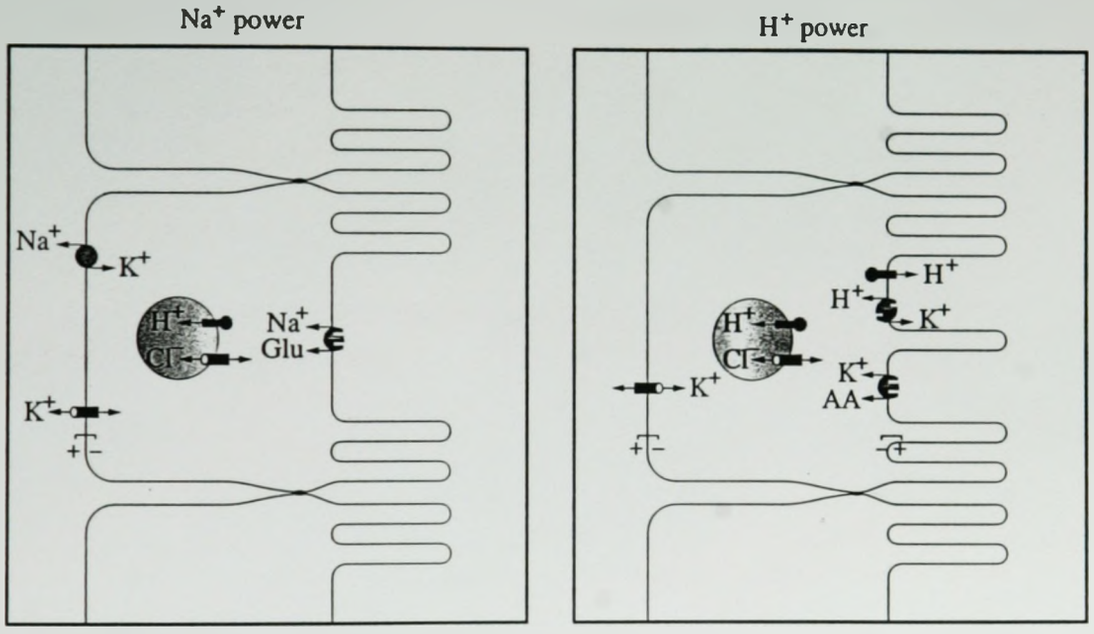

Mammal and 'all' animal cells

Insect cells

resulting transapical proton motive force (Harvey and Wieczorek, 1997; Figure 2.1). Vacuolar-type ATPase activity has been localized in various tissues by means of immunofluorescence and immunogold staining using monoclonal antibodies to specific subunits of the H^+-ATPase of *Manduca sexta* midgut apical membrane. The antibodies label not only the apical membrane of midgut goblet cells, but also the apical brush border of *Manduca sexta* Malpighian tubules (Klein *et al*, 1991). In addition, crude homogenates of Malpighian tubules cross-react with a polyclonal anti-holoenzyme serum to the midgut ATPase, further suggesting that a vacuolar-type H^+-ATPase is present in the tubules.

Inhibitor studies also support the involvement of a V-type H^+-ATPase in fluid and ion secretion by Malpighian tubules. This class of ATPases is insensitive to vanadate, an inhibitor of E_1E_2 -ATPases such as the Na^+,K^+-ATPase, but sensitive to the macrolide antibiotic bafilomycin A_1 (Bowman *et al*, 1988), the sulfhydryl reagent N-ethylmaleimide (NEM) and the nucleotide analog 7-chloro-4-nitrobenz-2-oxa-1,3 -diazole (NBD-Cl; Forgac, 1989). Secretion of fluid, Na^+ and K^+ by isolated tubules of *Drosophila hydei* decrease rapidly in response to sub-micromolar levels of bafilomycin, and 10-50 μM NEM and NBD-Cl (Bertram et al,1991). In contrast, the effects

of vanadate are less pronounced and develop slowly, and are accompanied by an increase in Na^+ content of the secreted fluid, consistent with inhibition of a basolateral Na^+,K^+-ATPase.

The operation an apical alkali cation/H^+ exchanger is suggested in part by the effects of amiloride on tubule function. In isolated tubules of *D. hydei* (Bertram, 1991) and *Rhodnius* (Maddrell and O'Donnell, 1992), application of amiloride results in acidification of the secreted fluid. It appears that acidification reflects continued operation of an H^+ pump across the apical membrane when the alkali cation/H^+ exchanger is blocked by amiloride. Intracellular pH (pH_i) does not decrease, as might be expected if amiloride blocks a Na^+/H^+ exchanger in the basolateral membrane (Bertram, 1991). Bafilomycin blocks recovery from experimental cytoplasmic acidification, and lowers the resting pH_i, consistent with the contribution of ATP-dependent mechanisms to cellular acid extrusion (Bertram, 1991). In Malpighian tubules of the ant *Formica polyctena*, the gradient of H^+ across the apical membrane is sufficient to energize movements of K^+ from cell to lumen through an electroneutral (*i.e.* $1K^+/1H^+$) antiporter (Zhang *et al*, 1994).

Fluid and ion secretion by Rhodnius Malpighian tubules

The hemipteran insect *Rhodnius prolixus* periodically ingests blood meals which may exceed its own body weight by a factor of 12. Surplus fluid, in the form of NaCl and water from the plasma, is eliminated for several hours after the blood meal. During this post-prandial diuresis, fluid secretion rates of the Malpighian tubules increase 1000-fold above the resting level, and each cell in the epithelium secretes a volume of fluid equal to its own volume every 15 s. The insect is thus able to eliminate urine at prodigious rates, equivalent to its original body weight every 20 - 30 min.

Fluid secretion is driven by ion transport across the tubule wall (Figure 2.2), and the current view is that active transport involves a V-type H^+ ATPase which works in concert with an alkali cation (Na^+, K^+/H^+) exchanger (Maddrell and O'Donnell, 1992). Fluid secretion is inhibited by the drugs furosemide and bumetanide, which block cotransport of Na^+ (and/or K^+) and Cl^- in vertebrate epithelia. In the case of *Rhodnius* tubules, transport of Cl^- across the basolateral membrane into the cell involves the movement of Cl^- against its electrochemical gradient. Favorable gradients for entry of Na^+ and/or K^+, however, are established by apical pumping of these ions from cell to lumen. The cotransporter couples the

Figure 2.2 -- The various transport processes, active and passive, involved in the operation of insect Malpighian tubules (From Madrell and O'Donnell, 1992).

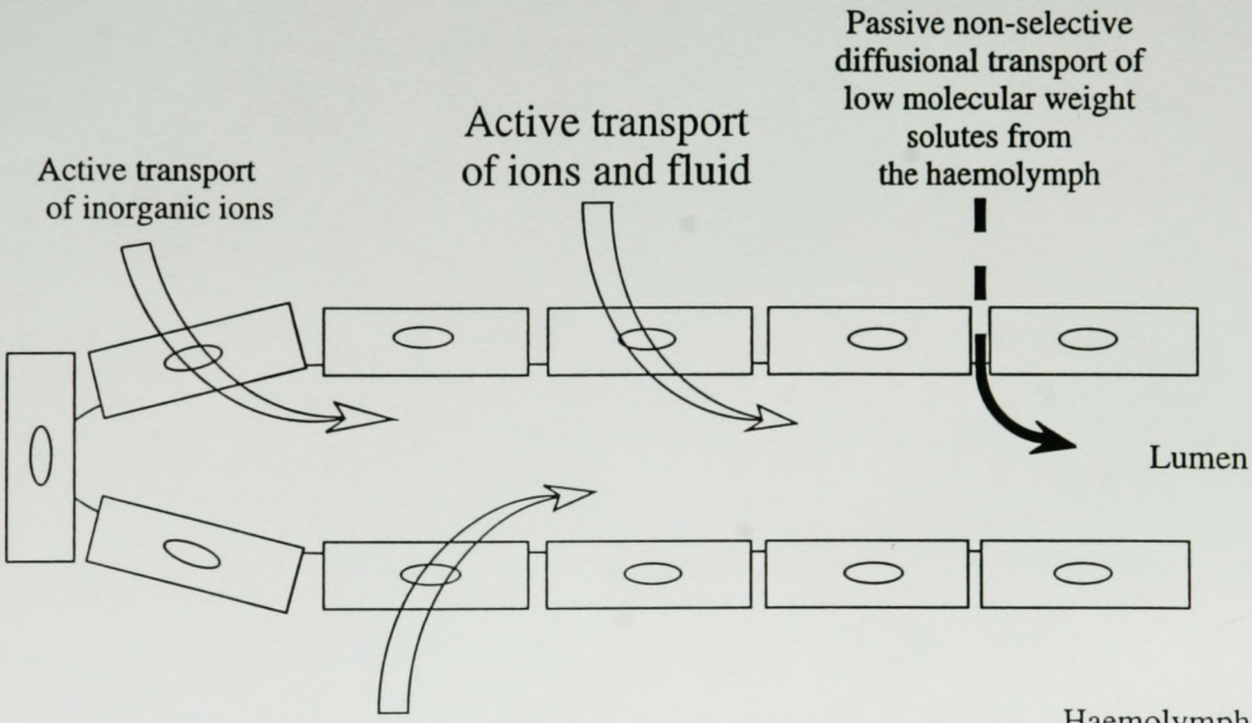
Passive non-selective diffusional transport of low molecular weight solutes from the haemolymph
Active transport of ions and fluid
Active transport of inorganic ions
Lumen
Haemolymph
Active transport of organic solutes (acylamides, sulphonates, alkaloids, cardiac glycosides, uric acid, etc.)

movement of Cl^- to the entry of Na^+ and/or K^+, thus energizing secondary active transport of Cl^-. Blockade of Cl^- influx into the cell by furosemide or bumetanide reduces the availability of Cl^- to act as a counterion for cations pumped electrogenically across the apical membrane, inhibiting fluid secretion and resulting in the build-up of a lumen-positive potential (O'Donnell and Maddrell, 1984). Similar changes in transepithelial potential are observed when tubules are bathed in chloride-free salines, or in Na^+-free salines, because entry of chloride into the cell is coupled to the entry of Na^+. In chloride-replete salines, anion movements from cell to lumen partially short-circuit the electrogenic effects of the apical cation pump, so that the apical membrane is partially depolarized and the net TEP is much less positive (O'Donnell and Maddrell, 1984).

Fluid secretion by Malpighian tubules is generally considered to result from passive osmotic water flux which is driven by active ion transport. The simplest explanation for coupling of salt and water flows in Malpighian tubules of *Rhodnius* involves transcellular osmosis. Small increases in osmolality of less than 0.7 mOsm kg^{-1} across the basolateral cell membrane and 2.6 mOsm kg^{-1} across the apical cell membrane are sufficient to account for the known flow rates and slight hypertonicity (1.3%) of the secreted fluid relative

to the hemolymph or bathing saline (O'Donnell and Maddrell, 1983). Transcellular osmosis is feasible because of the high measured osmotic permeability of the tubules, 4.3 x 10^{-3} cm s^{-1} $osmol^{-1}$ (O'Donnell *et al*, 1982). When the data are corrected for unstirred layer effects during measurement of P_{os} (Aldis, 1988), the true osmotic permeability increases by about 35%, to 5.8 x 10^{-3} cm s^{-1} $osmol^{-1}$ (O'Donnell *et al*, 1982).

Dual control by a peptide diuretic hormone and serotonin in Rhodnius Malpighian tubules

Many blood-feeding insects release hormones into the hemolymph in response to ingestion of the blood meal. In *Rhodnius* and the tsetse flies, diuretic hormones are released into the blood from the metathoracic ganglia, and hemolymph collected from fed individuals can stimulate fluid secretion by isolated tubules (Gee, 1975; Maddrell and Gardiner, 1976). Both chemical analyses (Lange *et al*, 1989) and bioassays have demonstrated that hemolymph levels of 5-hydroxy tryptamine (5HT) increase more than three-fold during feeding in *Rhodnius*, reaching values in the range of 0.5 - 1 x 10^{-7} M. Concentrations remain elevated for more than 1 h, and are sufficient to stimulate rapid fluid secretion by the Malpighian tubules (Lange *et al*, 1982; Maddrell *et al*, 1991).

Pharmacological studies employing the 5HT receptor antagonists ketanserin and spiperone (Lange *et al*, 1982; Maddrell *et al*, 1991) indicate that receptor sites distinct from those for the peptide diuretic hormone (Aston and White, 1974) are present on the Malpighian tubule cells. Orchard (Orchard, 1989) has shown that 5HT is produced by and released from the neurosecretory cells of the mesothoracic ganglion in Rhodnius, as well as from associated abdominal nerves. Moreover, the levels of 5HT in these cells is reduced during feeding (Orchard *et al*, 1988). The two hormones act synergistically, so that the dose-response curves for mixtures are 5 times steeper than for either hormone alone, and the response threshold concentration for either hormone is greatly reduced by the presence of a threshold dose of the other hormone (Maddrell *et al*, 1992). It is suggested that it may take less time to release small amounts of two synergistic hormones, rather than large quantities of a single hormone, and that such an arrangement may be advantageous to insects, which have sluggish circulation (Maddrell *et al*, 1993). Because minor changes in concentration substantially alter the rate of diuresis, not only can diuresis be rapidly initiated, but also rapidly terminated when sufficient urine has been voided. It is not known if KCl reabsorption by the lower tubule

(discussed below) and NaCl and fluid transport by the midgut also rely upon synergistic actions of 5HT and peptide diuretic hormone (DH). These actions can be stimulated by 5HT *in vitro*.

Reabsorption of ions by Malpighian tubules

The stimulated upper tubule of *Rhodnius* secretes a nearly isoosmotic solution containing approximately equimolar NaCl and KCl. The lower tubule selectively reabsorbs KCl. The resultant NaCl rich urine is 100 mOsm kg^{-1} hypo-osmotic to the blood, so that hemolymph osmolality and K^+ concentration are maintained when the animal feeds on blood which is hypoosmotic to the animal's hemolymph. In other insects, such as locusts, the reabsorption of KCl occurs primarily in the rectum. However, during rapid diuresis in *Rhodnius*, a tubular epithelium provides a much larger surface area, per unit of fluid in the lumen, than does the sac-like rectum. In other blood-feeders such as mosquitoes, the tubules secrete a NaCl-rich fluid, so the need for KCl reabsorption downstream is less pressing.

Most of the KCl reabsorbed from the lumen of *Rhodnius* lower tubule is transported across the 1/3 of the lower tubule closest to the junction with the gut (Maddrell, 1978). Moreover, the osmotic permeability (P_{os}) of the tubule wall

declines over the same region, and this reduction in P_{os} is more pronounced when KCl reabsorption is stimulated by 5HT (O'Donnell *et al*, 1982). This reduction in P_{os} in the length of the tubule responsible for KCl reabsorption minimizes osmotic movements of water which will tend to accompany KCl movements from lumen to hemolymph are limited. As a result, the final urine is hypoosmotic to the hemolymph.

Cooperative homeostatic mechanisms serve to match the K^+ concentration of the urine to the K^+ concentration of fluids absorbed from the gut, thereby maintaining hemolymph K^+ concentration nearly constant. Three mechanisms activated by a fall in the K^+ concentration of the medium bathing the tubules are: 1) a decrease in the rate of fluid secretion by the upper tubule, 2) a decrease in the K^+ concentration of the fluid secreted by the upper tubules, and 3) an increase in the rate of K^+ reabsorption by the lower tubules (Maddrell *et al*, 1993). Increases in bathing medium K^+ concentration produce the opposite effects.

Active K^+ reabsorption by the lower Malpighian tubule does not involve the amiloride-sensitive K^+/H^+ exchangers or V-type H^+-ATPases implicated in secretion of ions from haemolymph to lumen in the upper tubule (Haley and O'Donnell,

1997). Amiloride, N-ethylmaleimide, 4-chloro -7-nitrobenzo-2-oxa-1,3-diazol and bafilomycin A_1 inhibit haemolymph-lumen secretion of Na^+ and K^+ by the upper Malpighian tubule, but have little or no effect on lumen-haemolymph reabsorption of K^+ by the lower tubule. The effects of inhibitors of H^+/K^+-ATPases, including omeprazole and SCH 28080, suggest that a pump similar to the H^+/K^+-ATPase of the gastric mucosa is involved in KCl reabsorption. The presence of K^+ channels in the basolateral membrane in the lower Malpighian tubule is suggested by inhibition of KCl reabsorption by basolateral but not apical application of the K^+ channel blocker Ba^{2+}, and by blockade of K^+-dependent changes in membrane potential by Ba^{2+}. It is proposed, therefore, that K^+ is pumped from lumen to cell by an ATP-dependent pump resembling the H^+/K^+-ATPase of the gastric mucosa, and that K^+ leaks from cell to bathing saline (haemolymph) via an electrodiffusive pathway (*i.e.* K^+ channels). Cl^- reabsorption is inhibited by Cl^- channel blockers, including diphenylamine-2-carboxylate(DPC) and 5-nitro-2-(3-phenylpropylamino) benzoic acid (NPPB), but not by compounds which block $Na^+/K^+/Cl^-$ and K^+/Cl^- co-transporters (Haley *et al*, 1997). Measurements of transepithelial potential and basolateral membrane potential during changes in bathing saline chloride concentration indicate the presence of DPC- and NPPB-sensitive chloride channels in the basolateral

membrane. A working hypothesis of ion movements during KCl reabsorption proposes that Cl^- moves from lumen to cell through a stilbene-insensitive Cl^-/HCO_3^- exchanger and then exits the cell through basolateral Cl^- channels. Acetazolamide inhibits KCl reabsorption at more than one stage. By inhibiting the catalysis of CO_2 dehydration/rehydration by carbonic anhydrase (CA), acetazolamide may secondarily inhibit transporters dependent upon adequate supplies of H^+ and HCO_3^-. In other words, apical H^+/K^+-ATPases and Cl^-/HCO_3^- exchangers may both depend upon the H^+ and HCO_3^- provided by the actions of CA (Figure 2.3).

In this chapter, I describe the use of extracellular ion-selective microelectrodes for analysis of ion transport by two well-characterized epithelia which form the upper and lower segments of the Rhodnius Malpighian tubule. The gradients in ion concentration between USL and bathing saline have been measured by means of ion-selective microelectrodes positioned at various distances from the surface of the tubules. Results obtained with UMT and LMT, both isolated and *in situ*, demonstrate that the pH and concentrations of K^+ and Cl^- in the USL can be quite different from the corresponding values in the bathing saline. Measurements of USL ion concentrations can be used to indicate whether ions are secreted or reabsorbed by

different regions of MTs, and the rates of ion transport can be calculated from such measurements. The results of this chapter have been published in the *Journal of Experimental Biology* (Collier and O'Donnell, 1997; Appendix A).

Figure 2.3 -- Working hypothesis of ion movements during KCl reapbsorption in the LMT of Rhodnius prolixus. (From Haley *et al*, 1997)

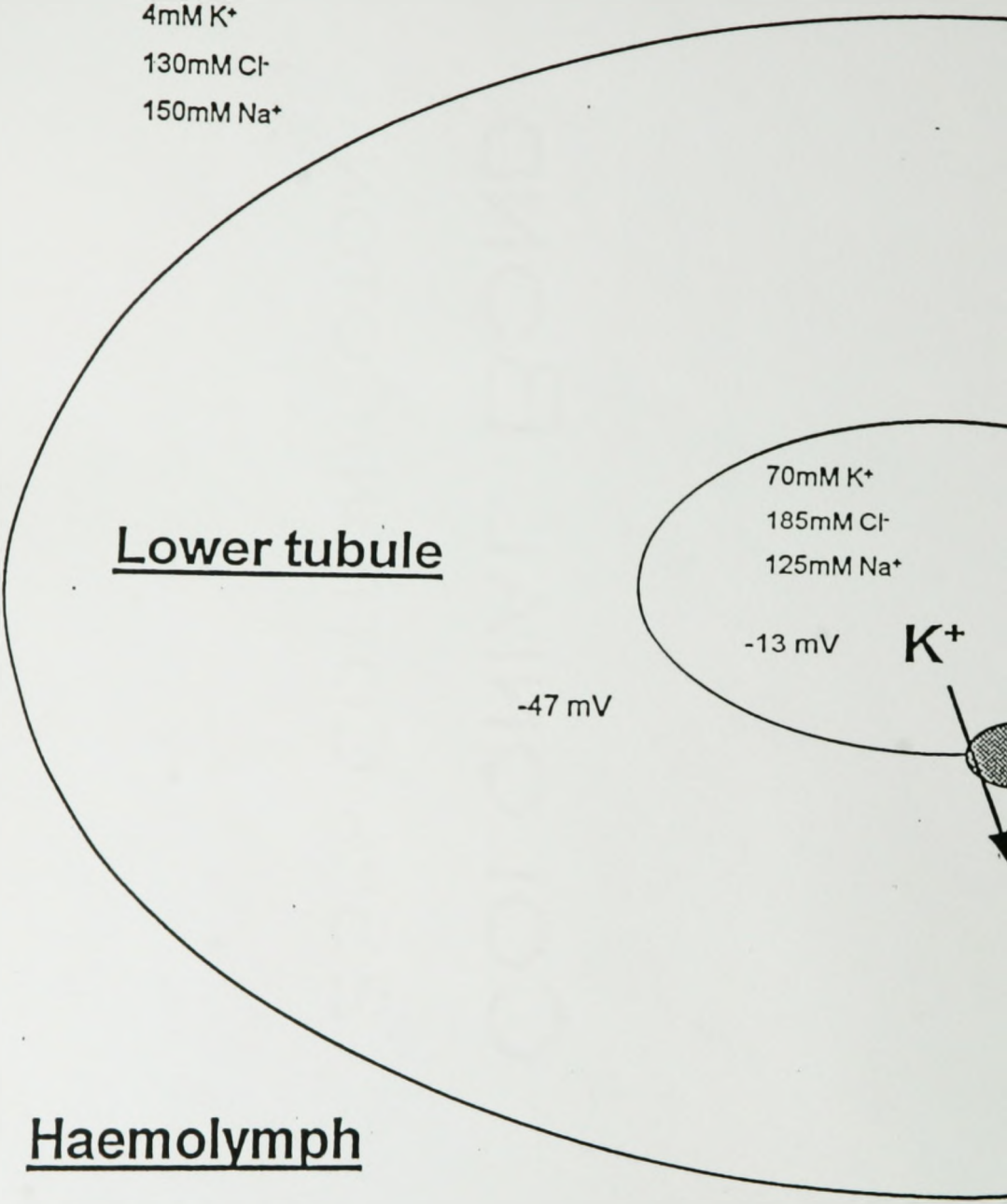
4mM K+
130mM Cl-
150mM Na+
Lower tubule
70mM K+
185mM Cl-
125mM Na+
-13 mV
K+
-47 mV
Haemolymph

Cl-
Cl-
HCO3-
H+ + HCO3-
H+
H2O + CO2
CA
K+

MATERIALS AND METHODS

Insects and experimental salines

Fifth instar *Rhodnius prolixus* from a laboratory culture maintained at 25°- 28°C and 60 % relative humidity were used 3 - 6 weeks after the previous blood meal. After insects were sacrificed by crushing the head with forceps, Malpighian tubules were dissected under physiological saline which consisted of (in mmol l^{-1}): NaCl (133.6), KCl (4.0), $MgCl_2.6H_2O$ (8.5), $CaCl_2.2H_2O$ (2.0), glucose (20.0), $NaHCO_3$ (10.2), NaH_2PO_4 (4.3), and HEPES (8.6). Saline was titrated with NaOH to pH 7.0. Salines with varying [K^+] were prepared by substitution with Na^+, maintaining the total concentration of NaCl and KCl at 137.6 mmol l^{-1}, and are referred to by their respective concentrations of K^+ (*e.g.* 4K for control saline). A saline with reduced buffering capacity was prepared using 1 mmol l^{-1} HEPES (omitting $NaHCO_3$ and NaH_2PO_4) and 154.7 mmol l^{-1} NaCl (for 4 mmol l^{-1} K^+ saline) to maintain osmolality. Saline containing 50 % of the control level of Cl^- was prepared by mixing equal parts of 4K saline and Cl^--free saline. The latter was prepared by using sulphate salts of calcium,

potassium and magnesium and substituting sodium isethionate for NaCl.

Isolation of Malpighian tubules

Upper and lower segments of isolated whole Malpighian tubules were placed in separate 200 µl droplets of saline (Figure 2.4). Lower tubules were bathed in 4K saline because this value approximates that found in the haemolymph (3.6 mmol l^{-1}; Maddrell *et al*, 1993). Upper tubules were bathed in 24K saline because the secreted fluid contains higher K^+ levels (*ca*. 100 mmol l^{-1}), and because they secrete fluid at constant rates for longer periods of time *in vitro* (Maddrell *et al*., 1993). The ampulla of the lower tubule was pulled out of the bathing droplet and anchored on a glass pin. Serotonin (5-hydroxytryptamine, 5HT) was added at 10^{-6} mol l^{-1} to both bathing saline droplets to stimulate fluid secretion by the upper tubule and KCl reabsorption by the lower tubule. Droplets of secreted fluid were collected from the ampulla at intervals. Droplet diameters were measured with an eyepiece micrometer and droplet volume (nl) was calculated using a standard formula (*e.g.* Haley and O'Donnell, 1997). Secretion rates (nl min^{-1}) were calculated by dividing droplet volumes by the time over which the droplet was formed.

Figure 2.4 -- Schematic diagram showing the experimental arrangement for measurement of extracellular ion activity of whole Malpighian tubules. Droplets of calibration solutions (not shown) and bathing saline were placed under mineral oil in a petri dish lined with Sylgard. For most experiments, UMT and LMT were bathed in 24K and 4K saline, respectively. Ion activity was measured with the ion-selective microelectrode positioned near the basolateral membrane of the tubule, and with the reference electrode placed > 5 mm away from the tubule in the bathing droplet. Axial positions are referred to in subsequent figures in units of % of the LMT's length, where 0% and 100% (indicated by arrows) correspond to the junction of the LMT and ampulla and the junction of the LMT and UMT, respectively. In some experiments, small volumes (10 - 15 nl) of saline containing drugs were ejected onto the tubule surface by a micropipette positioned adjacent to the ion-selective electrode. Pressure was applied through a 25 ml syringe connected to the back of the micropipette by polyethylene tubing.

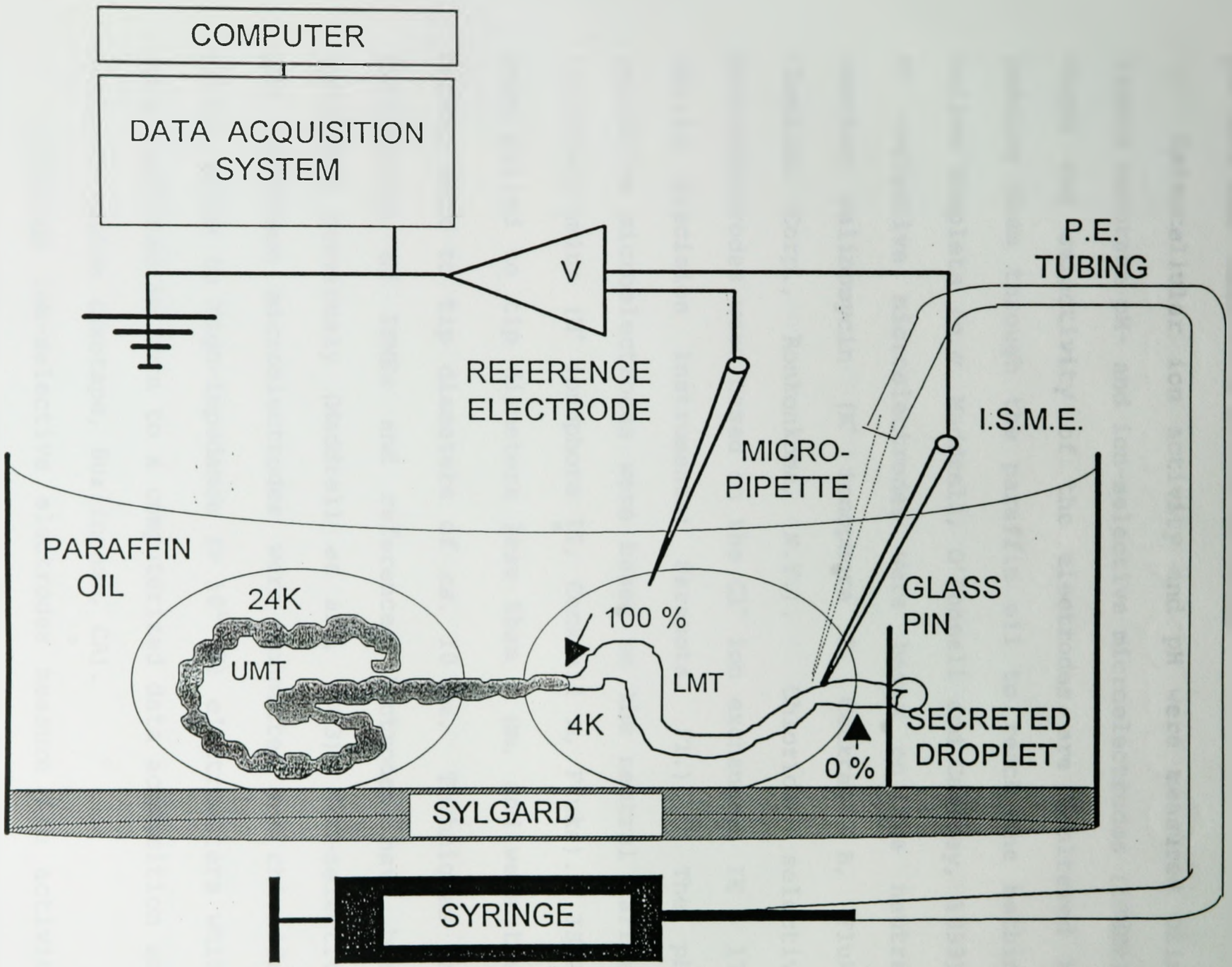
COMPUTER
DATA ACQUISITION SYSTEM
V
P.E. TUBING
REFERENCE ELECTRODE
I.S.M.E.
MICRO-PIPETTE
PARAFFIN OIL
24K
UMT
100 %
LMT
4K
GLASS PIN
SECRETED DROPLET
0 %
SYLGARD
SYRINGE

pH- and ion- selective microelectrodes

Extracellular ion activity and pH were measured using liquid membrane pH- and ion-selective microelectrodes (ISMEs). Slope and selectivity of the electrodes are unaltered by passing them through the paraffin oil to reach the bathing saline droplets (*e.g.* Maddrell, O'Donnell and Caffrey, 1993). K^+ -selective microelectrodes were based on the neutral carrier valinomycin (K^+ ionophore I, Cocktail B, Fluka Chemical Corp., Ronkonkoma, N.Y.). Chloride- selective microelectrodes were based on the Cl^- ion exchanger, IE - 173 (World Precision Instruments; Sarasota, Fl.). The pH-selective microelectrodes were based on the neutral carrier tridodecylamine (H^+ ionophore II, Cocktail A, Fluka). ISMEs were pulled to tip diameters less than 1 μm, and were then broken back to tip diameters of *ca.* 10 μm. Techniques for fabrication of ISMEs and reference electrodes have been described previously (Maddrell *et al.*, 1993). Ion-selective and reference microelectrodes were connected by chlorided silver wires to high-impedance (> 10^{15} Ω) electrometers which were connected in turn to a computerized data acquisition and analysis system (Axotape, Burlingame, CA).

Although ion-selective electrodes measure ion activity and not concentration, data can be expressed as concentrations

if it is assumed that the activity coefficient is the same in both the calibration solutions and the bathing saline. Over the range of ionic strengths of fluids encountered in this study (80 - 180 mmol l^{-1}), errors resulting from this assumption are less than 5% (Maddrell *et al*, 1993b). Expressing ISME data as concentrations simplifies comparisons with previous studies in which ion concentrations were measured by flame photometry.

Potassium and chloride concentrations were calculated with the following equation:

$$[I]_{USL\ or\ Bath} = [I]_c\ 10^{(\Delta V/S)}$$

where $[I]_{USL\ or\ Bath}$ is the concentration of K^+ or Cl^- in the USL or bathing saline, and $[I]_c$ is the corresponding concentration in the calibration droplet. ΔV is the change in electrical potential (mV) between the calibration solution and the USL or bathing saline, and S is the slope (mV) measured for a 10 - fold change in potassium or chloride concentration. Calibration solutions for K^+ and Cl^- electrodes were prepared from mixtures of 150 mmol l^{-1} NaCl and KCl.

Values of pH were calculated with the equation:

$$pH_{USL\ or\ Bath} = pH_c - (\Delta V/S)$$

where $pH_{USL\ or\ Bath}$ refers to the pH of the USL or bathing saline and pH_c to the pH of a calibration solution. S is the slope (mV), measured for a 1 unit pH difference. Calibration solutions were prepared from salines adjusted to two pH values, usually differing by 1 pH unit.

Ion concentrations or pH were measured at varying distances from the basolateral surface, and at several positions along the tubule's length. Distances were measured using a calibrated eyepiece micrometer in the dissecting microscope. Positions along the length of the lower tubule are expressed as percentages of its length (approximately 17 mm tubule in 5th instar *Rhodnius*), where 0% corresponds to the ampulla and 100% to the junction of upper and lower tubules. Reference electrodes were positioned > 5 mm away from the tubule.

In situ measurements

Measurements of $[K^+]_{USL}$ and pH_{USL} were also made on MTs *in situ*. Insects were sacrificed by crushing the head with forceps, the dorsal cuticle of the posterior half of the abdomen was removed, and 100 µl of 4K saline was added to the haemocoel. The animal was pinned down by the legs to a dissecting dish lined with Sylgard and the fat body and heart

were pulled slightly to one side to expose the tubules and the gut. Evaporation of the saline was prevented by covering the saline surface with 50 µl of paraffin oil. The preparation was illuminated from the ventral side. Ion-selective, and reference electrodes were placed in the saline/haemolymph to measure ion activity. Mean ion concentrations were measured 5 µm from the basolateral surface. The reference electrode was placed at least 5 mm away from the tubules.

Preliminary measurements indicated that $[K^+]_{USL}$ and pH_{USL} did not vary along the length of the UMT and a mean value was determined for three measurements for 3 tubules from each animal. For the lower tubule, $[K^+]_{USL}$ and pH_{USL} were calculated as the mean of 3 measurements at the same site 20% - 30% along the length of each of 3 tubules in each insect.

Pressure ejection of drugs to localized regions of the basolateral surface of Malpighian tubules

Micropipettes pulled to tip diameters of less than 1 µm were broken back to tip diameters of 3-4 µm. Each pipette was filled with paraffin oil and attached to polyethylene tubing and a 25 ml syringe filled with distilled water. Drugs were dissolved in saline and droplets of known volume were expelled under paraffin oil (See Results). The tip of the

micropipette was placed into the droplet containing the dissolved drug, and the entire droplet was taken up into the micropipette by creating a slight negative pressure in the syringe. The micropipette was then placed adjacent the ion selective microelectrode in the USL. While observing the saline/oil interface in the micropipette through the microscope, sufficient pressure was applied to the syringe plunger to eject the entire volume of saline within the micropipette.

Data analysis

All experiments were performed at room temperature, 20°-25°C. Values are reported as means ± S.E.M. Significance of differences between means were evaluated by paired or unpaired Student's t-tests (two-tailed), using a critical value of $p < 0.05$ for significance. Previous studies by Boutilier and Shelton (1980) justify the calculation of mean values and standard errors for pH data, and the pH measurements were not converted, therefore, to $[H^+]$ (mol l^{-1}) before statistical treatment.

RESULTS

Extracellular potassium and chloride concentrations near the basolateral surface of the lower tubule

Potassium concentrations were measured in the USL within 5μm of the basolateral surface at 10%, 25%, 50%, 75%, and 95 % along the length of the lower tubule (inset, Fig. 2.5a). This minimum distance was a consequence of the wall thickness of the ISME. For unstimulated tubules, the mean $[K^+]$ in the fluid of the unstirred layer of the basolateral surface of the lower tubule ($[K^+]_{USL}$) did not vary significantly along the length of the tubule (Fig. 2.5a) , and the data were therefore pooled. $[K^+]_{USL}$ of unstimulated tubules (4.49 ± 0.03 mmol l^{-1}; n = 30 sites on 6 tubules) was slightly but significantly ($p<0.05$) above $[K^+]_{BATH}$ (4.33 ± 0.01 mmol l^{-1}, n=6). This small difference may reflect passive leakage of K^+ from lumen to bath in unstimulated lower tubules. In stimulated tubules the concentration of K^+ in the unstirred layer adjacent to the basolateral surface increased, relative to the bath, and these differences were most dramatic at 10% and 25% along the lower tubules' length (Fig. 2.5a). The increase in $[K^+]_{USL}$ relative to $[K^+]_{BATH}$ is consistent with accumulation of potassium in the

USL as potassium is transported from lumen to bath by the LMT. The pattern of changes in $[K^+]_{USL}$ was examined in greater detail by scanning at 8 positions along the length of the lower tubule (Fig. 2.5b). The lower values of $[K^+]_{USL}$ at distances greater than or less than the peak at 25% along the lower tubule's length presumably reflects both the reabsorptive capacity of the epithelium and the lumenal concentration of K^+ (see discussion). The differences in bathing saline $[K^+]$ in figures 2.5a and 2.5b reflect the gradual increase in $[K^+]_{BATH}$ with time as K^+ is reabsorbed from lumen to bath in stimulated tubules. For tubules isolated in 200 µl droplets of $4K^+$ bathing saline, this increase was less than 2 mmol l^{-1} over a period of 60 minutes. In all subsequent experiments, therefore the duration of the experiments after addition of 5HT was restricted to 50 min.

Previous studies have shown that equal amounts of K^+ and Cl^- are reabsorbed by the lower tubule (Maddrell and Phillips, 1975). Measurement of $[Cl^-]_{USL}$ was not feasible in salines containing the control Cl^- concentration (148.1 mmol l^{-1}); an increase of 2 mmol l^{-1} above the bath, for example, would result in a voltage change of only 0.3 mV for a Cl^- selective microelectrode with a slope of 58 mV / 10 - fold change in $[Cl^-]$. For this reason, measurements of $[Cl^-]_{USL}$ near the lower

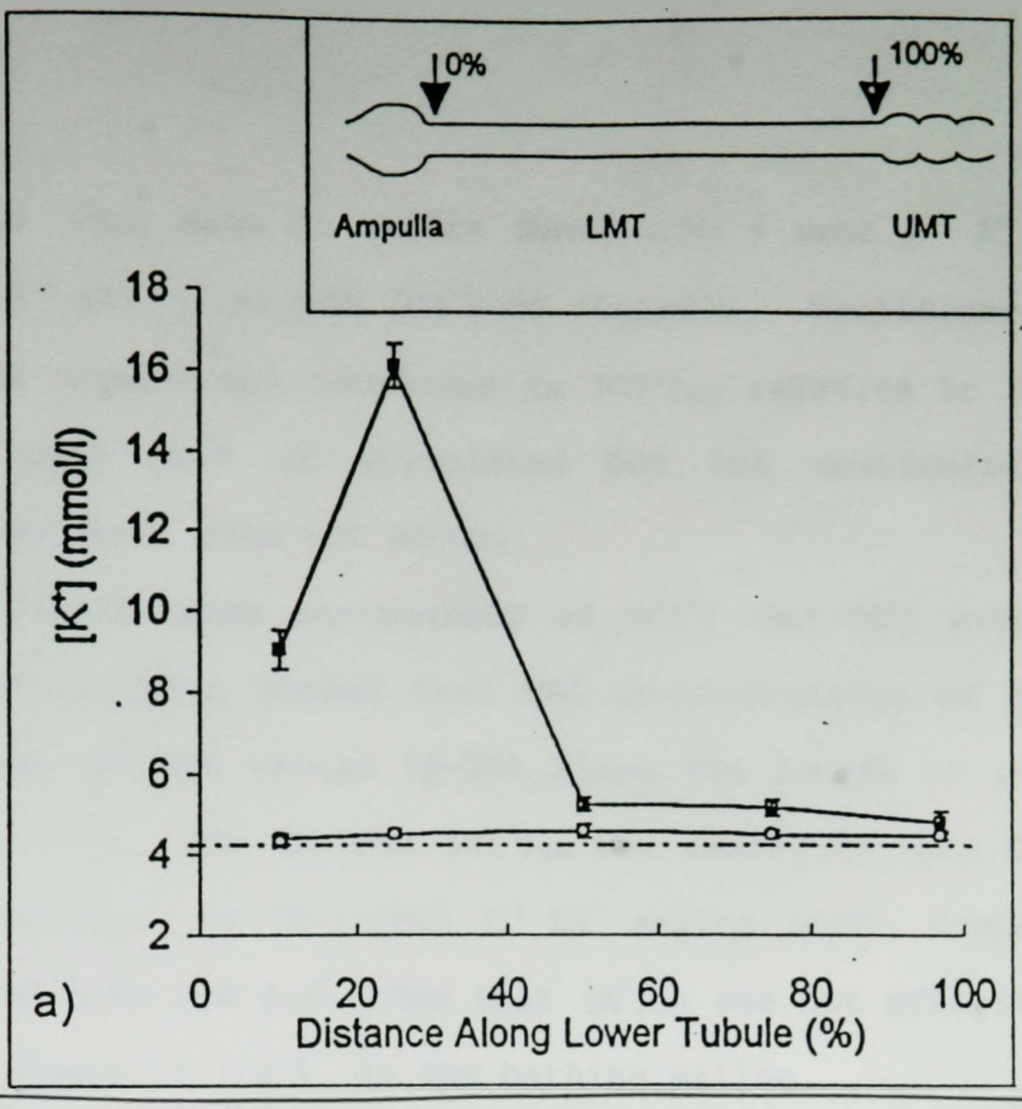
0%
100%
Ampulla
LMT
UMT
[K+] (mmol/l)
18
16
14
12
10
8
6
4
2
0
20
40
60
80
100
Distance Along Lower Tubule (%)
a)

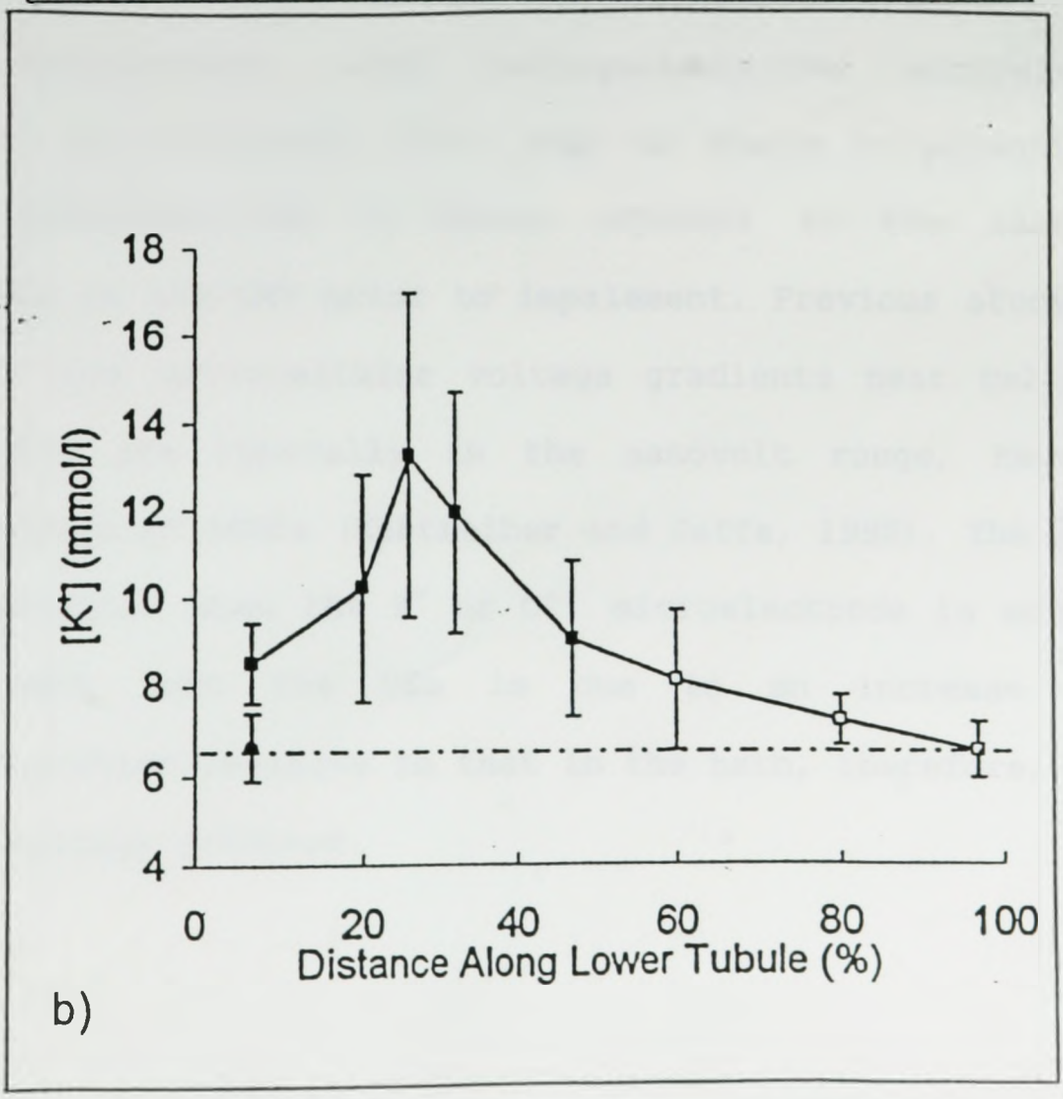
[K+] (mmol/l)
18
16
14
12
10
8
6
4
0
20
40
60
80
100
Distance Along Lower Tubule (%)
b)

tubule were made in saline containing 4 mmol l^{-1} K^+ and 74.1 mmol l^{-1} Cl- (*i.e.* 50% $[Cl^-]$ of control). Preliminary results showed significant increases in $[Cl^-]_{USL}$ relative to $[Cl^-]_{BATH}$ in the lower half of stimulated but not unstimulated lower tubules (n=5, data not shown).

Simultaneous measurement of $[Cl^-]$ and $[K^+]$ with double-barrelled ISMEs showed that USL concentrations of both ions reached maximum values 15-30% along the length of the tubule (Fig. 2.6). The maximum $[Cl^-]_{USL}$ was nearly 24 mmol l^{-1} higher than $[Cl^-]_{BATH}$ in 74.1 mmol l^{-1} Cl^- saline (n=6). Comparison of figures 2.5b and 2.6 shows that $[K^+]_{USL}$ was not affected by a 2 fold change of $[Cl^-]$ in the bathing saline.

Measurements with voltage-sensitive microelectrodes (Haley and O'Donnell, 1997) show no change in potential when the microelectrode is moved adjacent to the basolateral surface of the LMT prior to impalement. Previous studies have shown that extracellular voltage gradients near cells, when present, are typically in the nanovolt range, beyond the resolution of ISMEs (Kuhtreiber and Jaffe, 1990). The increase in potential when the K^+ or Cl^- microelectrode is moved from the bath into the USL is due to an increase in ion concentration relative to that in the bath, therefore, and not to a voltage gradient.

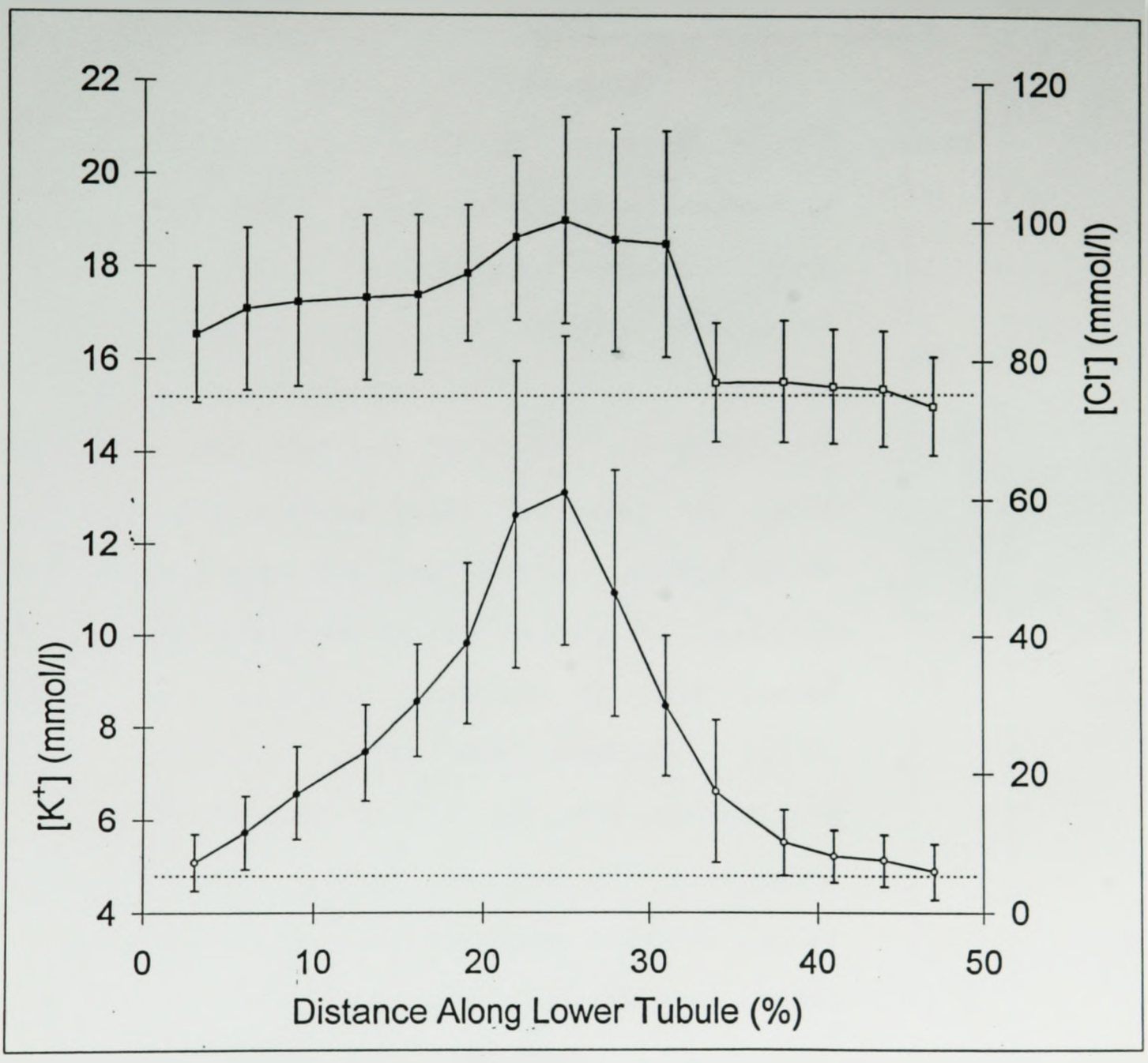
22
20
18
16
14
12
10
8
6
4
[K+] (mmol/l)
120
100
80
60
40
20
0
[Cl-] (mmol/l)
0
10
20
30
40
50
Distance Along Lower Tubule (%)

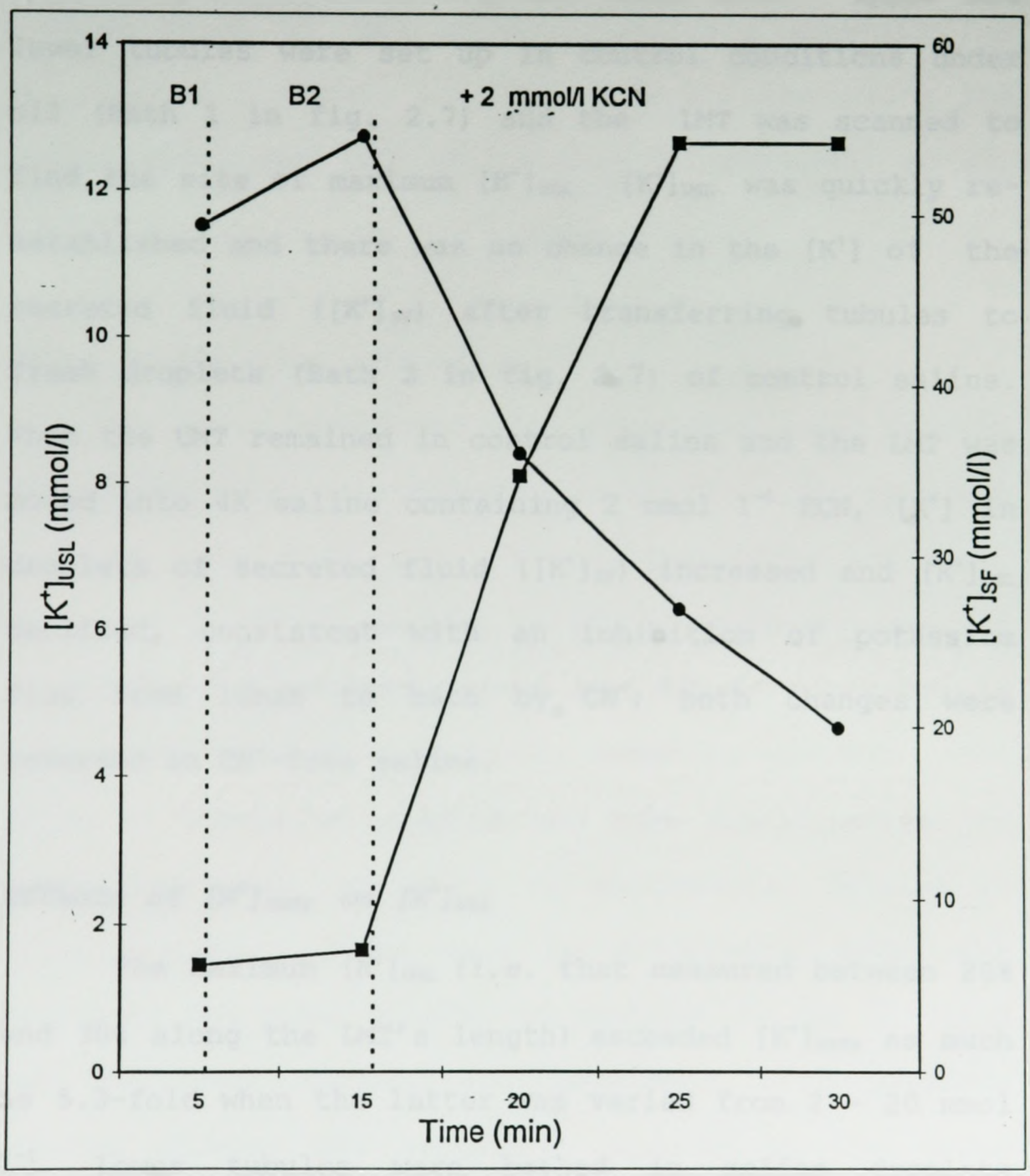
B1
B2
+ 2 mmol/l KCN
$[K^+]_{USL}$ (mmol/l)
$[K^+]_{SF}$ (mmol/l)
Time (min)
0
2
4
6
8
10
12
14
0
10
20
30
40
50
60
5
15
20
25
30

Dependence of elevated $[K^+]_{USL}$ on active transport in 5HT-stimulated lower tubules was demonstrated by inhibiting metabolism with KCN (Fig. 2.7). Upper and lower tubules were set up in control conditions under oil (Bath 1 in fig. 2.7) and the LMT was scanned to find the site of maximum $[K^+]_{USL}$. $[K^+]_{USL}$ was quickly re-established and there was no change in the $[K^+]$ of the secreted fluid ($[K^+]_{SF}$) after transferring tubules to fresh droplets (Bath 2 in fig. 2.7) of control saline. When the UMT remained in control saline and the LMT was moved into 4K saline containing 2 mmol l^{-1} KCN, $[K^+]$ in droplets of secreted fluid ($[K^+]_{SF}$) increased and $[K^+]_{USL}$ declined, consistent with an inhibition of potassium flux from lumen to bath by CN^-; both changes were reversed in CN^--free saline.

Effects of $[K^+]_{BATH}$ on $[K^+]_{USL}$

The maximum $[K^+]_{USL}$ (*i.e.* that measured between 20% and 30% along the LMT's length) exceeded $[K^+]_{BATH}$ as much as 5.3-fold when the latter was varied from 2 - 20 mmol l^{-1}. Lower tubules were bathed in saline droplets containing 2, 4, 6, 8.6 or 20 mmol l^{-1} K^+; the corresponding values of $[K^+]_{USL}$ (in mmol l^{-1}, mean ± S.E., for the number of tubules indicated in brackets) were:

10.6 ± 0.8 (9), 11.8 ± 0.4 (59), 12.0 ± 1.0 (5), 15.4 ± 1.3 (6) and 28.2 ± 1.8 (5). These data show that the maximum value of $[K^+]_{USL}$ was relatively constant for $[K^+]_{BATH}$ of 2 - 6 mmol l^{-1} (fig. 2.8a,b), bracketing the normal haemolymph $[K^+]$ of 3.6 mmol l^{-1} (Maddrell *et al*, 1993b).

$[K^+]_{USL}$ of the upper tubule

The $[K^+]_{USL}$ associated with stimulated upper tubules was slightly but significantly *lower* ($P< 0.05$) than the bath in both 8.6K and 24K salines (fig. 2.9a,b). Reduction in $[K^+]_{USL}$ relative to $[K^+]_{BATH}$ is consistent with a depletion of potassium from the USL as potassium is transported from bath to tubule lumen by the UMT. The $[K^+]_{USL}$ of stimulated tubules was also significantly ($P< 0.05$) lower than the $[K^+]_{USL}$ of unstimulated tubules in either saline. There were no differences along the length of the upper tubule, in contrast to the findings for the lower tubule, and consistent with previous studies showing the secretory capacity of the upper tubule to be homogeneous along its length (Maddrell, 1969). Measurements were taken at evenly-spaced points

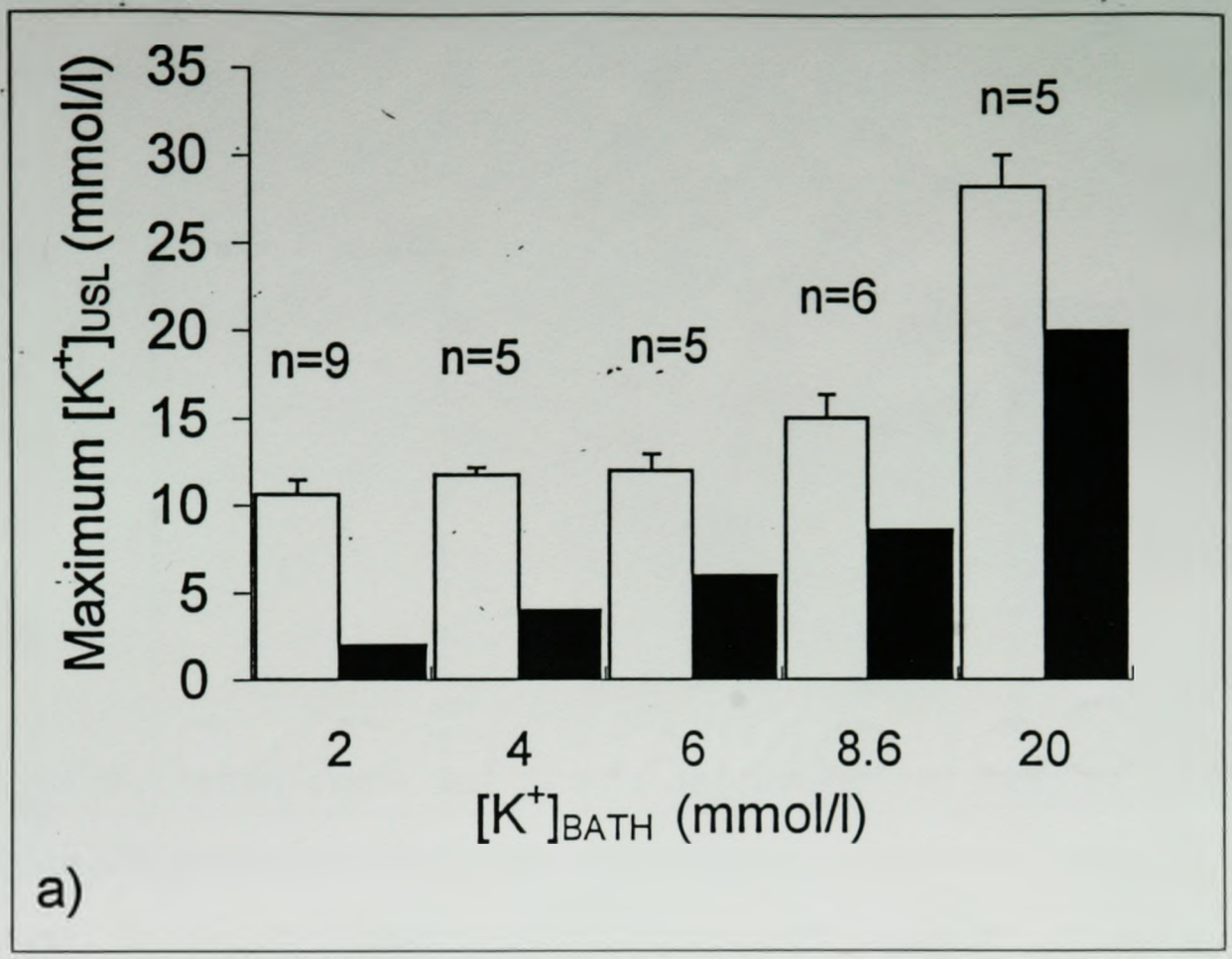
Maximum $[K^+]_{USL}$ (mmol/l)
35
30
25
20
15
10
5
0
n=9
n=5
n=5
n=6
n=5
2
4
6
8.6
20
$[K^+]_{BATH}$ (mmol/l)
a)

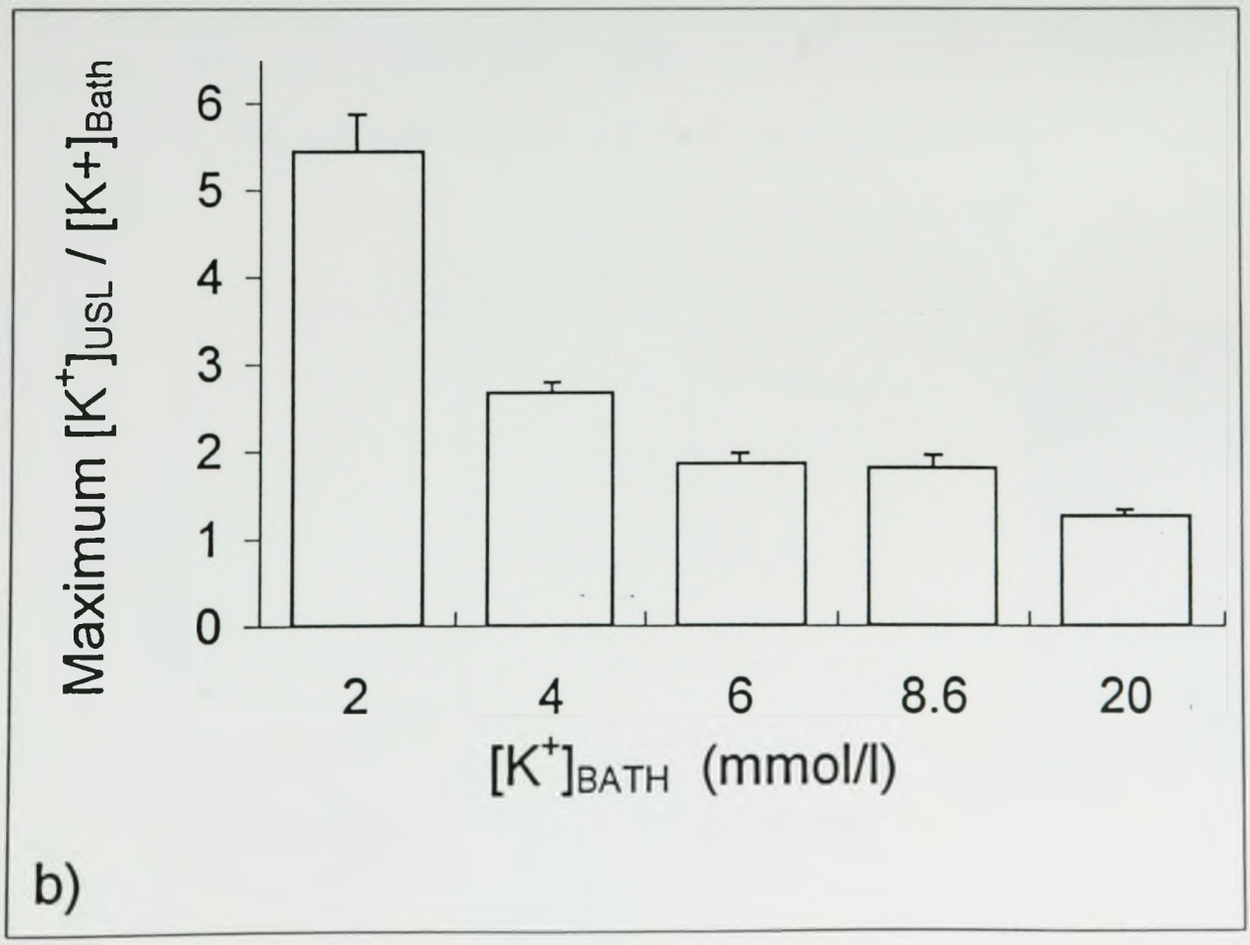
Maximum $[K^+]_{USL}$ / $[K+]_{Bath}$
6
5
4
3
2
1
0
2
4
6
8.6
20
$[K^+]_{BATH}$ (mmol/l)
b)

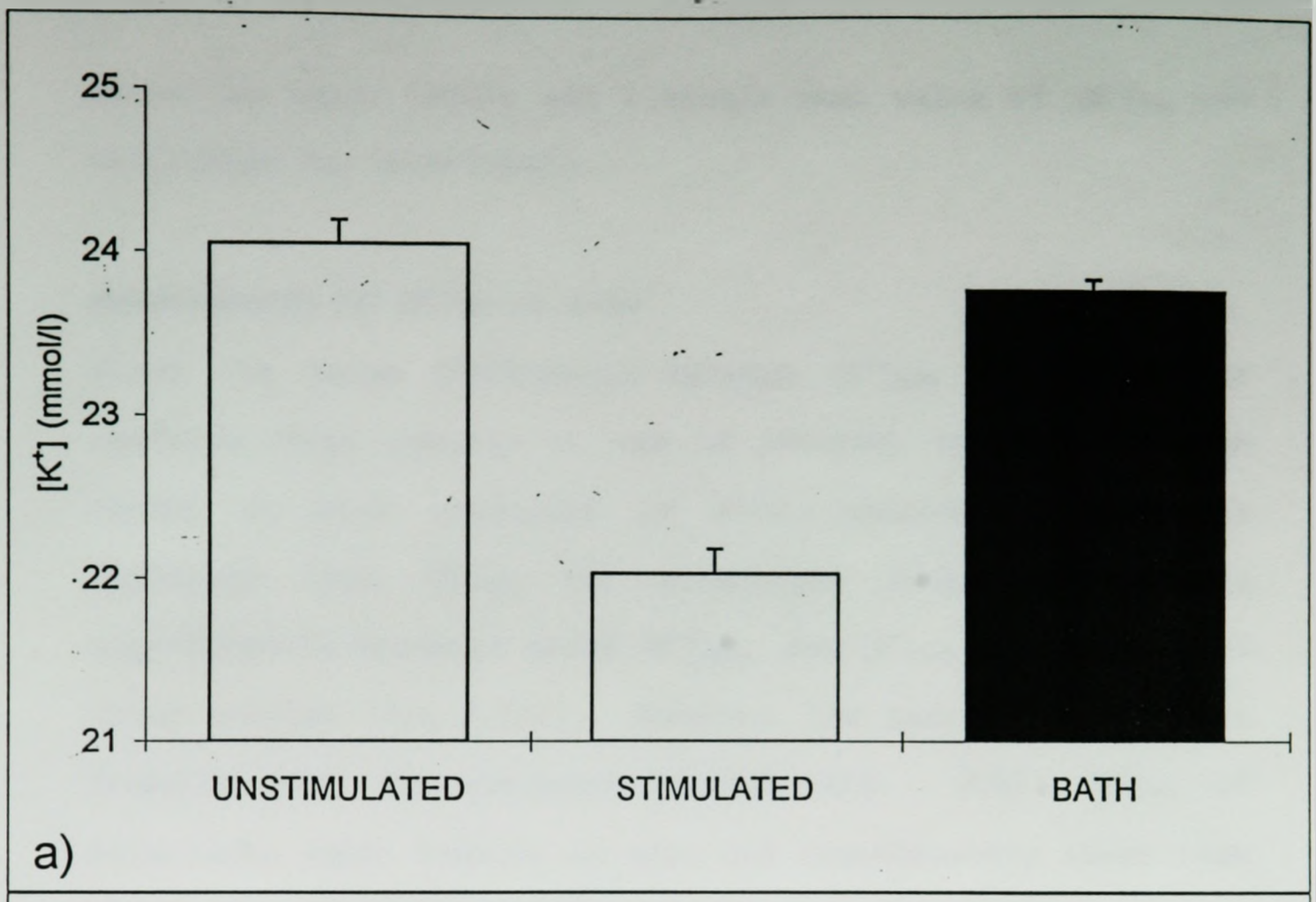
25
24
23
22
21
[K+] (mmol/l)
UNSTIMULATED
STIMULATED
BATH
a)

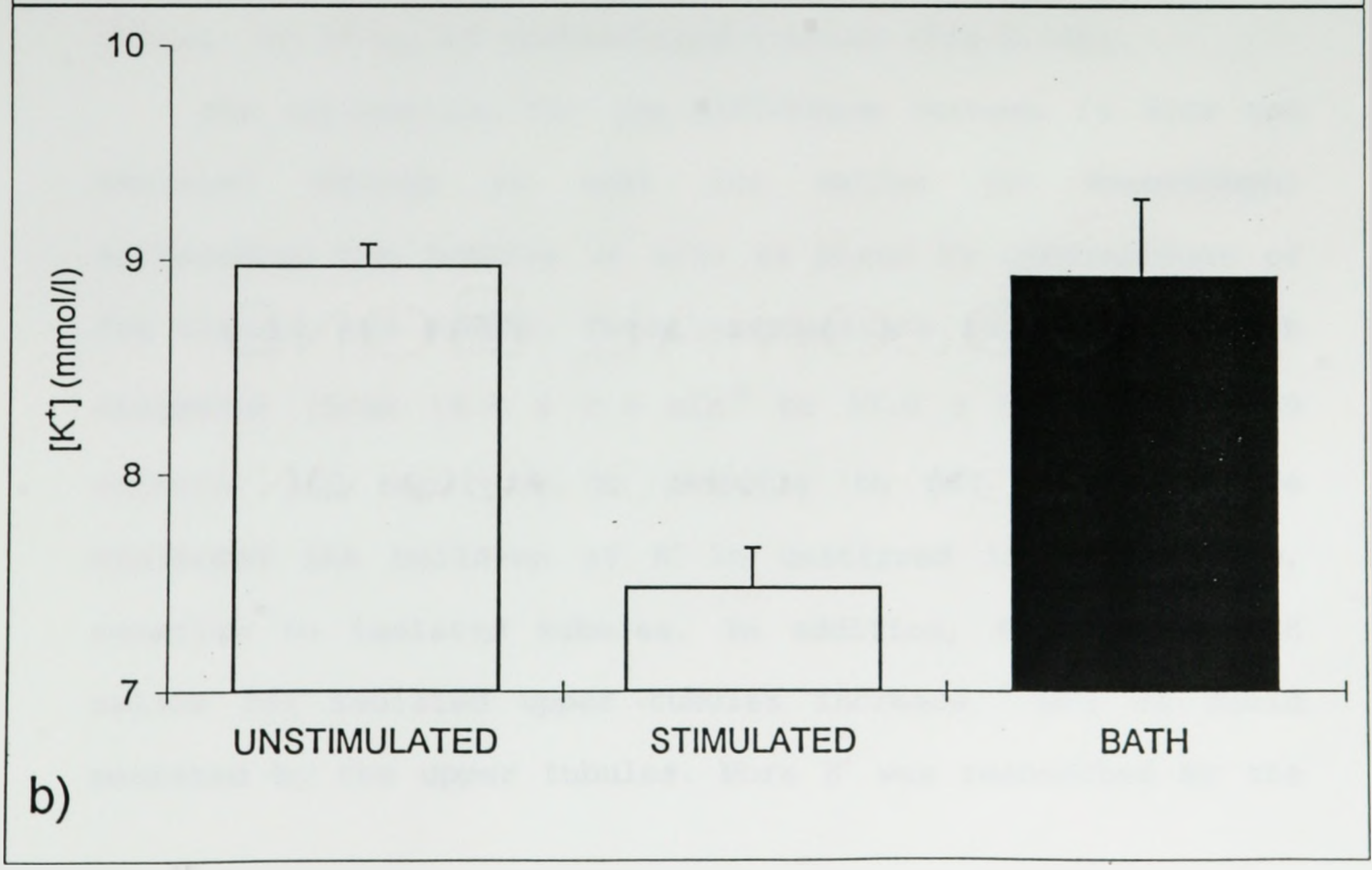
10
9
8
7
[K+] (mmol/l)
UNSTIMULATED
STIMULATED
BATH
b)

along the upper tubule and a single mean value of $[K^+]_{USL}$ was calculated for each tubule.

Measurements of $[K^+]_{USL}$ in situ

Given the large differences between $[K^+]_{BATH}$ and $[K^+]_{USL}$ for isolated lower tubules it was of interest to determine the extent of such gradients *in situ*. Measurements *in situ* indicated that $[K^+]_{USL}$ for stimulated lower tubules was significantly elevated above $[K^+]_{BATH}$ and $[K^+]_{USL}$ of unstimulated lower tubules (fig 2.10a). However, the increases were less dramatic than for isolated tubules (Fig. 2.5). $[K^+]_{USL}$ of stimulated upper tubules *in situ* was significantly lower than $[K^+]_{BATH}$ or $[K^+]_{USL}$ of unstimulated tubules (fig 2.10b).

One explanation for the difference between *in situ* and isolated tubules is that the saline (or haemolymph) surrounding the tubules *in situ* is mixed by contractions of the hindgut and midgut. These contractions increased in both frequency (from 15.8 ± 0.8 min^{-1} to 37.0 ± 0.9 min^{-1}, n =9 animals) and amplitude in response to 5HT, and may have minimised the build-up of K^+ in unstirred layers *in situ*, relative to isolated tubules. In addition, the use of 24K saline for isolated upper tubules increase $[K^+]$ of fluid secreted by the upper tubules. More K^+ was reabsorbed by the

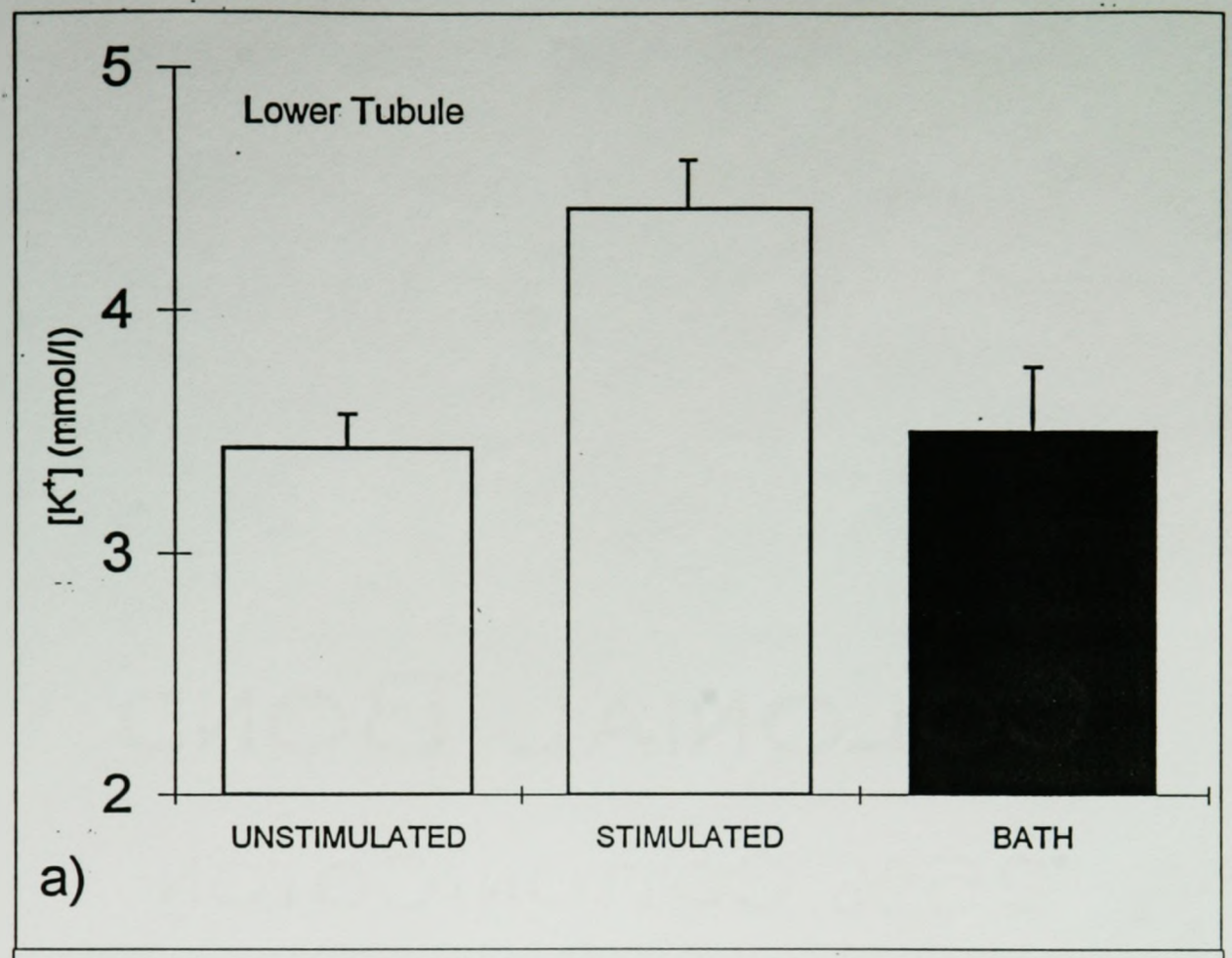
Lower Tubule
5
4
3
2
[K+] (mmol/l)
UNSTIMULATED
STIMULATED
BATH
a)

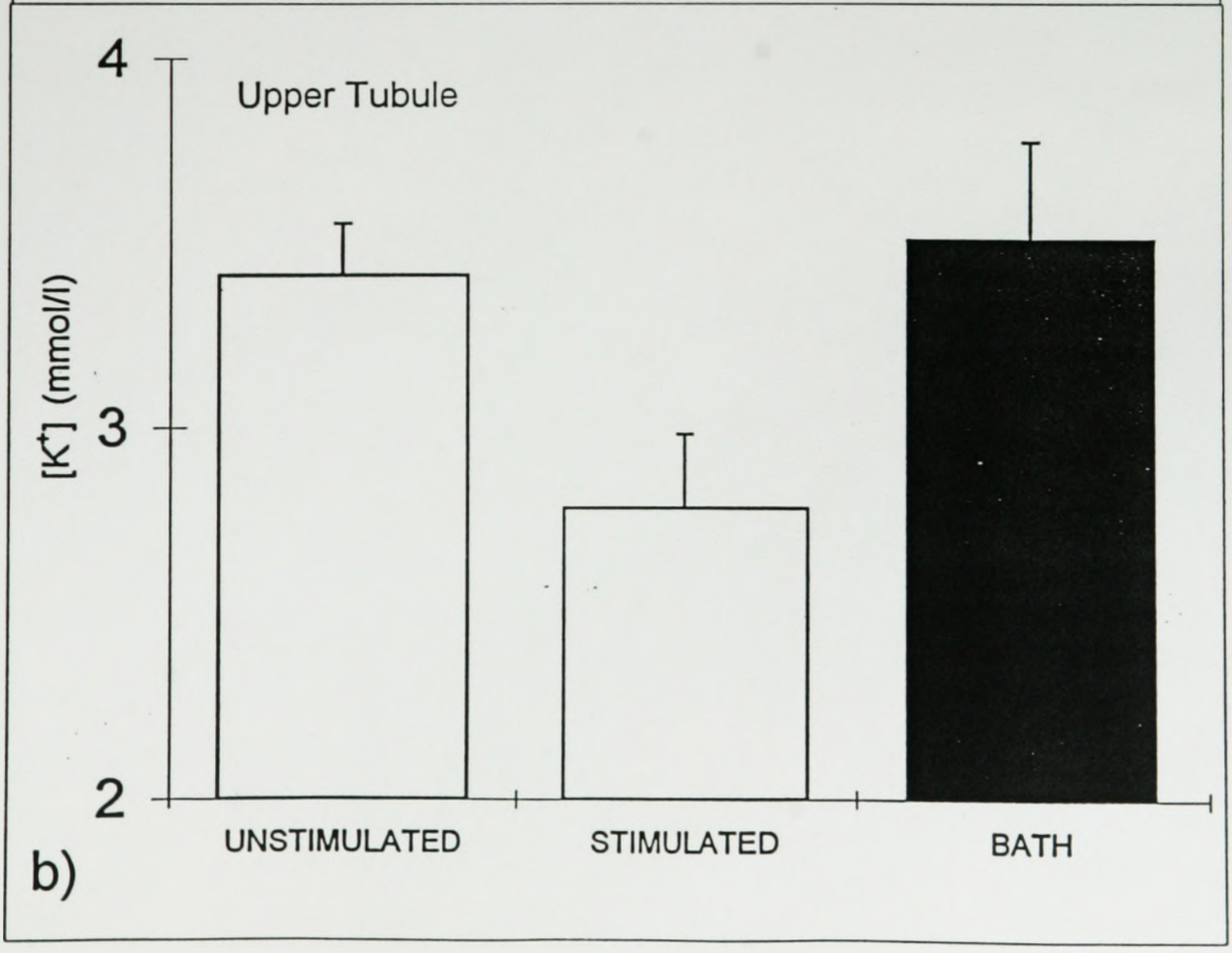
Upper Tubule
4
3
2
[K+] (mmol/l)
UNSTIMULATED
STIMULATED
BATH
b)

LMT, therefore, and the difference between $[K^+]_{USL}$ and $[K^+]_{Bath}$ increased.

USL acidification

pH was measured in the USL within 5 µm of the basolateral surface of upper or lower tubules. Measurements were taken at 10%, 25%, 50%, 75%, and 95% along the length of upper and lower tubules. Upper tubule measurements taken at these various points whether unstimulated or stimulated, showed no minimum pH (*i.e.* maximum $[H^+]$) at a particular position along its length, and data for each upper tubule were therefore pooled. The pH_{USL} of unstimulated upper tubules was slightly but significantly acidic to pH_{USL} in saline of reduced buffering capacity (fig 2.11a). In both salines, stimulation with 5HT resulted in significant acidification of pH_{USL} relative to the values measured for the same tubules prior to stimulation. The extent of acidification exceeded 0.3 pH units in saline with reduced buffering capacity (fig 2.11b).

Values of pH_{USL} for unstimulated lower tubules were not acidic relative to pH_{Bath} (Fig. 2.12). Stimulation of the lower tubule alone, or both upper and lower tubules,

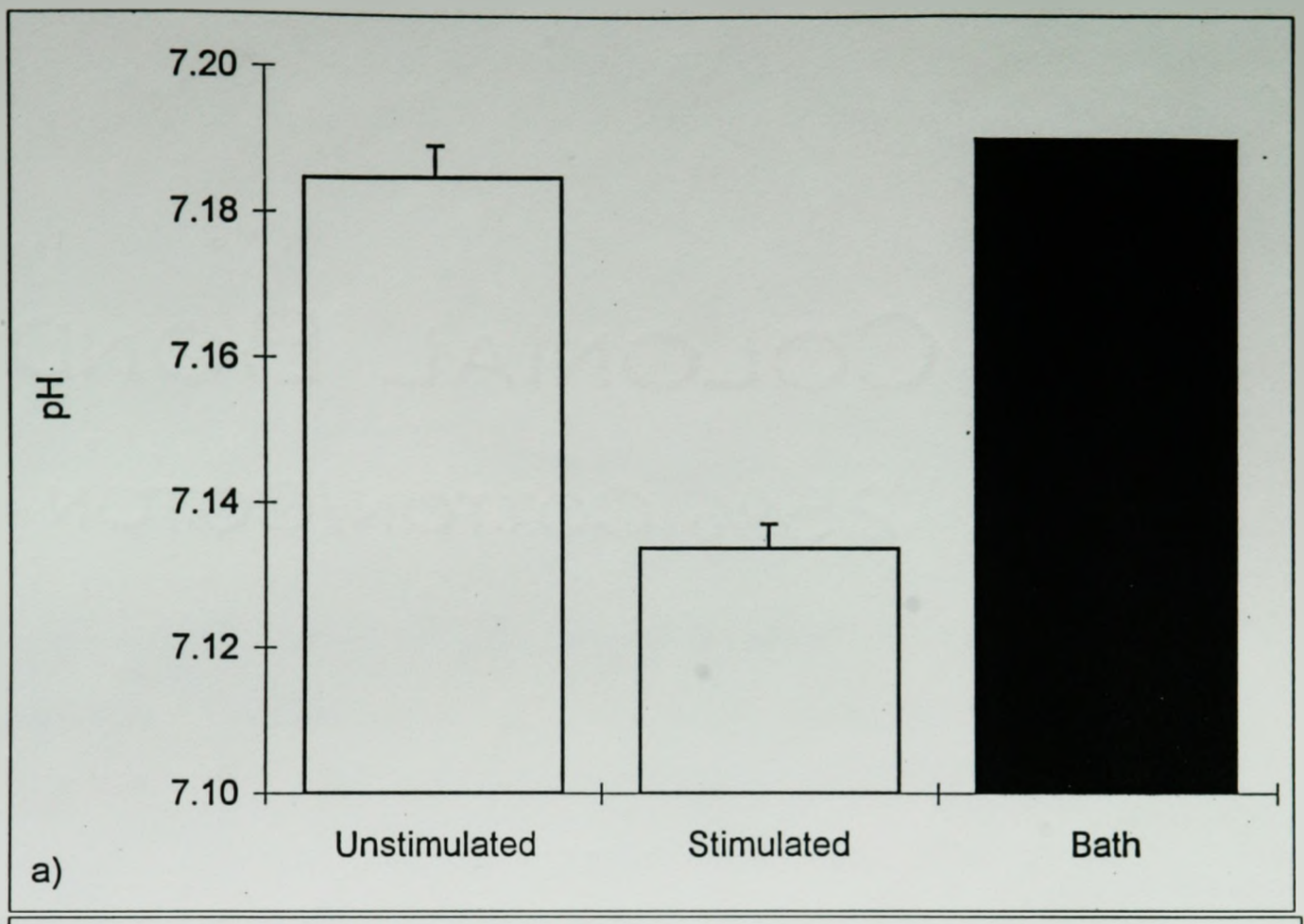
7.20
7.18
7.16
7.14
7.12
7.10
pH
Unstimulated
Stimulated
Bath
a)

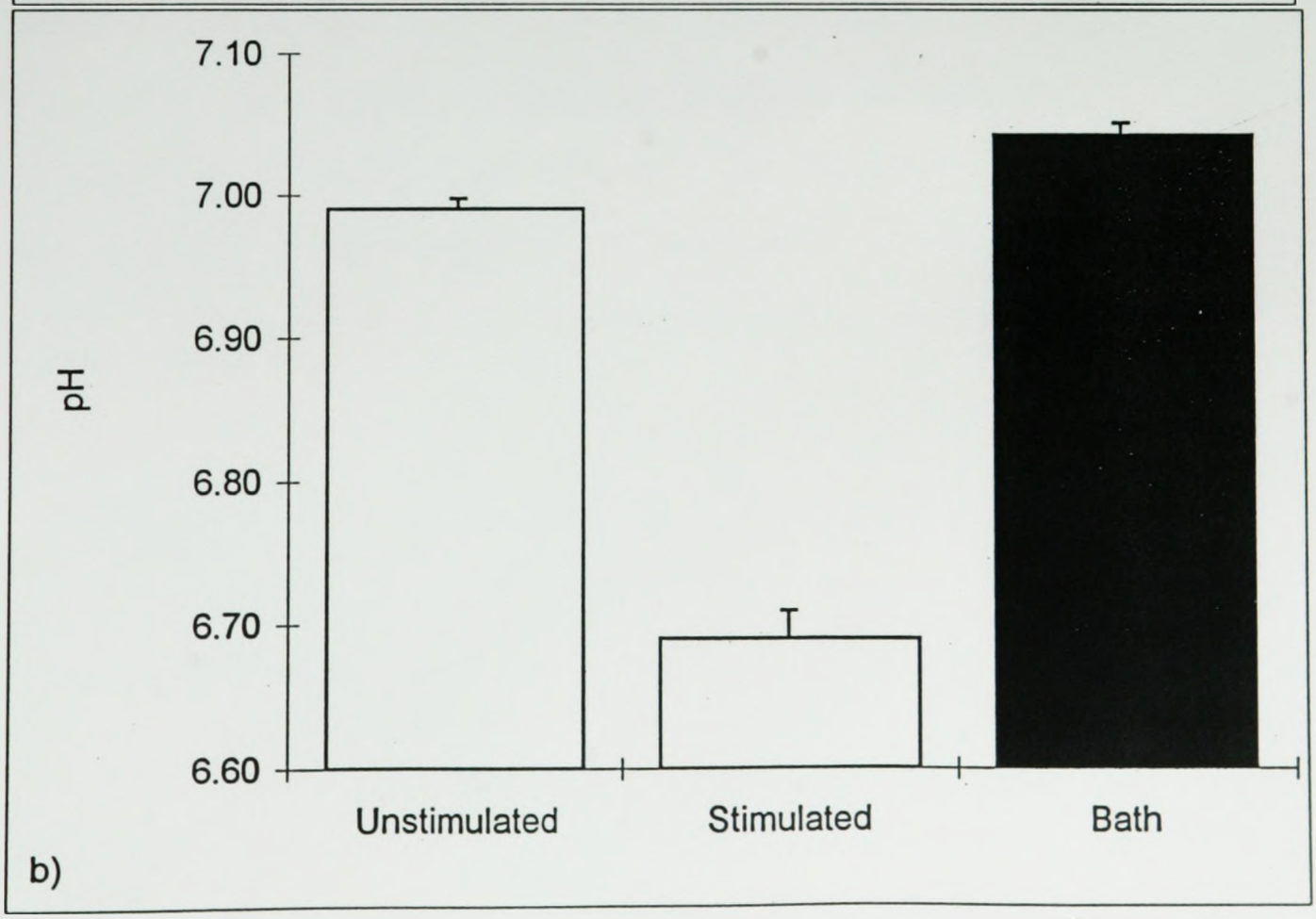
7.10
7.00
6.90
6.80
6.70
6.60
pH
Unstimulated
Stimulated
Bath
b)

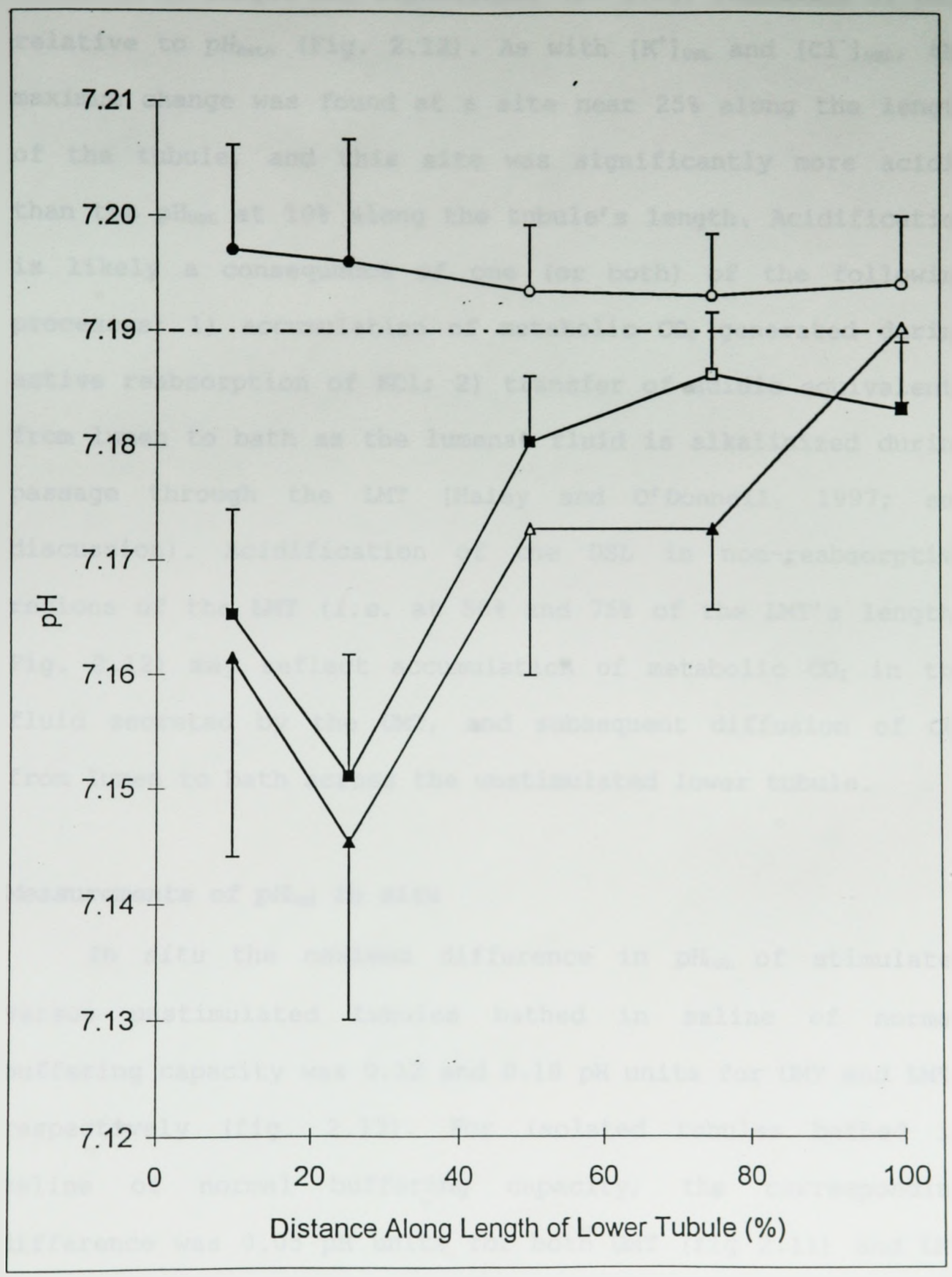
7.21
7.20
7.19
7.18
7.17
7.16
7.15
7.14
7.13
7.12
pH
0
20
40
60
80
100
Distance Along Length of Lower Tubule (%)

resulted in slight but significant ($P < 0.05$) reduction of pH_{USL} relative to pH_{Bath} (Fig. 2.12). As with $[K^+]_{USL}$ and $[Cl^-]_{USL}$, the maximum change was found at a site near 25% along the length of the tubule, and this site was significantly more acidic than the pH_{USL} at 10% along the tubule's length. Acidification is likely a consequence of one (or both) of the following processes: 1) accumulation of metabolic CO_2 generated during active reabsorption of KCl; 2) transfer of acidic equivalents from lumen to bath as the lumenal fluid is alkalinized during passage through the LMT (Haley and O'Donnell, 1997; see discussion). Acidification of the USL in non-reabsorptive regions of the LMT (*i.e.* at 50% and 75% of the LMT's length, Fig. 2.12) may reflect accumulation of metabolic CO_2 in the fluid secreted by the UMT, and subsequent diffusion of CO_2 from lumen to bath across the unstimulated lower tubule.

Measurements of pH_{USL} in situ

In situ the maximum difference in pH_{USL} of stimulated versus unstimulated tubules bathed in saline of normal buffering capacity was 0.12 and 0.18 pH units for UMT and LMT, respectively (fig. 2.13). For isolated tubules bathed in saline of normal buffering capacity, the corresponding difference was 0.05 pH units for both UMT (fig 2.11) and LMT

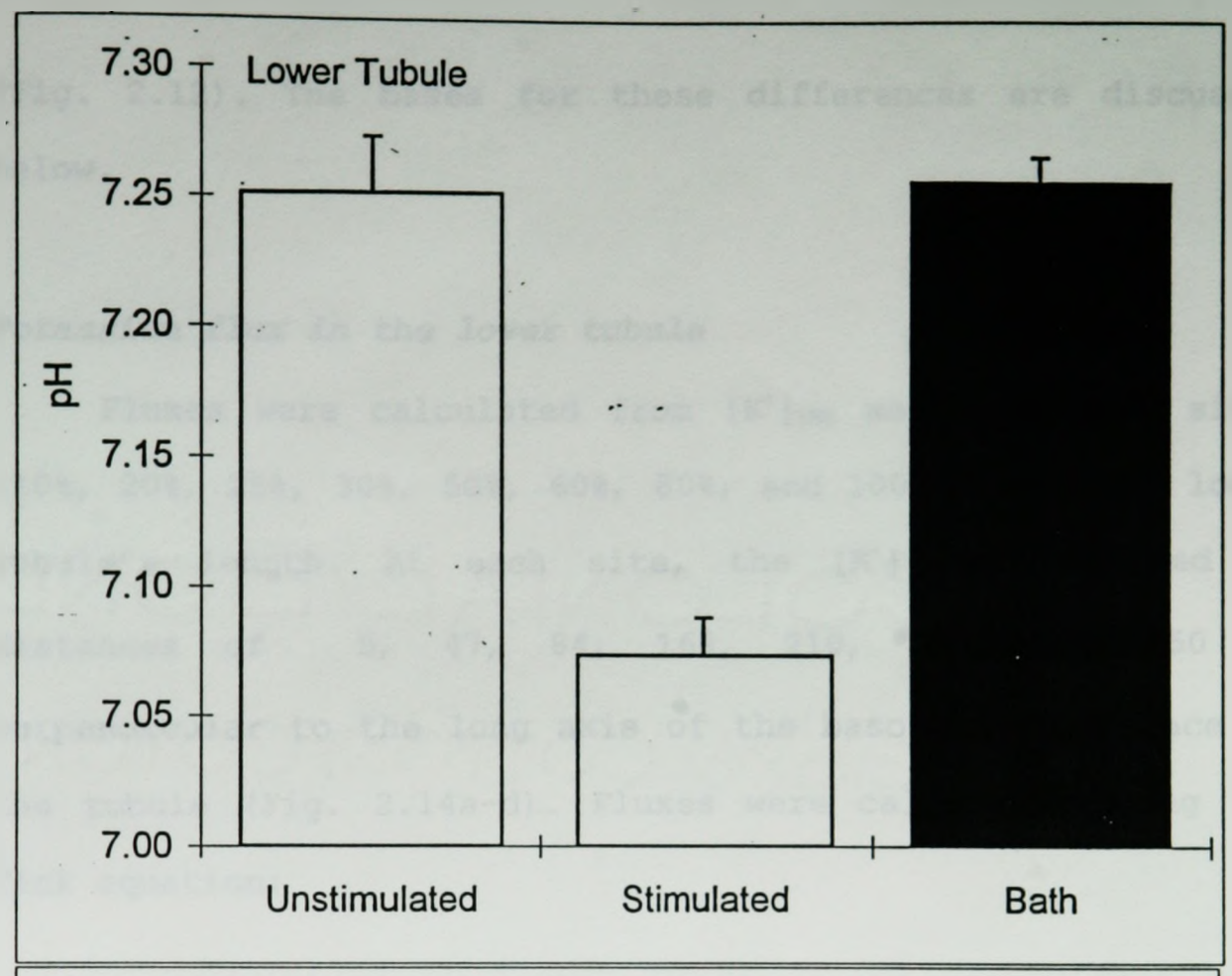
Lower Tubule
7.30
7.25
7.20
7.15
7.10
7.05
7.00
pH
Unstimulated
Stimulated
Bath

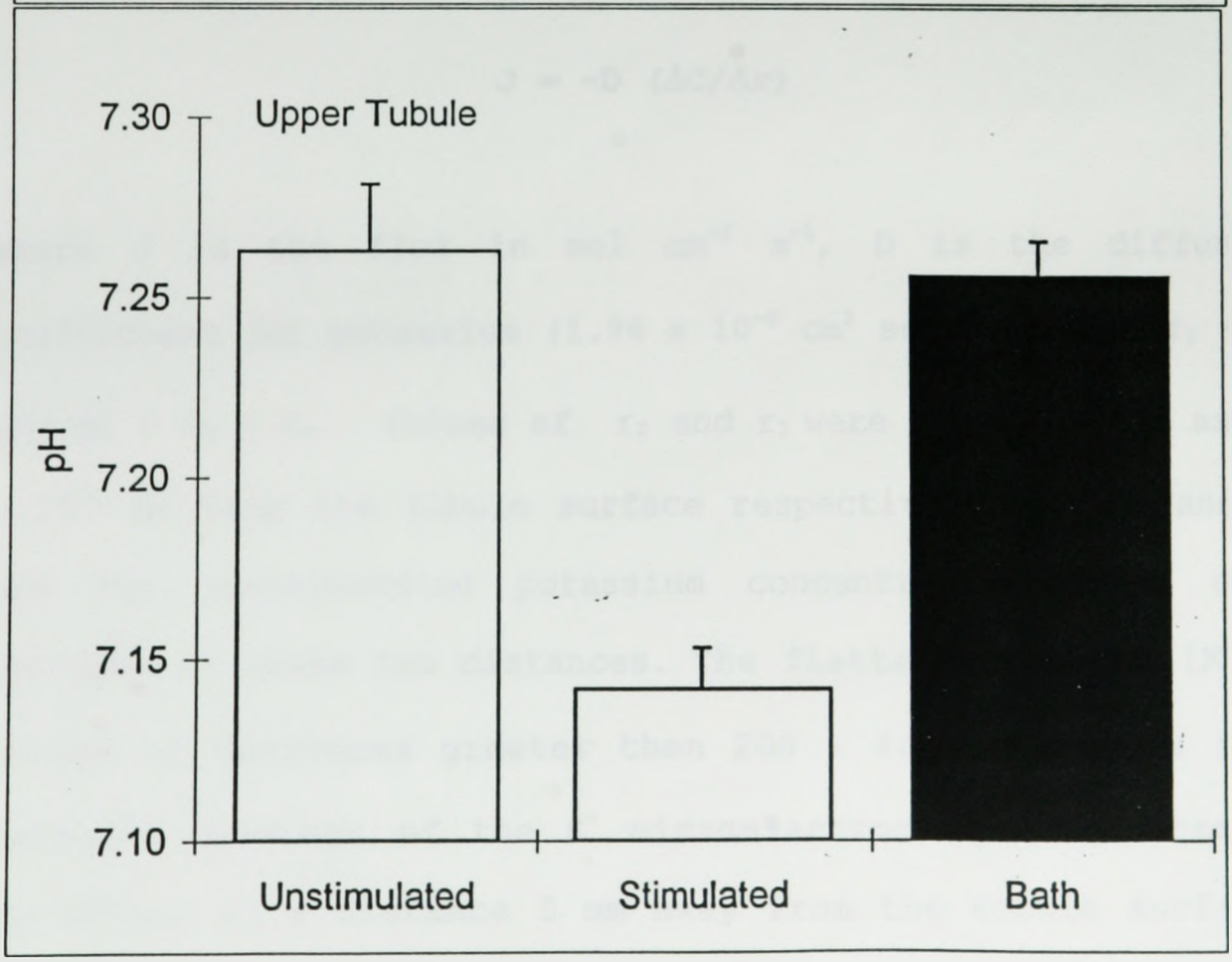
Upper Tubule
7.30
7.25
7.20
7.15
7.10
pH
Unstimulated
Stimulated
Bath

(Fig. 2.12). The bases for these differences are discussed below.

Potassium flux in the lower tubule

Fluxes were calculated from $[K^+]_{USL}$ measured at 8 sites (10%, 20%, 25%, 30%, 50%, 60%, 80%, and 100%) along the lower tubule's length. At each site, the $[K^+]$ was measured at distances of 5, 47, 84, 168, 210, 315, and 550 μm perpendicular to the long axis of the basolateral surface of the tubule (Fig. 2.14a-d). Fluxes were calculated using the Fick equation:

$$J = -D\ (\Delta C/\Delta r)$$

where J is the flux in mol cm^{-2} s^{-1}, D is the diffusion coefficient for potassium (1.96×10^{-5} cm^2 sec^{-1}), $\Delta r = r_2 - r_1$ and $\Delta C = C_2 - C_1$. Values of r_2 and r_1 were 4.7×10^{-3} cm and 5×10^{-4} cm from the tubule surface respectively, and C_2 and C_1 are the corresponding potassium concentrations (mol cm^{-3}) measured at these two distances. The flattening of the $[K^+]_{USL}$ curves at distances greater than 200 - 400 μm results from periodic movement of the K^+ microelectrode for measurement of $[K^+]_{BATH}$ at a distance 5 mm away from the tubule surface.

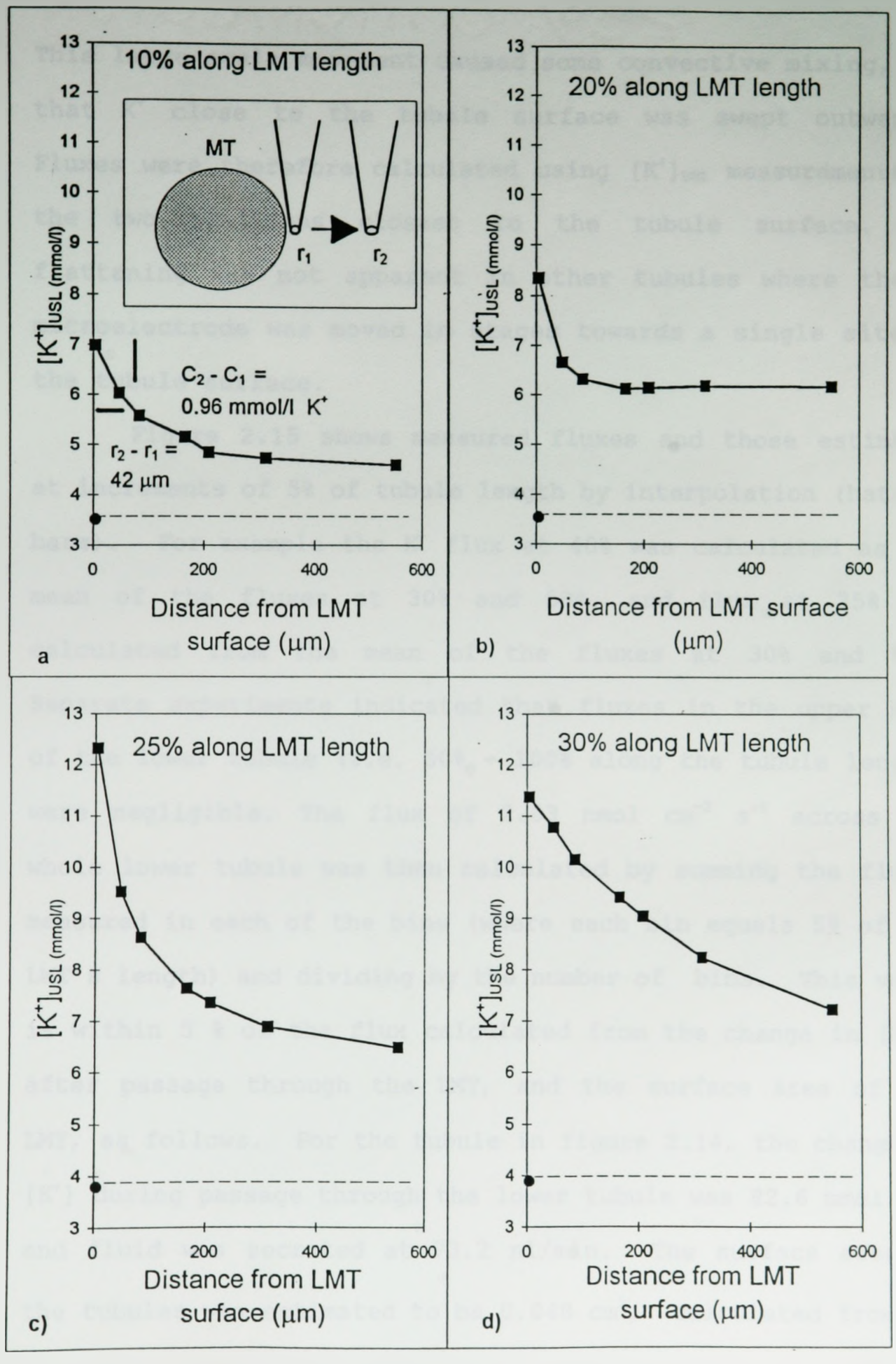
10% along LMT length
MT
r1
r2
C2 - C1 =
0.96 mmol/l K+
r2 - r1 =
42 µm
[K+]USL (mmol/l)
Distance from LMT surface (µm)
a
20% along LMT length
[K+]USL (mmol/l)
Distance from LMT surface (µm)
b)
25% along LMT length
[K+]USL (mmol/l)
Distance from LMT surface (µm)
c)
30% along LMT length
[K+]USL (mmol/l)
Distance from LMT surface (µm)
d)

This large-scale movement caused some convective mixing, so that K^+ close to the tubule surface was swept outwards. Fluxes were therefore calculated using $[K^+]_{USL}$ measurements at the two positions closest to the tubule surface. The flattening was not apparent in other tubules where the K^+ microelectrode was moved in stages towards a single site on the tubule surface.

Figure 2.15 shows measured fluxes and those estimated at increments of 5% of tubule length by interpolation (hatched bars). For example the K^+ flux at 40% was calculated as the mean of the fluxes at 30% and 50%, and flux at 35% was calculated from the mean of the fluxes at 30% and 40%. Separate experiments indicated that fluxes in the upper half of the lower tubule (i.e. 50% - 100% along the tubule length) were negligible. The flux of 2.03 nmol cm^{-2} s^{-1} across the whole lower tubule was then calculated by summing the fluxes measured in each of the bins (where each bin equals 5% of the LMT's length) and dividing by the number of bins. This value is within 5 % of the flux calculated from the change in $[K^+]_{SF}$ after passage through the LMT, and the surface area of the LMT, as follows. For the tubule in figure 2.14, the change in $[K^+]$ during passage through the lower tubule was 82.6 mmol l^{-1}, and fluid was secreted at 73.2 nl/min. The surface area of the tubules was estimated to be 0.048 cm^2, calculated from (Π

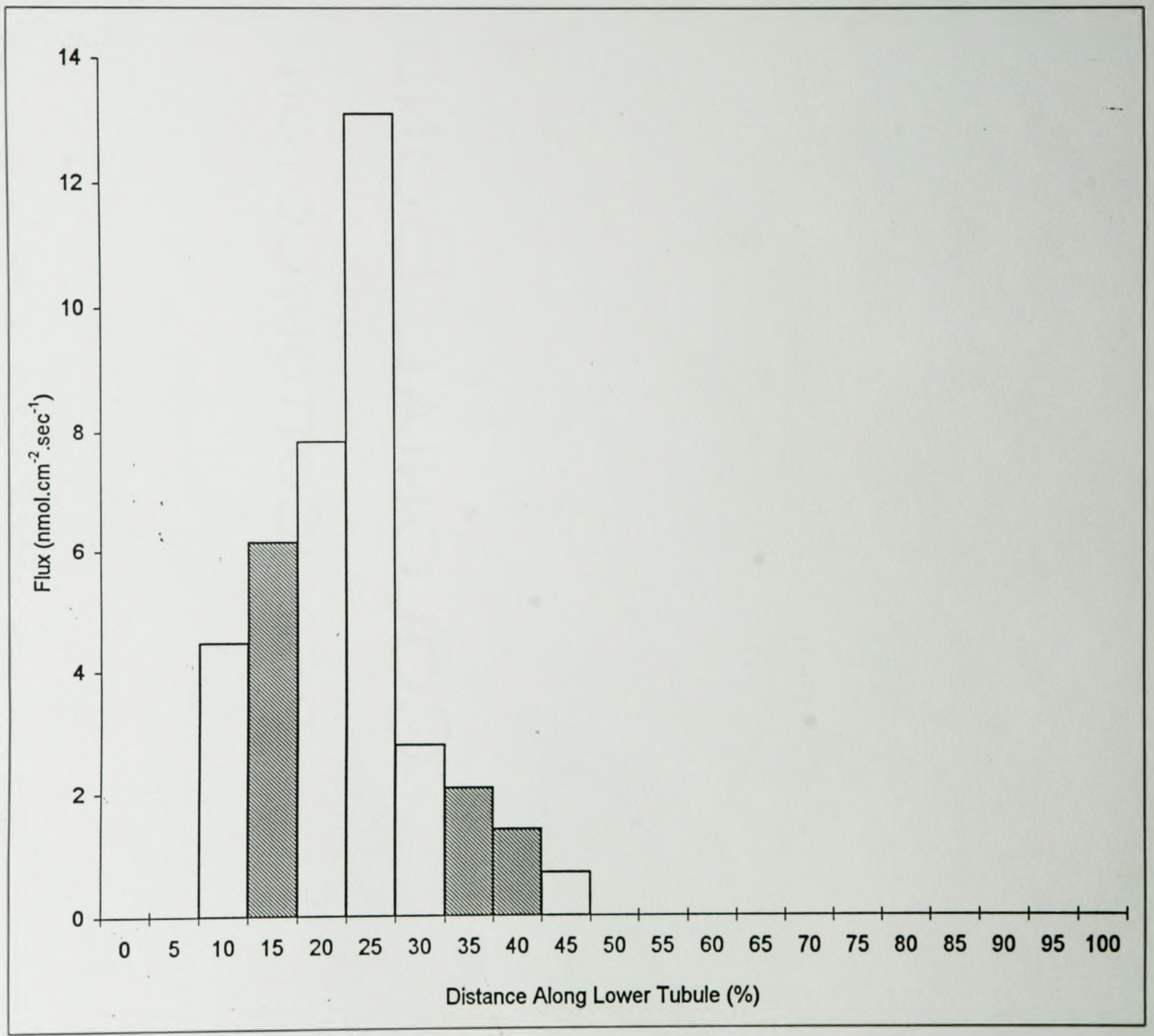
14
12
10
8
6
4
2
0
Flux (nmol.cm-2.sec-1)
0 5 10 15 20 25 30 35 40 45 50 55 60 65 70 75 80 85 90 95 100
Distance Along Lower Tubule (%)

$\cdot d \cdot L$), where d is the tubule diameter (90 μm), and L its length (17 mm). The K^+ secretion rate of 0.101 nmol sec^{-1} [= (73.2 x 10^{-9} l/min)(82.6 x 10^{-3} mols/l)(1/60)] then corresponds to an area specific flux of 2.10 nmol cm^{-2} sec^{-1} [= (0.101 nmol$\cdot sec^{-1}$/0.048 cm^2)].

Effects of furosemide and bumetanide on $[K^+]_{USL}$ in upper tubules.

Measurements of changes in $[K^+]_{USL}$ of the upper tubule could also be used as an assay for drugs known to inhibit MT fluid secretion, and the changes in $[K^+]_{USL}$ could be correlated with a decrease in K^+ flux. For example, the presence of a basolateral $Na^+/K^+/2Cl^-$ co-transporter in the Malpighian tubules of *Rhodnius* (O'Donnell and Maddrell, 1894), *Aedes* (Hegarty *et al*, 1991), and *Formica* (Leyssens *et al*, 1994) has been proposed on the basis of inhibition of fluid secretion by 10^{-5} - 10^{-4} mol l^{-1} bumetanide, or 10^{-4} mol l^{-1} furosemide. Fluid secretion by the upper Malpighian tubules of *Rhodnius* is reduced 79% - 80% by 10^{-4} mol l^{-1} furosemide, or 10^{-5} mol l^{-1} bumetanide (O'Donnell and Maddrell, 1984).

Figure 2.16 shows that bumetanide (4 x 10^{-5} mol l^{-1}) significantly ($p<0.05$) increased $[K^+]_{USL}$, consistent with less depletion of potassium from the USL (*i.e.* a decrease in K^+

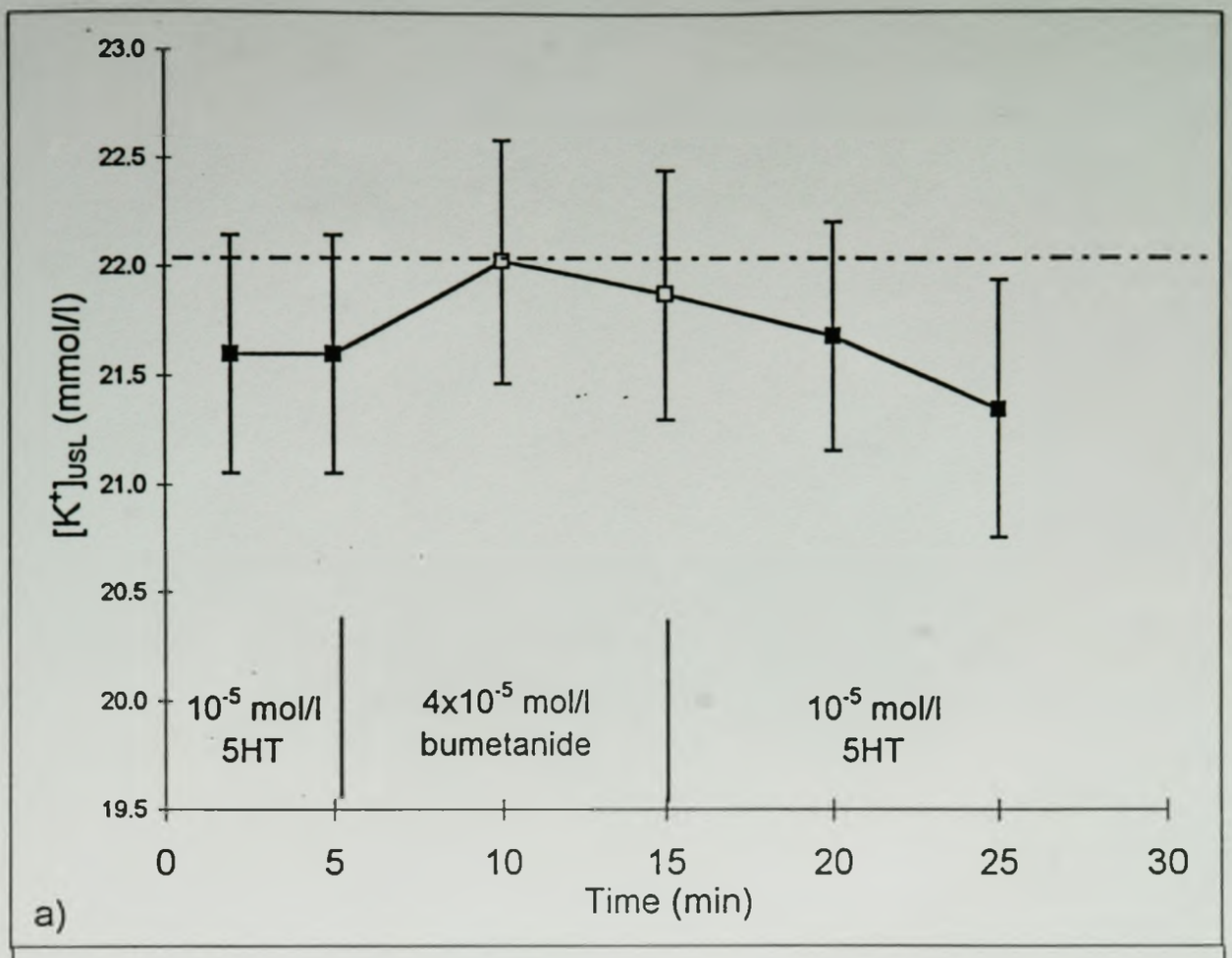
23.0
22.5
22.0
21.5
21.0
20.5
20.0
19.5
$[K^+]_{USL}$ (mmol/l)
10^{-5} mol/l 5HT
$4x10^{-5}$ mol/l bumetanide
10^{-5} mol/l 5HT
0
5
10
15
20
25
30
Time (min)
a)

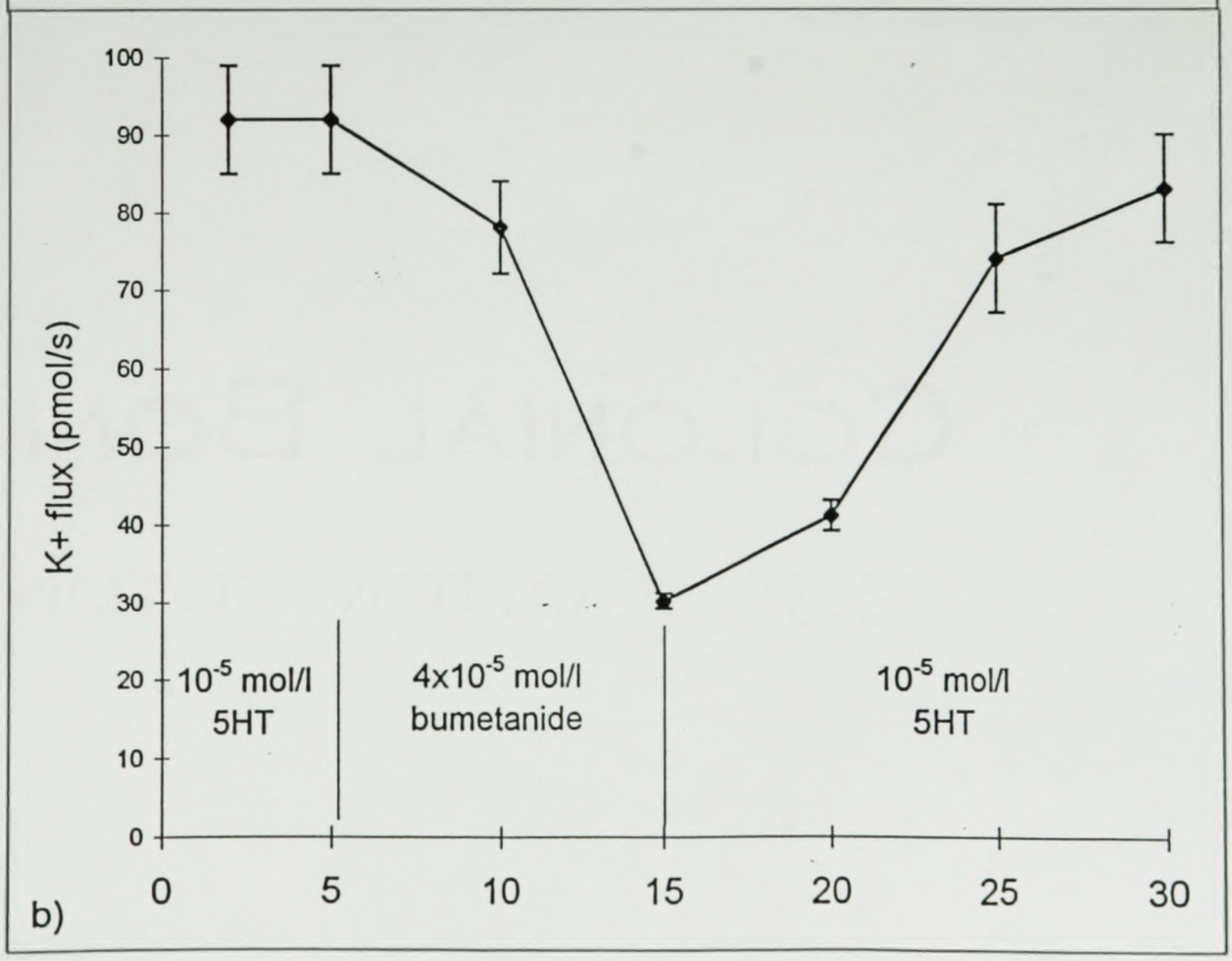
100
90
80
70
60
50
40
30
20
10
0
K+ flux (pmol/s)
10^{-5} mol/l 5HT
$4x10^{-5}$ mol/l bumetanide
10^{-5} mol/l 5HT
0
5
10
15
20
25
30
b)

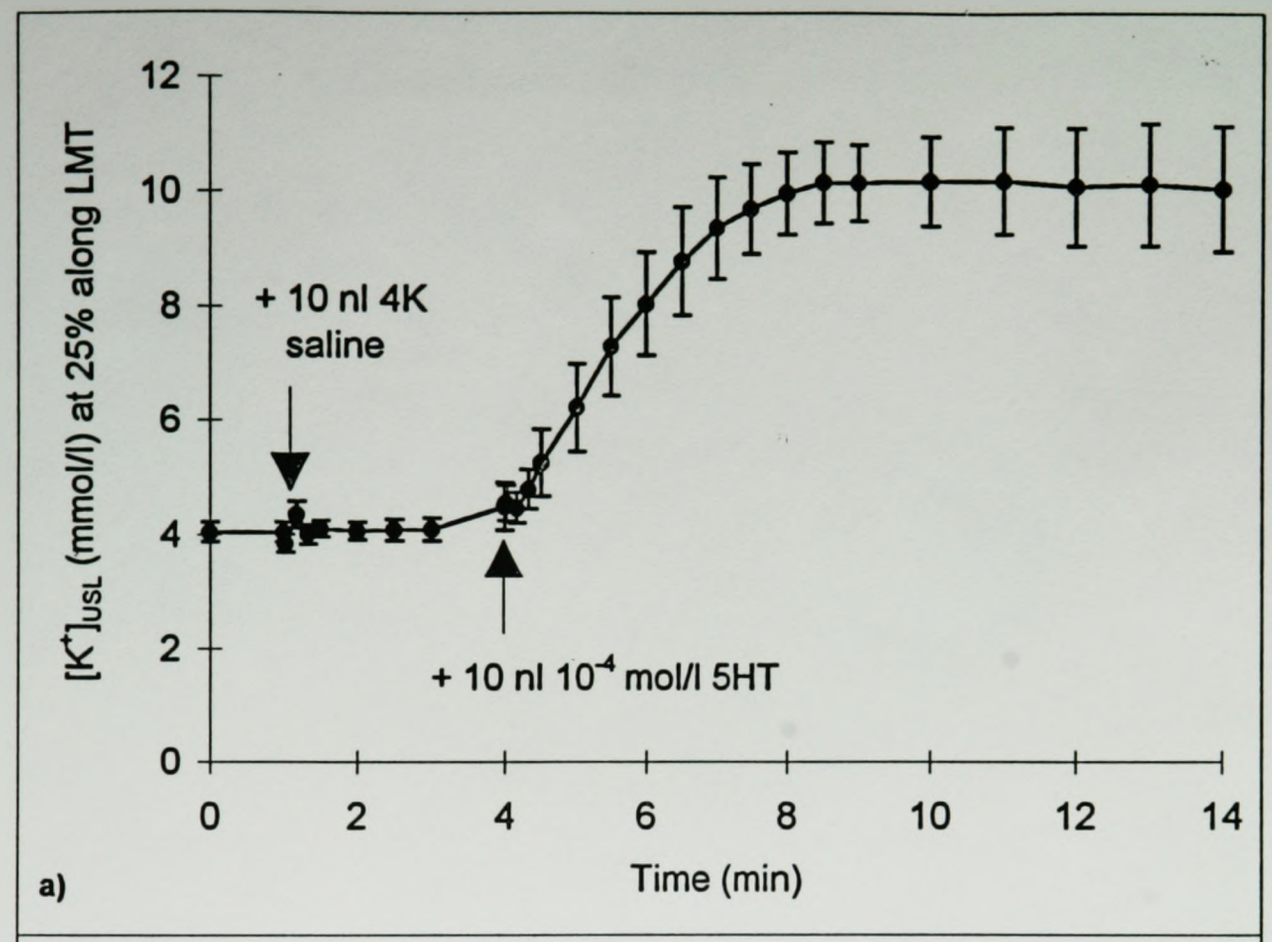
12
10
8
6
4
2
0
[K+]USL (mmol/l) at 25% along LMT
+ 10 nl 4K saline
+ 10 nl 10-4 mol/l 5HT
0
2
4
6
8
10
12
14
Time (min)
a)

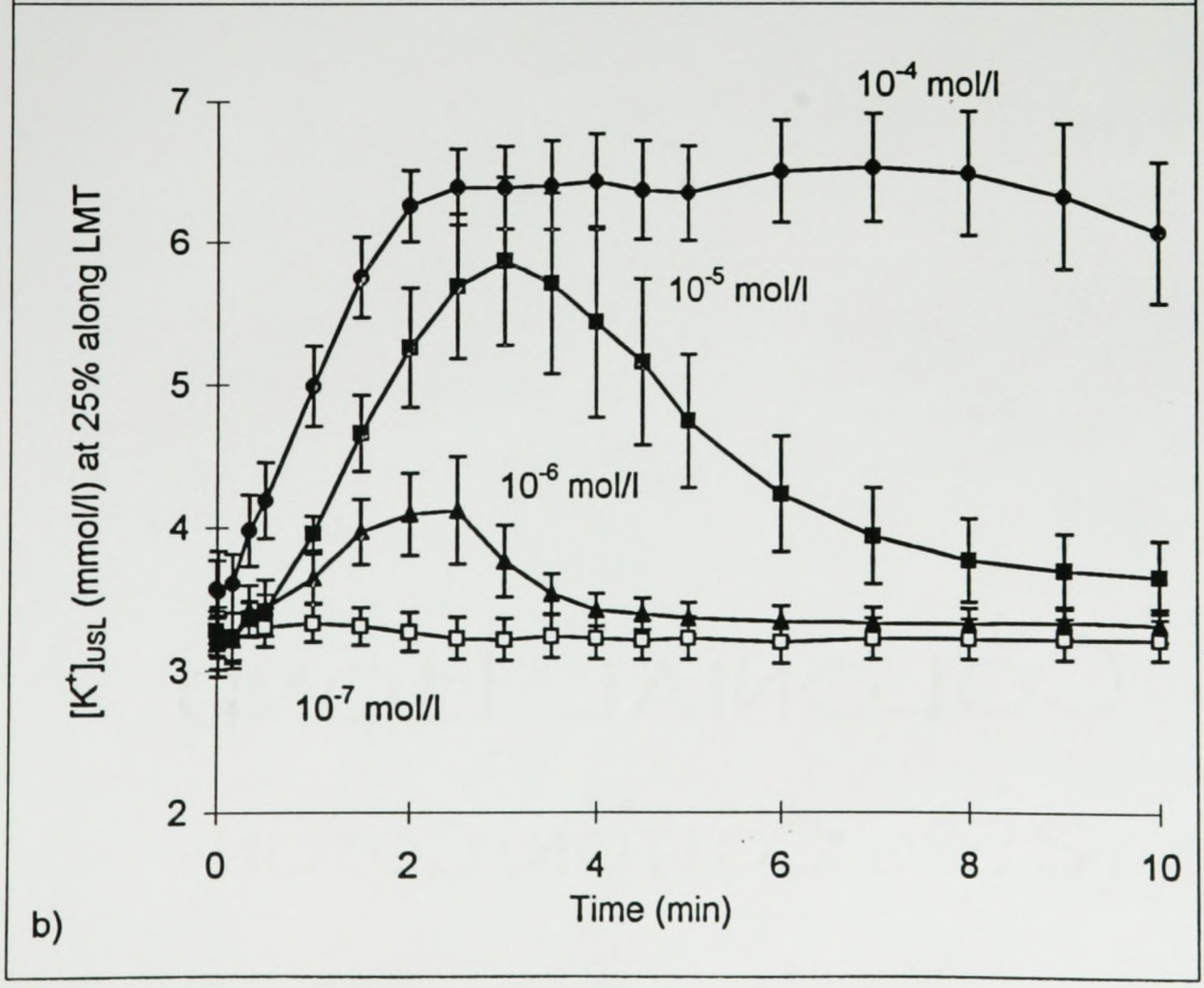
7
6
5
4
3
2
[K+]USL (mmol/l) at 25% along LMT
10-4 mol/l
10-5 mol/l
10-6 mol/l
10-7 mol/l
0
2
4
6
8
10
Time (min)
b)

$[K^+]_{USL}$ increased over a period of 10 minutes following localized application of 5HT (Fig. 2.17a). The mean time taken to produce 50% of the maximal stimulation was 1.5 min (n=5). A 10 - 15 nl pulse of control saline at the same site, in contrast showed no sustained increase in $[K^+]_{USL}$ over a period of 3 minutes (Fig. 2.17a). The maximum $[K^+]_{USL}$, and the duration of the rise in $[K^+]_{USL}$ increased with higher doses of 5HT (Fig. 2.17b). $[K^+]_{USL}$ subsequently declined as 5HT diffused into the 200 µl droplet of bathing saline, reducing the concentration of 5HT to less than 5 nmol l^{-1}, below the threshold for stimulation of KCl reabsorption (Maddrell *et al.*, 1993b).

Extracellular potassium near the basolateral membrane of single upper tubule cells.

The results demonstrate that information about ion transport by isolated or *in situ* tubules can be inferred from analysis of USL ion concentrations measured with ISMEs. Importantly, we have found that it is feasible to measure the effects of ion transport by a single cell on USL ion concentrations. These measurements exploited the finding that near the junction of the upper and lower Malpighian tubule, one or more UMT cells may be isolated from the rest of the UMT and surrounded by LMT cells (Fig. 2.18, inset). As noted

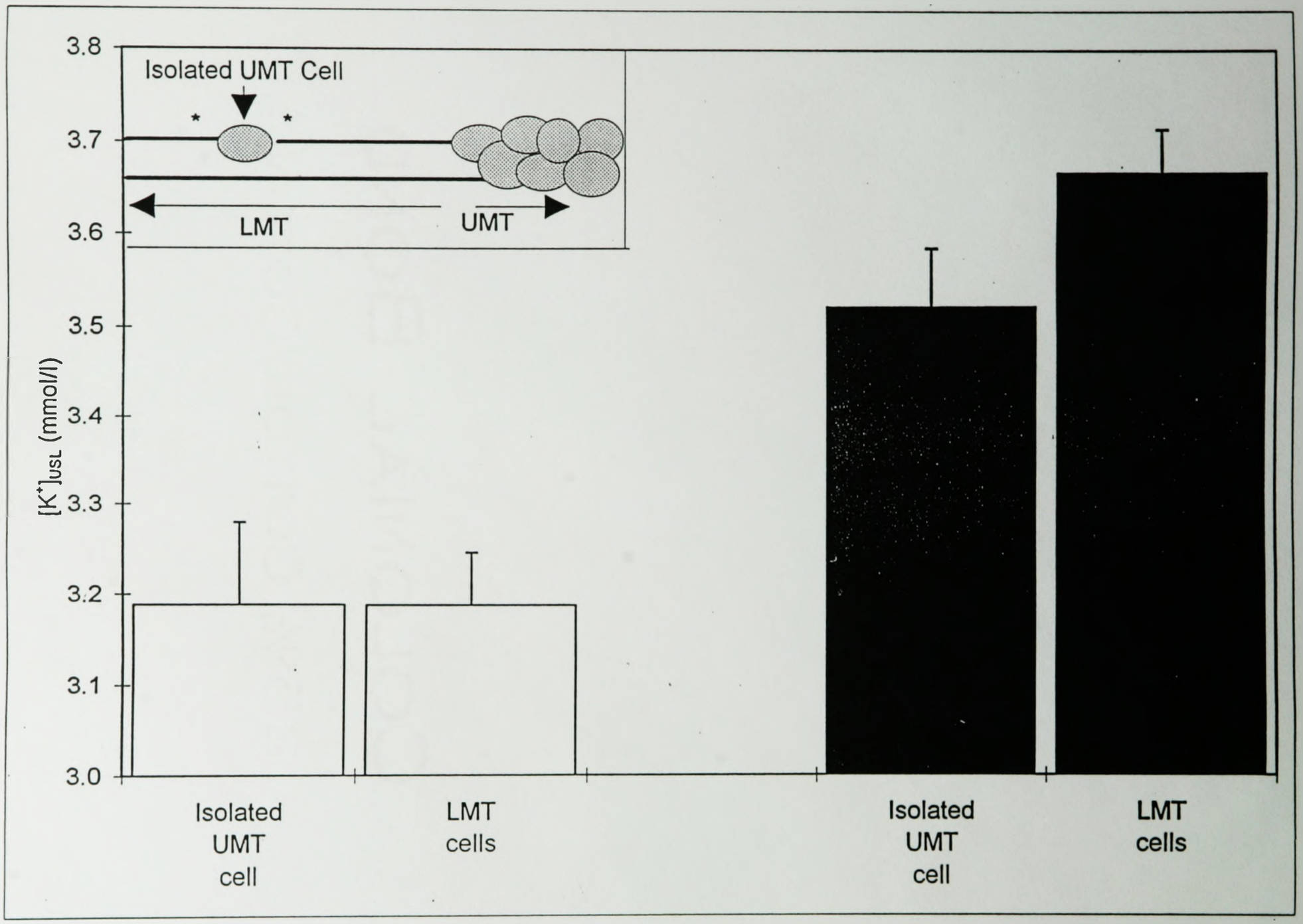
Isolated UMT Cell
LMT
UMT
3.8
3.7
3.6
3.5
3.4
3.3
3.2
3.1
3.0
[K+]USL (mmol/l)
Isolated UMT cell
LMT cells
Isolated UMT cell
LMT cells

DISCUSSION

This study demonstrates that both secretion and reabsorption of ions by *Rhodnius* Malpighian tubules can be assessed both qualitatively and quantitatively by ISME measurement of ion concentrations in the USL associated with the basolateral cell surface. This technique can be used to measure anions or cations, provided that there is a appropriately selective ionophore. Also, basolateral measurements of ion transport capacity can be determined before and after putative stimulants or inhibitors are added to the bathing saline droplets. Very small differences in electrical potential (*ca.* 0.1 - 0.2 mV) can be consistently resolved with a temporal resolution of about 2 - 10 s. The spatial resolution of this technique is comparable to that of an individual cell (100 μm). Importantly, the techniques described in this paper can be used for Malpighian tubules *in situ*, as well as *in vitro*.

This technique revealed several new features of ion transport in a well characterized transporting epithelium, the Malpighian tubule of *Rhodnius*. The effects of 5HT and KCN indicate that elevation of $[K^+]$ and $[Cl^-]$ within the USL

is a direct consequence of 5HT stimulation of metabolically dependent KCl reabsorption by the lower tubule. The decline in $[K^+]_{USL}$ as the electrode is moved from 30% to 50% of the LMT's length is consistent with previous studies which demonstrate that KCl reabsorption is restricted to the lower one third of the lower tubule (Maddrell, 1978). Moreover, our data reveal a new finding: K^+ reabsorption within the lower 1/3 of the tubule is not constant. K^+ flux between 20% - 30% of the LMT's length is higher than flux calculated from $[K^+]_{USL}$ measurements closer to the ampulla. The decline in $[K^+]_{USL}$ closer to the ampulla may reflect a decline in $[K^+]$ as fluid in the tubule lumen passes through the lower 1/3 of the LMT. K^+ reabsorption becomes progressively more difficult and both $[K^+]_{USL}$ and K^+ flux decline. Double-barreled ISME measurements confirm that both K^+ and Cl^- are reabsorbed across the same regions of the lower tubule.

The $[K^+]$ in the USL of the lower tubule may be more than 5-fold greater than that in the bathing saline when $[K^+]_{BATH}$ is in the range 2 - 6 mmol l^{-1}, bracketing the normal haemolymph $[K^+]$ of 3.6 mmol l^{-1}. These findings are of relevance for development of models of ion transport by rapidly transporting epithelia such as Malpighian tubules. Such models often involve calculations of electrochemical gradients for ion movements across epithelia, and it is

usually assumed that the concentration of an ion in contact with the apical or basolateral surface is equal to the concentration in the bulk solution at a distance from the surface. Our results indicate that this assumption would lead to errors in calculated electrochemical gradients; estimates of electrochemical gradients should be made, therefore, using tubules which are superfused so as to minimize USL effects.

Measurements of $[K^+]_{USL}$ surrounding the basolateral membrane of the upper tubule confirm findings from previous studies regarding the homogeneous secretory capacity of the UMT along its' length (Maddrell, 1969). Experiments with bumetanide and furosemide indicate that effects of these drugs can be detected not just through changes in fluid secretion rates (O'Donnell and Maddrell, 1984), and K^+ flux (this thesis) but also through the decline in the potassium concentration gradient between the USL and the bathing saline.

Acidification of the USL of upper and lower tubules presumably reflects the transfer of acid-base equivalents into or out of the USL, and also accumulation of metabolic CO_2 and its subsequent hydration to form bicarbonate and H^+. The increase in USL acidification *in situ* may be related to higher rates of ion transport of *in situ* relative to isolated

tubules (Maddrell, 1991). Experiments with microelectrodes which measure pH and P_{CO2} simultaneously (Bomsztyk and Calalb, 1986) will be of use in determining the contributions of various processes to USL acidification. During KCl reabsorption the LMT alkalinizes the fluid produced by the UMT by 1.2 pH units, and the secreted fluid is 1.4 pH units alkaline to the bath after passage through the LMT (Haley and O'Donnell, 1997). Acidification of the basolateral USL may be a consequence, in part, therefore of lumenal alkalinization; if base is transported into the lumen, then maintenance of cytoplasmic pH will require an equivalent transfer of acidic equivalents into the bathing saline or haemolymph. Acidification of the USL in unstimulated upper tubules may reflect metabolism associated with secretion of KCl at slow rates, and with homeostatic and excretory processes. The UMT secretes fluid of near neutral pH and this is unaffected when pH_{BATH} is varied between 6.9 and 8.1 (Maddrell and O'Donnell, 1992). When pH_{BATH} is 7, therefore, there does not appear to be a requirement for transfer of acid-base equivalents from lumen to bath. Reductions in upper tubule pH_{USL} relative to pH_{BATH} are more likely, therefore, to reflect diffusion of CO_2 into the USL or acid-base exchange across the basolateral cell membrane.

Conversion of CO_2 to H^+ and HCO_3^- may introduce a small error into our measurements of $[Cl^-]_{USL}$, because the Cl^--selective liquid ion exchanger microelectrodes used here are only 20 times more sensitive to Cl^- than to HCO_3^- (Walker, 1971). The electrode may therefore overestimate the extent of Cl^- accumulation in the USL if HCO_3^- concentrations rise dramatically above those of the bath (10.2 mmol l^{-1}). Measurements with solid-state Cl^--selective microelectrodes, which are insensitive to HCO_3^-(*e.g.* Wright and O'Donnell, 1992) could resolve the extent of this error.

Previous studies have shown that bathing saline $[K^+]$ above 30 mmol l^{-1} inhibits KCl reabsorption (Maddrell and Phillips, 1977), consistent with blockade of passive efflux from cell to bath through basolateral K^+ channels (Haley and O'Donnell, 1997). Our data indicate that the effective concentration of K^+ at the basolateral surface of the tubule will in fact, be much higher than this value because of accumulation of K^+ in the USL. Our *in situ* measurements suggest that the convective mixing of the haemolymph by 5HT-stimulated contractions of the midgut and hindgut minimizes the build up of K^+ within the USL. This decrease in the boundary layer concentrations of $[K^+]$ *in situ* was detected in both upper and lower tubules. These findings raise the possibility that in intact animals, the contractions of the

hindgut are stimulated by the hormones released at diuresis, and that this increase in contraction frequency serves to minimize the establishment of a large differences in $[K^+]$ between the bath and the USL. The build-up of Cl- in the USL will be much less inhibitory since the levels of Cl^- in the bathing saline are high (148 mmol l^{-1} in 4K saline), and the proportionate change in $[Cl^-]_{USL}$ relative to $[Cl^-]_{BATH}$ will be much less.

Flux measurements determined from measurements of $[K^+]_{USL}$ are in good agreement with those determined from measurements of fluid secretion rates and secreted fluid $[K^+]$. The technique described in this paper, therefore, may be useful in characterizing Malpighian tubules of other species. This may be of particular interest for species such as the hemipteran *Cenocorixa bifida* (Cooper *et al.*, 1989) in which MTs have several identifiable segments, each of which may have different transport functions; or for species having Malpighian tubules composed of heterogeneous cell types, such as the Malpighian tubules of *Drosophila* which contain stellate cells and principal cells (*e.g.* O'Donnell *et al.*, 1996).

CHAPTER 3: Analysis of Epithelial Transport By Measurement of K+, Ca+2, and Cl- gradients in Extracellular Unstirred Layers: Ion Secretion and Reabsorption By Malpighian Tubules of *Drosophila melanogaster*

INTRODUCTION

The results of Chapter 2 showed that extracellular ion selective electrodes could detect ion concentrations in the USL adjacent the basolateral membrane of two well characterised transporting epithelia each composed of a single cell type, which form the UMT and LMT of *Rhodnius*. Therefore it was of interest for this chapter to determine how effectively this non- invasive approach would be in measuring the ion transport capacity of a less well characterised transporting epithelium-- the Malpighian tubules of *Drosophila melanogaster*, which contains more than one type of cell.

The tubules of *Drosophila* secrete fluid at higher rates than any other epithelium, including the Malpighian tubules of *Rhodnius* (Maddrell, 1991). The length of the main segment of the *D. melanogaster* tubule is 1.5 mm, with an outside diameter of about 35 μm and luminal diameter of

17 µm. Tubules typically secrete fluid at rates of 0.7 - 1.0 nl/min unstimulated, with a maximum secretion rate exceeding 6 nl/min when stimulated (Dow *et al*, 1994*b*). This corresponds to each cell secreting fluid at a rate equal to its own volume in less than 15 s.

Drosophila have four Malpighian tubules arranged as two pairs: one anterior, and one posterior (fig. 3.1). Each pair is connected to the gut through a short ureter. The anterior pair of tubules are each divided into three regions (Wessing and Eichelberg, 1978): a reabsorptive proximal segment, a fluid secretory main segment, and a distal segment which neither secretes nor reabsorbs fluid (Dow *et al*, 1994*b*). The posterior pair of tubules each lack a distal segment (fig. 3.1). The proximal segment of the *Drosophila* tubule, i.e. the 30% of total length closest to the ureter, is involved in reabsorption of KCl and water (O'Donnell and Maddrell, 1995).

Malpighian tubules in most Diptera, including *Drosophila*, are composed of two cell types: principal and stellate (Satmary and Bradley, 1984). Stellate cells are found between principal cells in the main segment of the tubule (Alkassis and Schoeller-Raccaud, 1984), and are fewer in number than the principal cells (Satmary and Bradley,

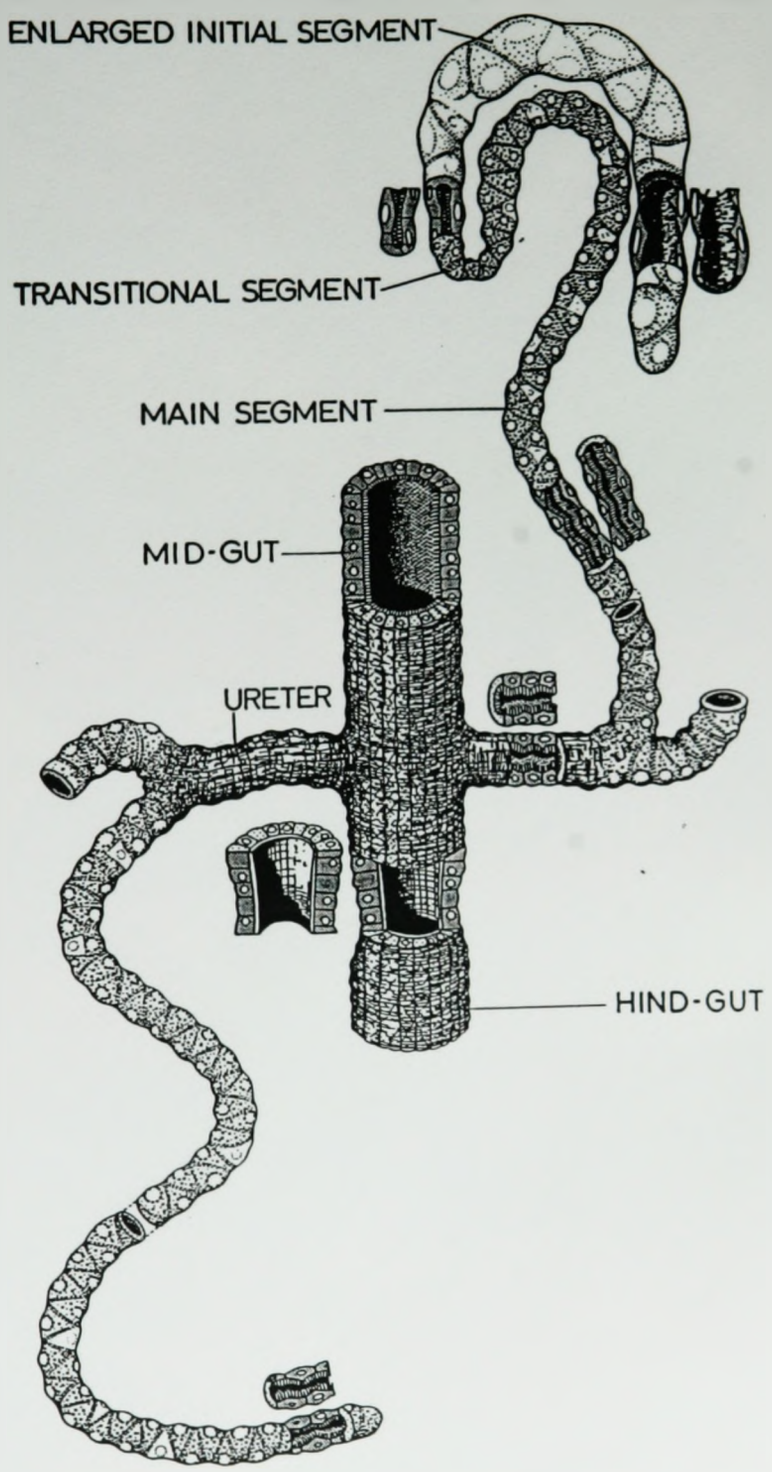
ENLARGED INITIAL SEGMENT
TRANSITIONAL SEGMENT
MAIN SEGMENT
MID-GUT
URETER
HIND-GUT

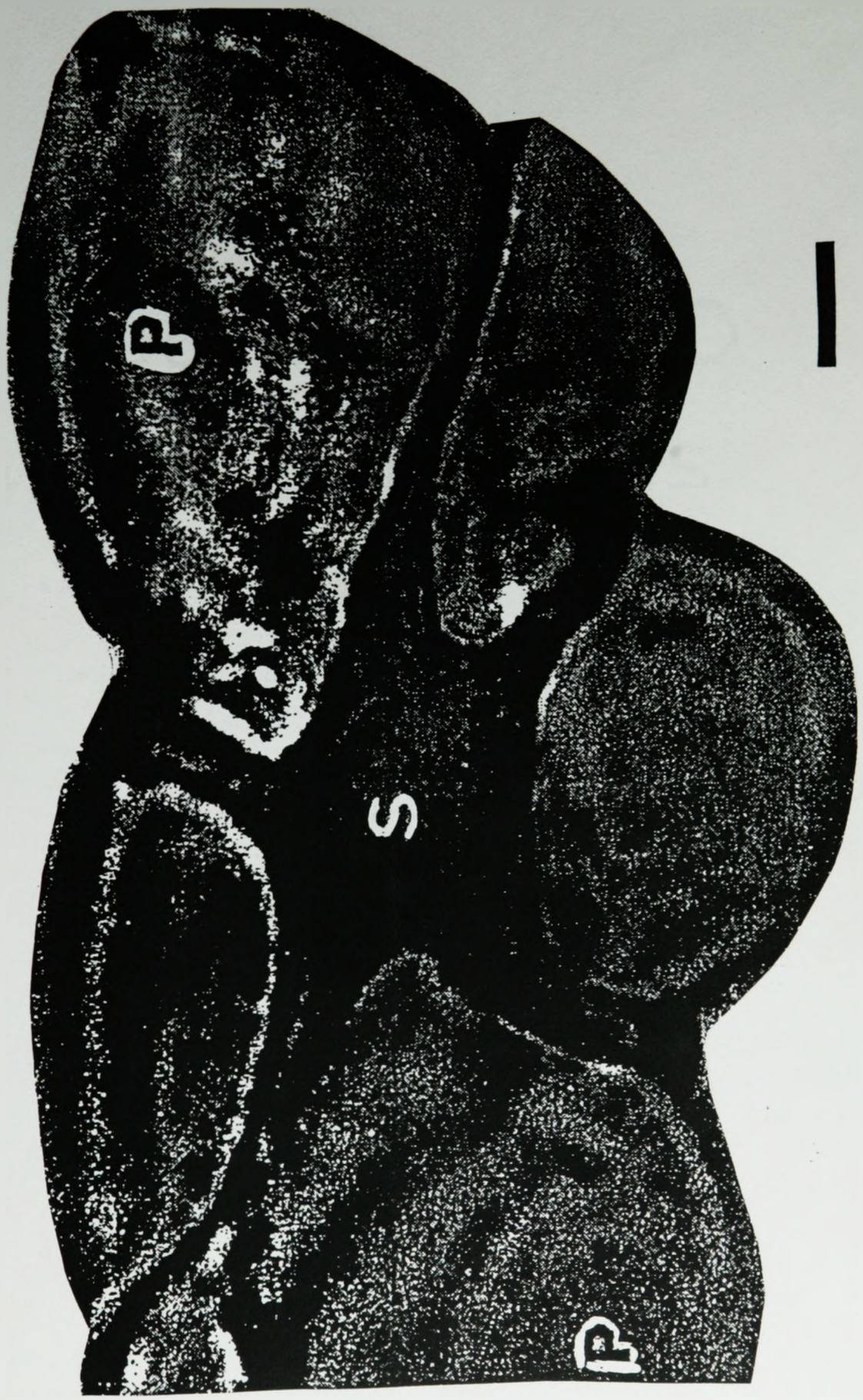
P
S
P

1984; fig. 3.2). By contrast, the UMT of *Rhodnius* is composed of a single cell type. The stellate cells are smaller, have fewer mitochondria, and have shorter microvilli than principal cells (Alkassis and Schoeller-Raccaud, 1984; fig. B1, Appendix B).

The current model of ion transport by *Drosophila* Malpighian tubules involves separate pathways for the control of transport of cations and anions in the MT (O'Donnell *et al*, 1996). Potassium movements across the basolateral membrane involve K^+ channels and possibly a Na^+/K^+ - ATPase, but not the furosemide-sensitive $Na^+/K^+/2Cl^-$ co-transporter implicated in ion transport by the Malpighian tubules of *Rhodnius* and *Aedes*. A vacuolar-type H^+-ATPase which is inhibited by bafilomycin A_1 and is insensitive to ouabain is found on the apical membrane (Bowman *et al*, 1988; Bertram *et al*, 1991; Wessing *et al*, 1993). This electrogenic pump maintains a pH gradient for potassium movement from cell to lumen through an electroneutral amiloride sensitive potassium/proton antiport. This antiport may also accept sodium ions as well, at increasing intracellular sodium levels. The proton pump also maintains a lumen positive electrical gradient which favours the movement of Cl^- from the cell to lumen

(Williams and Beyenbach, 1984). Fluid transport is seen as a secondary and passive osmotic consequence of ion transport (O'Donnell *et al*, 1982; O'Donnell and Maddrell, 1983), with water movement perhaps facilitated by water channels (Dow *et al*, 1995).

The control of fluid secretion of *Drosophila* Malpighian tubules involves several different intracellular second messenger pathways. Cyclic AMP accelerates fluid secretion in tubules of many species, including *Drosophila* (Maddrell *et al*, 1971; Dow *et al*, 1994a). Secretion rates increased more than 2-fold in response to 5×10^{-5} mol l^{-1} cAMP. The first messenger (i.e. hormone)resulting in cAMP production in the tubule is unknown (Davies *et al*, 1995; O'Donnell *et al*, 1996). Transport can also be stimulated by cGMP. Davies *et al* (1995), found that an endogenous cardio-acceleratory peptide(CAP_{2b}) raises fluid secretion rates through production of NO, which in turn lead to elevation of cGMP concentrations (Dow *et al*, 1994a). The effects of cyclic GMP with cAMP on fluid secretion are not additive, which suggests that the two cyclic nucleotides stimulate the same transporter(s) (Dow *et al*, 1994*a*; O'Donnell *et al*, 1996).

Several myogenic octapeptides called leukokinins (LK) also stimulate fluid secretion. LK-1 (10^{-6} M) stimulates *Drosophila* tubules, producing secretion rates similar to saturating doses of cAMP (Maddrell *et al*, 1994). However, LK-1 acts via the elevation of intracellular Ca^{+2}, independent of the cAMP and cGMP pathway (Maddrell *et al*, 1994; fig. 3.4). Manipulation of intracellular Ca^{+2} levels with ionophores (A23187) or Ca^{+2} -mobilizing agents (thapsigargin) increases fluid secretion rates (O'Donnell *et al*, 1996), and the increase in secretion rate is indistinguishable from, and not additive to, the effects of leukokinins (Davies *et al*, 1995). The cell-permeant Ca^{+2} chelator BAPTA-AM suppresses the actions of leukokinins, but not those of cAMP, or CAP_{2b} and its second messenger cGMP, again indicating the involvement of Ca^{+2} as a second messenger for the leukokinins. The suggestion of separate anion and cation control is further indicated by the additive effects of cGMP or cAMP to those of LK or thapsigargin (Davies *et al*, 1995; O'Donnell *et al*, 1996).

Electrophysiolgical data provide further support for the theory of separate control of cation and anion transport in MTs. Cyclic nucleotides and CAP_{2b} drive the apical membrane potential (V_{ap}) to more positive levels and thereby

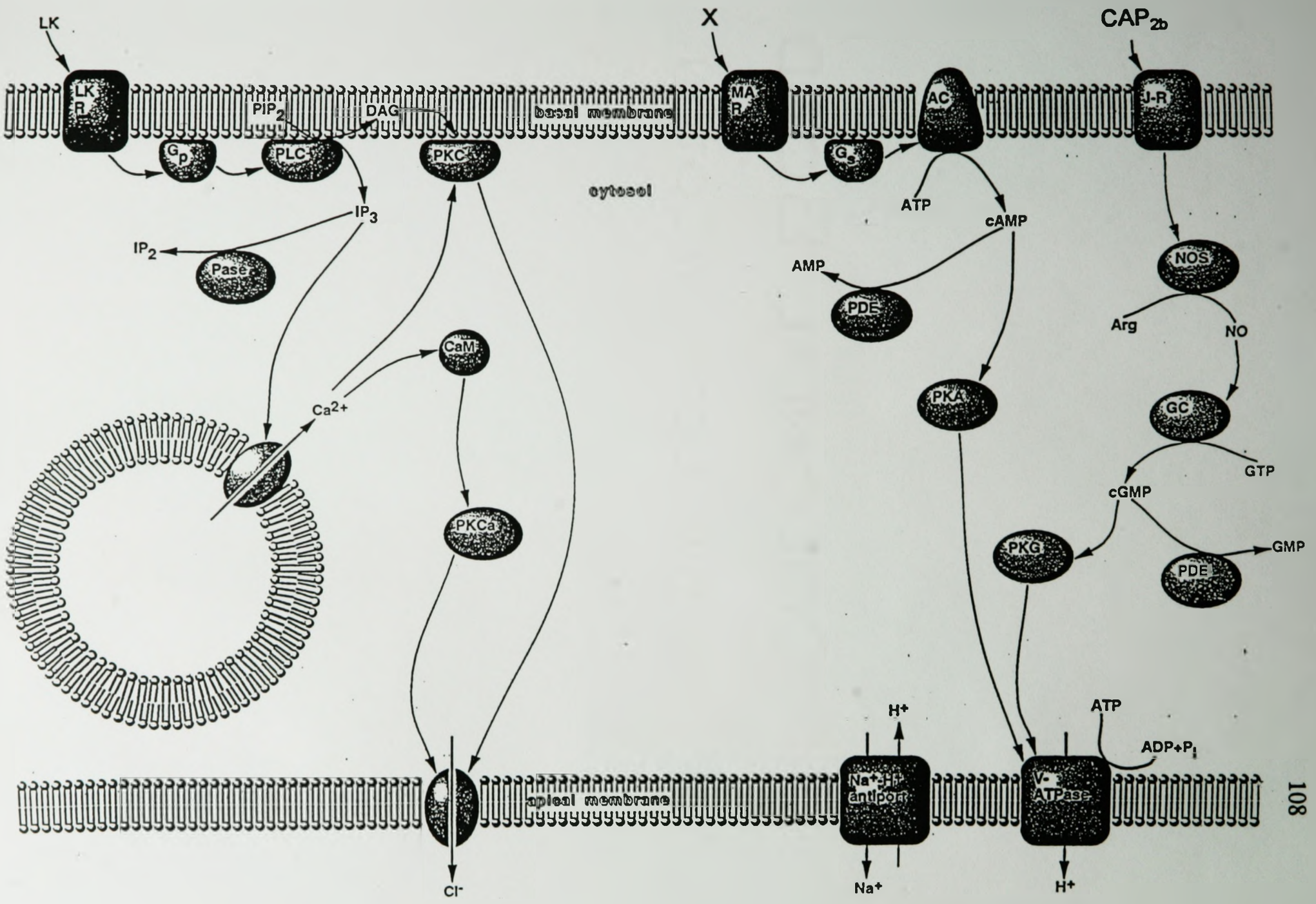
LK
LK R
X
MA R
CAP2b
J-R
AC
PIP2
DAG
basal membrane
Gp
PLC
PKC
Gs
cytosol
ATP
cAMP
IP3
IP2
Pase
AMP
PDE
NOS
Arg
NO
CaM
Ca2+
PKA
GC
GTP
cGMP
PKCa
PKG
GMP
PDE
H+
ATP
ADP+Pi
Na+-H+ antiport
V-ATPase
apical membrane
Cl-
Na+
H+

increasing the TEP (hyperpolarization). These messengers act by stimulating the electrogenic cation transporting apical V-ATPase and have little effect on anion conductance, or intracellular Ca^{+2} (O'Donnell *et al*, 1996). By contrast, leukokinin or thapsigargin increases transepithelial Cl^- permeability, thereby causing the TEP to become less positive (O'Donnell *et al*, 1996).

Thus far, it is clear that there exists a functional separation between the pathways controlling cation and anion transport in *Drosophila* MT. Pannabecker *et al* (1993) have proposed that Cl^- may move paracellularly between stellate cells and adjacent principal cells. O'Donnell (1997), believe that a transcellular route through the stellate cells is more likely. Figure 3.5 shows the summary of transport mechanisms believed to occur on both principal and stellate cells to date.

In addition, O'Donnell and Maddrell (1995), have found the proximal lower segment, and the main segment of *Drosophila* MTs to rapidly transport Ca^{+2} into the lumen. The main segment of the MT actively transports Ca^{+2} even when the TEP is made considerably more lumen positive when stimulated with cAMP. When the tubule is further stimulated with LKI (causing depolarization of the TEP), Ca^{+2}

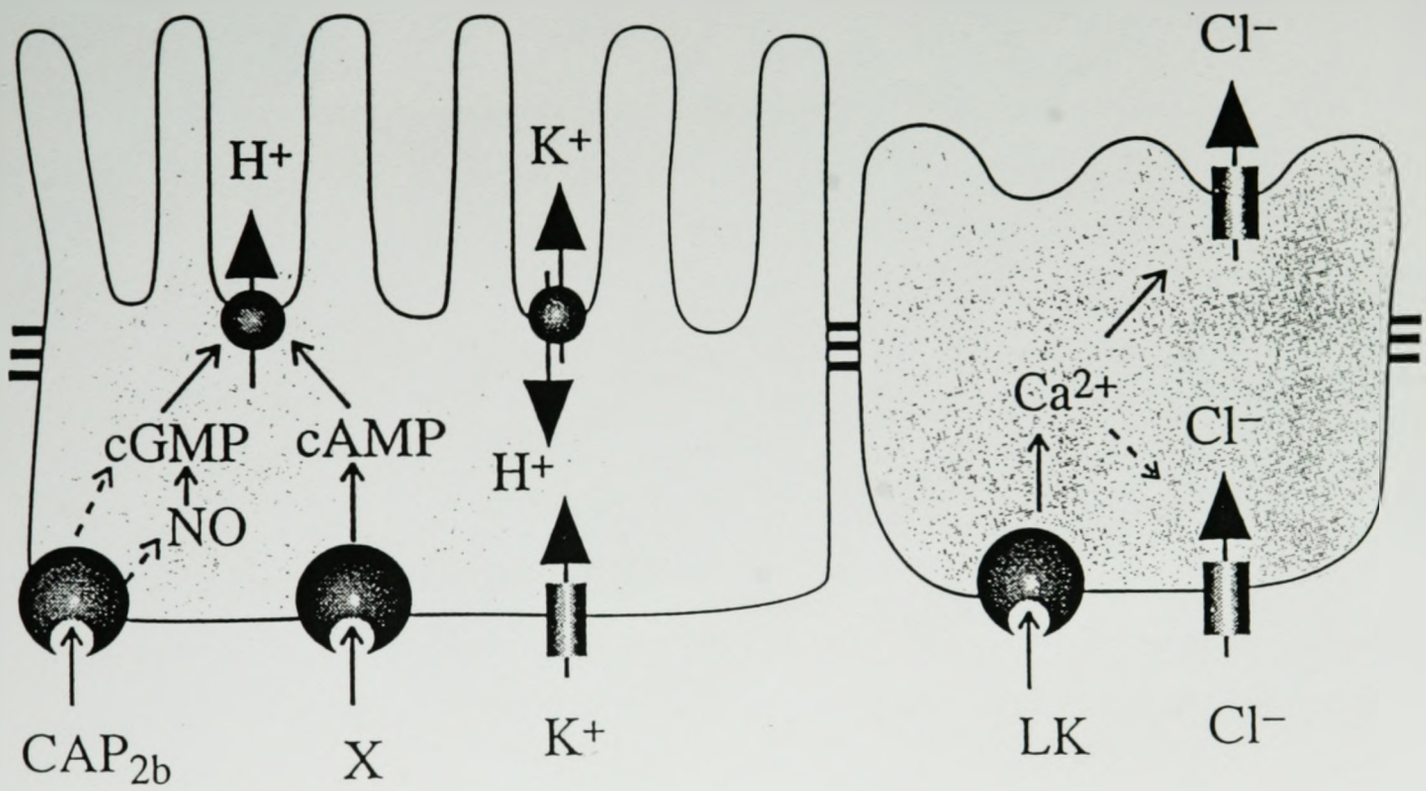
Cl⁻
H+
K+
Ca2+
cGMP
cAMP
NO
H+
Cl⁻
CAP2b
X
K+
LK
Cl⁻

transport is further accelerated. In addition, the proximal lower segment of the tubule transports Ca^{+2} at a higher rate per unit length than does the main segment of the the MT, as the TEP in the former segment is much more favourable for movement of Ca^{+2} into the lumen (O'Donnell and Maddrell, 1995).

This chapter examines if transport of ions to specific segments or cells of the *Drosophila* MT can be detected through changes in USL ion concentrations. The results of experiments in which static K^{+}, Ca^{+2}, and Cl^{-}-selective microelectrodes, in the USL are described. I also attempted to achieve greater resolution using a vibrating Cl^{-} selective microelectrode. This technique incorporates a self-referencing electrode and signal averaging, thereby allowing a greater improved signal-to- noise ratio relative to a static microelectrode (Smith *et al*, 1994). ISME measurements were correlated with fluid secretion analyses (Ramsay, 1952).

MATERIALS AND METHODS

Insects

Oregon R strain *Drosophila melanogaster* were grown on standard fly medium at room temperature and ambient humidity (Ashburner, 1989). Adult flies were fed on a yeast diet which lightly covered approximately two thirds of the surface of the standard fly medium. The second generation of adult flies emerged approximately 10 days later, and were transferred to new tubules with fresh yeast. The remaining larvae and pupae remained in the initial tube, and the newly emerged adults were transferred to new tubules on a daily basis. Age of adult flies could thus be determined within a 24 hour range.

Isolation of Malpighian tubules

Adult females, 4 - 7 days post-emergence were used, partly because their tubules are larger than those of the smaller males, and also to preclude any undetected differences between the sexes (Dow *et al*, 1994b). Post-emergent adults were dissected in saline by gripping vicinal abdominal tergites with fine forceps, and pulling away the

posterior half of the abdomen. With the fly's body now in two halves, the alimentary canal and the attached Malpighian tubules became uncoiled. Fine glass probes were used as required to free either the anterior or posterior pair of tubules. Only the anterior pair of tubules were used. Tubules were transferred to a 5 ml Falcon dish and bathed in a 300 µl droplet of saline. A 1.25 cm diameter hole was punched out of the bottom of the dish and a 22 x 22 mm glass slide (Fisher Scientific Co, thickness #1) was sealed in place with wax in order to improve optics. The glass slide was covered with a drop of poly-lysine (125 µg/ml) rinsed with distilled water, and air dried in order to facilitate tubule adhesion. Anterior tubules were positioned on the glass slide such that the pair of tubules spanned a straight line, with the ureter bisecting the line. Stimulants (cAMP, LK1) were added at various concentrations to the bathing saline to stimulate fluid secretion by the principal cells, and the stellate cells. Tubules were viewed under an inverted microscope with phase contrast optics.

Experimental salines

Insects were dissected in control saline consisting of (in mM): NaCl (117.5), KCl (20.0), $CaCl_2$(2.0), $MgCl_2$-$6H_2O$ (8.5), glucose (20.0), $NaHCO_3$ (10.2), NaH_2PO_4 (4.3),

HEPES (8.6), and adjusted to pH 7.2. The osmolality of the standard saline was 340 mOsm.

A saline containing 50% of the control level of Cl^- was prepared by mixing equal parts of control saline and Cl^--free saline. The latter was prepared by substitution of SO_4^{-2} for Cl^-. Following the advice of J. Kunkel (personal communication), a second type of Cl^--free saline was prepared and used on a trial basis at Wood's Hole MA. This saline used methane sulphonic acid to preclude possible harmful effects of SO_4^{-2}. NaH_2PO_4 was also omitted to preclude tissue damage and interference with metabolic processes (J. Kunkel, personal communication). Trehalose was substituted for glucose to maintain an osmolality of 360 mOsm. The final composition of this Cl^--free saline consisted of (in mM) NaOH (117.5), KOH (20.0), $CaOH_2$ (2.0), $MgOH_2$ (8.5), $NaHCO_3$ (10.2), HEPES (8.6), Methane sulphonic acid (158.5), trehalose (30.0), and was titrated to pH 7.2. Experiments testing Ca^{+2} transport were set up in either control saline (2 mM Ca^{+2}) or 4.2 mM Ca^{+2}.

Secretion rates

Isolated anterior tubules were placed in a 20 µl droplet of saline under oil. One tubule of the pair and the ureter was pulled out of the bathing droplet and anchored on

a glass pin. Cyclic AMP and LK1 were added consecutively at 10^{-3} M and 2 x 10^{-4} M, respectively, to stimulate fluid secretion. Droplets of secreted fluid were collected from the ureter at intervals. Droplet diameters were measured with an eyepiece micrometer and droplet volume (nl) was calculated using a standard formula. Secretion rates ($nl.min^{-1}$) were calculated by dividing droplet volumes by the time over which the droplet was formed.

Ion-selective microelectrodes and ionophores

Extracellular ion activities were measured using liquid membrane ion-selective microelectrodes. K^+-selective microlectrodes were based on the neutral carrier valinomycin (K^+ ionophore I, Cocktail B, Fluka Chemical Corp., Ronkonkoma, NY, USA). Cl^--selective microlelectrodes were based on the Cl^- exchanger IE-173 (World Precision Instruments; Sarasota., FL, USA). The Ca^{+2}-selective microelectrodes were based on the neutral carrier N,N,N',N'-Tetracyclohexyl-3-oxapentanediamide (Ca^{+2} ionophore II, ETH 1001,cocktail A, Fluka Chemical Corp., Ronkonkoma, NY, USA).

I- Static Microelectrodes

Manufacture of electrodes

Techniques for fabrication of ISME's and reference electrodes have been described previously in Chapter 2.

Data aquisition

Ca^{+2}, K^{+} and Cl^{-}-selective as well as reference microelectrodes were connected by chlorided silver wires to high-impedance (> 10^{15} Ω) electrometers, which were connected in turn to a PC-based data aquisition and analysis system (Axotape, Burlingame, CA, USA).

Probe positioning and data collection

Sampling of ion activity was taken with the electrode positioned at 90° to the long axis of the tubule. The sampling speed was set at 5 Hz and each sample trial ran for 7 secs. When the sampling trial was finished at one site along the tubule, the ISME was moved at least 100 µm away from the tubule surface to the bath. The sample trial for the bath measurement proceeded once again for 7 secs. This method continued by alternating measurements between the bath and the sites along the tubule length.

Data was exported from Axotape to a spreadsheet software package (Excel 7.0, Microsoft) which facilitated signal averaging calculations. Voltage signals at each site were averaged over 5 secs to give one resultant value for calculation of ion concentration.

II- Vibrating Microelectrodes

Manufacture of electrodes

Bee-stinger type micropipettes (Smith *et al*, 1994) were pulled from 1.5 mm diameter borosilicate glass capillary tubes in 2 stages to a tip diameter of 2 µm (Model BB-CH Mecanex). After pulling, the pipettes were baked for 2 hours at 180° C and then silanized in the vapor of 50 µl N,N-Dimethyltrimethylsilylamine under a bell jar for 10 minutes. The pipettes were then baked over night in the absence of silanizing vapour, then stored in a bell jar over disiccant. Cl^--selective electrodes were backfilled with 100 mM KCl and front-loaded by capillarity with the liquid ion-exchanger (LIX). Reference electrodes were made with borosilicate glass capillary tubes filled with 3M sodium acetate in 3% agar. The electrodes were calibrated

using KCl of different concentrations, differing 10 fold (i.e. 1 mmol l^{-1}, and 10 mmol l^{-1} KCl).

Data aquisition

The Cl^--selective microelectrode and chlorided silver wires were connected to an orthogonal array of computer-controlled stepper motors which could control the vibrational angle and amplitude of the probe in 3 axes with submicron accuracy (0.4 μm). The stepper motors were connected to a preamplifier, and both probe and preamplifier were vibrated together to reduce mechanically generated noise and preclude capacitative changes. The preamplifier was linked to another amplifier with a gain of 1000, in which signals passed through a high pass filter, then a low pass filter in series which in combination filter and removed signals higher than 30 Hz. The resulting signal was fed to a PC-based computer data aquisition and analysis system (3DVIS; National Vibrating Probe Facility, MA, USA). The experimental setup was mounted over a Zeiss IM35 inverted microscope positioned on an air table. The entire experimental set up was enclosed in a Faraday cage and images were viewed remotely by video through the microscope side port.

Probe positioning and data collection

Ion activity was measured with the electrode positioned at 90° to the long axis of the tubule using a sampling speed of 1000 points per second, vibrational frequency of 0.3 Hz, vibrational amplitude between 30 and 100 µm, blanking constant of 3, and a running average based on 14 bins of data. The blanking number is the number of discrete averages (out of 10) which were not used as the electrode moved to the opposite extreme of its vibrational amplitude. In other words, if you were to assume that measurements taken by the probe in position 1 (P_1 *i.e.* at the tubule surface) could be arranged with equal data points divided into 10 bins. As the probe moved to position 2 (P_2 *i.e.* the bath), the same data collection would follow with equal number of data points arranged into 10 bins. If all 20 of these data bins were averaged to find the ΔmV for one cycle (*i.e.* movement from P_1 to P_2) then a large amount of noise/error would result by including those data points gathered while the probe was in transition from P_1 to P_2. In order to minimize this error, the data points collected in the first 3 bins at both P_1 and P_2 were rejected. Seven bins of data at P_1 were compared to the 7 bins of data points at P_2 for each cycle of vibrational amplitude.

Therefore every cycle would give one resultant running average of ΔmV based on 14 bins.

Measurements of ion concentrations in bath and USL

K^+, Cl^-, and Ca^{+2} concentrations were calculated using the following equation:

$$[I]_{USL} \text{ or } [I]_{Bath} = [I]_c \times 10^{(\Delta V/S)}$$

where $[I]_{USL}$ or $[I]_{Bath}$ is the concentration of K^+, Cl^-, or Ca^{+2} in the USL or bathing saline, and $[I]_c$ is the corresponding concentration in the calibration droplet. ΔV is the change in electrical potential (in mV) between the calibration solution and the USL or bathing saline, and S is the slope (in mV) measured for a 10- fold change in K^+, Cl^-, or Ca^{+2} concentration. Calibration solutions for K^+ and Cl^- electrodes were prepared from mixtures of 150 mmol l^{-1} NaCl and KCl. Calibration solutions for Ca^{+2} electrodes were prepared from mixtures of 2 mmol l^{-1} $CaCl_2$ and 150 mmol l^{-1} NaCl.

Cl^- Flux in the anterior tubule

The vibrating electrode was used to measure fluxes at 8 or more sites along the length of the tubule. The probe vibrated between the site perpendicular to the long axis of the tubule and the bath (at either 30 µm or 100 µm away). Fluxes were calculated using the Fick equation:

$$J = [-D (\Delta C / \Delta r)] / (E)$$

where J is the flux in $\mu mol.cm^{-2}.sec^{-1}$, D is the diffusion coefficient for Cl^- (2.0×10^{-5} cm^2sec^{-1}), Δr is the vibrational amplitude of the probe in cm, and E is the efficiency of the chloride electrode. Electrode efficiency was determined by measuring the ion efflux from a source of a known concentration at a specific frequency and comparing the measured value of ΔC to the actual value. For Cl^- measurements, the efficiency of the ionophore was found to be 0.75 (J. Kunkel, personal communication). ΔC is the concentration of Cl^- in $mol \cdot cm^{-3}$ and is calculated using the following derivation from Smith *et al* (1994):

$$\Delta C \cong [2.3 (\Delta V) (C_B)] / S$$

where ΔV was the measured voltage difference from the vibrating probe measured in mV, C_B is the background $[Cl^-]$ in $\mu mol \cdot cm^{-3}$, and S was the slope obtained from a 3 point calibration of static measurements with 3 different bath concentrations each differing by a decade change in mV.

Data Analysis

All experiments were performed at room temperature,20-25° C. Values are reported as means ± S.E. M. Significance of differences between means was evaluated by paired Student's *t*-tests (two-tailed), using a critical value of $p < 0.05$ for significance.

RESULTS

$[K^+]_{USL}$ of the main segment principal and stellate cells measured with static K^+-SMEs

$[K^+]_{USL}$ was calculated from positioning the ISME within 5 µm of the basolateral surface of either a main segment principal cell, or a main segment stellate cell. Two different principal cells, and two different stellate cells were chosen as measurement sites on each tubule. $[K^+]_{USL}$ was measured before and after stimulation with both 2 x 10^{-4} mol l^{-1} LKI and 10^{-3} mol l^{-1} cAMP. $[K^+]_{USL}$ associated with stimulated principal or stellate cells was significantly lower ($p<0.05$) than $[K^+]_{USL}$ of unstimulated tubules, and $[K^+]_{Bath}$ (fig. 3.6). The reduction of $[K^+]_{USL}$ in stimulated tubules relative to $[K^+]_{Bath}$ is consistent with a depletion of K^+ from the USL as K^+ is transported from bath to tubule lumen by both cell types. The $[K^+]_{USL}$ of stimulated stellate cells was also significantly lower ($p<0.05$) than the $[K^+]_{USL}$ of stimulated principal cells in the main segment (fig. 3.6). This suggests that the secretory capacity of the main segment is heterogenous along its length. Previous studies by O'Donnell *et al* (1996)

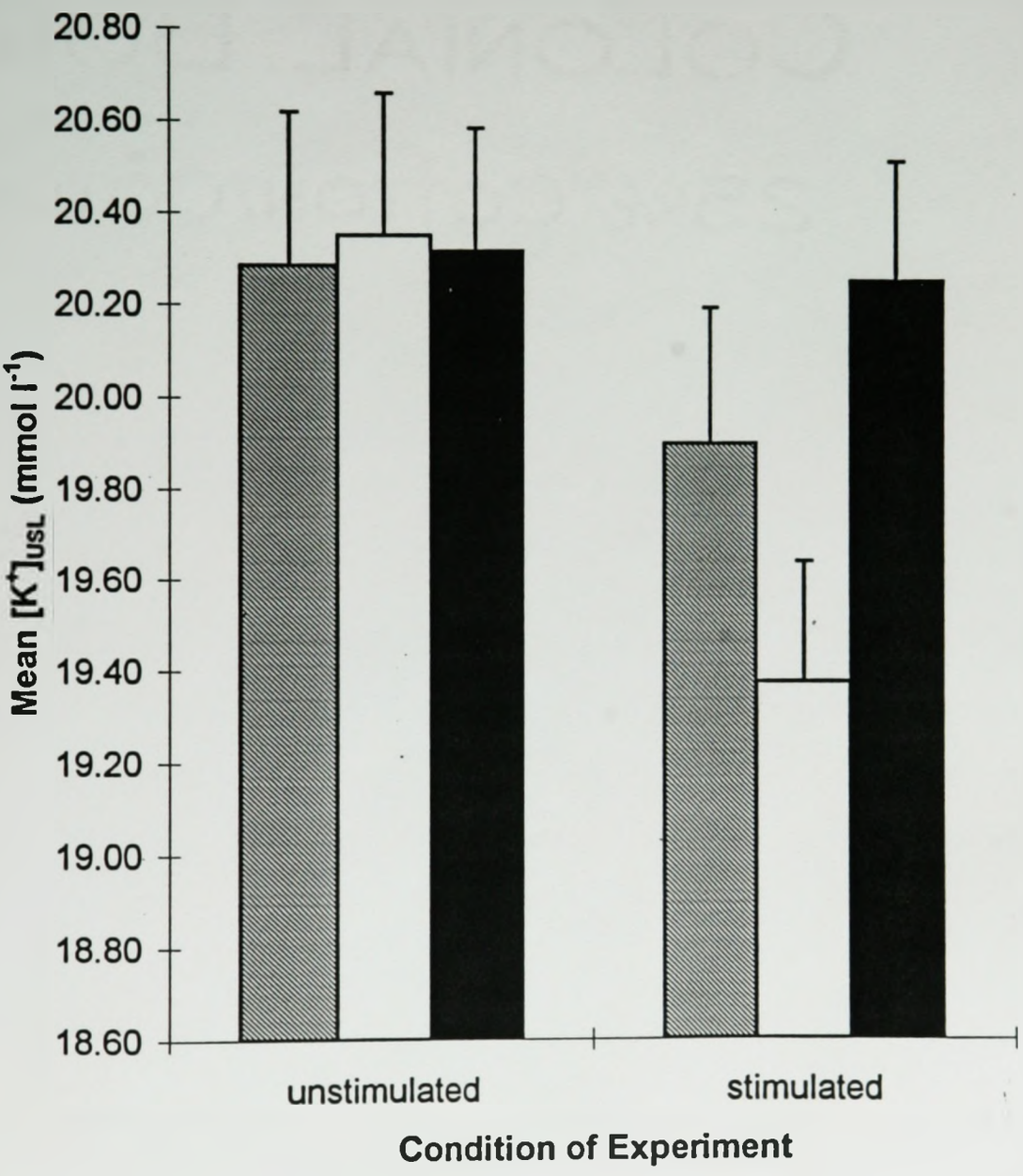
20.80
20.60
20.40
20.20
20.00
19.80
19.60
19.40
19.20
19.00
18.80
18.60
Mean [K+]USL (mmol l-1)
unstimulated
stimulated
Condition of Experiment

suggest that it is unlikely that stellate cells actively secrete K^+. One possible explanation for this apparent increase in stellate K^+ secretion may be due to local differences in transepithelial potential (TEP; see discussion). Figure 3.7 also confirms the increase in secretion rate when tubules were stimulated with 10^{-3} mol l^{-1} cAMP, and then further stimulated with 2×10^{-4} mol l^{-1} LKI. This additive effect of stimulants correlates with previous studies by O'Donnell *et al* (1996), which proposes that cAMP stimulates cation secretion and LKI stimulates anion secretion through a cAMP independent pathway.

$[K^+]_{USL}$ of the Principal Cells in the Proximal and Distal Regions of Anterior Tubules

K^+ activity was measured by positioning the K^+ selective microelectrode within 5 μm of the basolateral surface of principal cells in either the proximal or distal region. Two different principal cells in each region were selected as sites of measurement for each tubule. The ion concentration at each site was measured before and after stimulation with the combination of 2×10^{-4} mol l^{-1} LKI and 10^{-3} mol l^{-1} cAMP. $[K^+]_{USL}$ at either region did not change significantly ($p>0.05$) with stimulation. All sites in

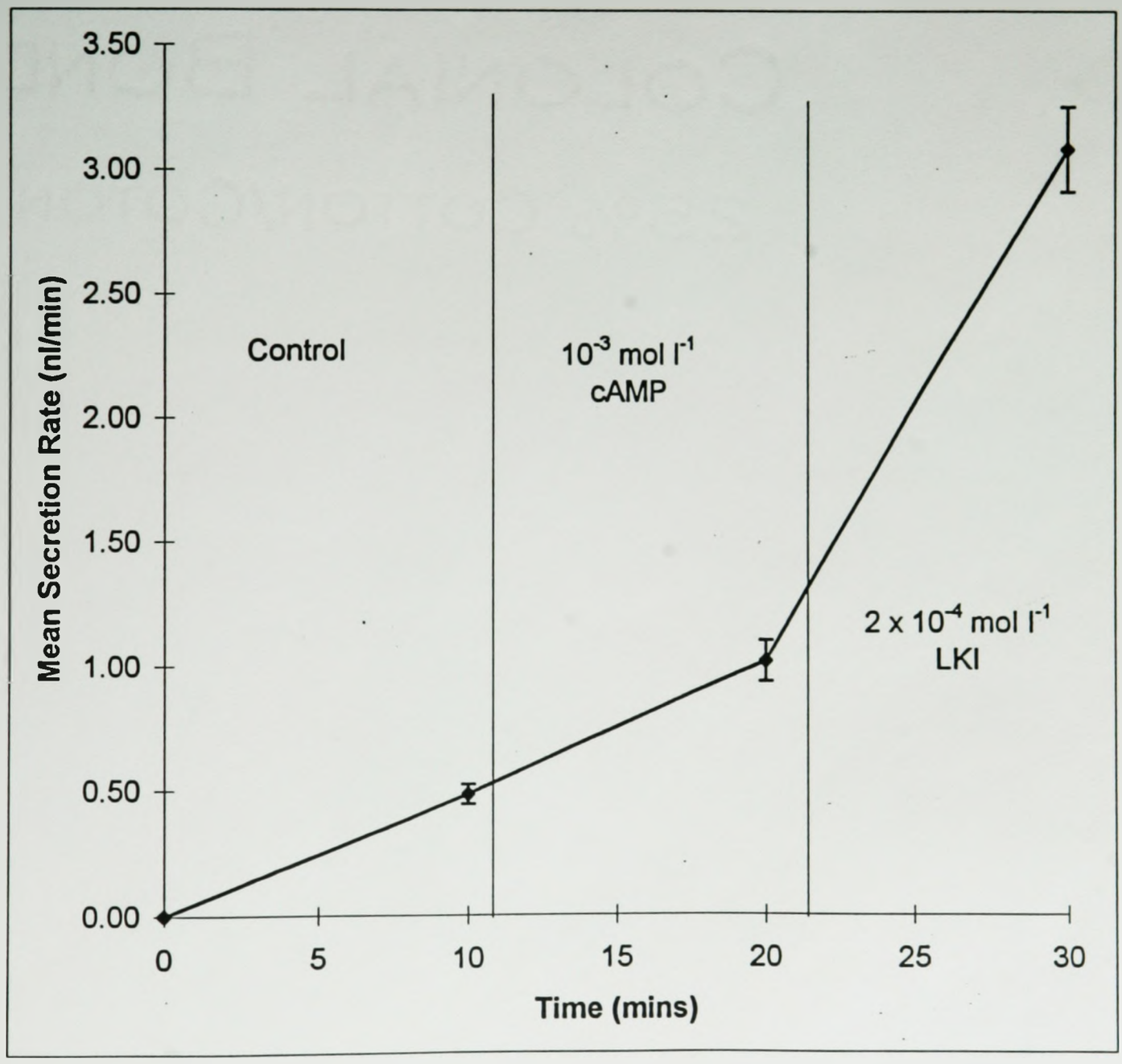
3.50
3.00
2.50
2.00
1.50
1.00
0.50
0.00
Mean Secretion Rate (nl/min)
Control
10-3 mol l-1
cAMP
2 x 10-4 mol l-1
LKI
0
5
10
15
20
25
30
Time (mins)

proximal and distal regions however, had a $[K^+]_{USL}$ higher than $[K^+]_{Bath}$ (fig. 3.8). This increase in $[K^+]_{USL}$ relative to bath in both regions is consistent with an accumulation of K^+ in the USL as K^+ is transported from tubule lumen to bath. The proximal region is known to function in ion reabsorption (O'Donnell and Maddrell, 1995). The apparent K^+ reabsorption capacity by the distal region is a new finding.

Measurement of $[Cl^-]_{USL}$ with static microelectrodes

No differences in the $[Cl^-]_{USL}$ relative to $[Cl^-]_{Bath}$ were detected with static Cl^--SMEs. Eight sites were sampled on each tubule: 2 sites were principal cells in the proximal region, 4 sites were in the main segment (2 sites adjacent stellate cells and 2 sites adjacent principal cells), and the final 2 sites were in the distal segment. Tubules bathed in either control saline (150 mmol l^{-1} Cl^-), 50% chloride free saline (75 mmol l^{-1} Cl^-), or control saline with 4.2 mmol l^{-1} Ca^{+2}, showed no differences in $[Cl_-]_{USL}$ when compared to $[Cl^-]_{Bath}$. Similarly, no appreciable depletion or buildup of Cl^- ions in the USL was detectable with static Cl^- microelectrodes after stimulation with either 2×10^{-4} mol l^{-1} LKI or the combination of 10^{-3} mol l^{-1} cAMP and 2×10^{-4} mol l^{-1} LKI, (N>10, data not shown).

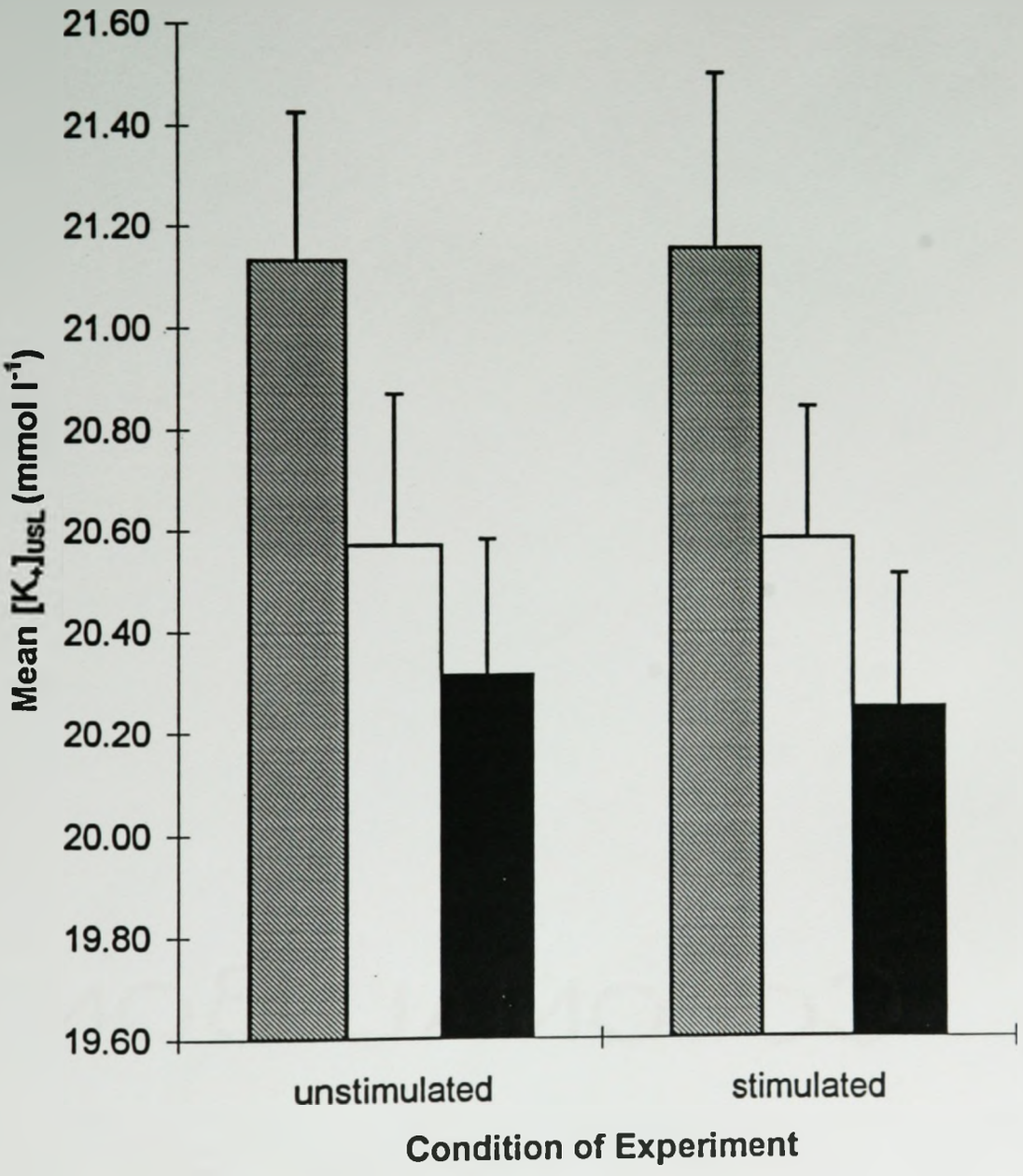
21.60
21.40
21.20
21.00
20.80
20.60
20.40
20.20
20.00
19.80
19.60
Mean [K+]USL (mmol l-1)
unstimulated
stimulated
Condition of Experiment

Measurement of $[Ca^{+2}]_{USL}$ with static Ca^{+2}-SMEs

Ca^{+2} ion activity was measured with a static microelectrode positioned within 5 µm of the basolateral surface of isolated tubules at the same 8 sites selected for static Cl^- measurements. Tubules bathed in control saline (2 mmol l^{-1} Ca^{+2}) or in 4.2 mmol l^{-1} Ca^{+2} saline did not show any increase or decrease in $[Ca^{+2}]_{USL}$ when compared to $[Ca^{+2}]_{Bath}$ either unstimulated or stimulated with the combined addition of 10^{-3} mol l^{-1} cAMP and 2 x 10^{-4} mol l^{-1} LKI in any of the sampled sites (n=12, data not shown).

Cl^- flux in the anterior Malpighian tubule: vibrating Cl- microelectrode

Cl^- fluxes were calculated by positioning the vibrating microelectrode in the USL within 5 µm of the basolateral surface of the tubule. The electrode was positioned at 6 different sites: 1. A principal cell in the proximal region (reabsorptive region), 2. Between a principal cell and one side of a stellate cell, 3. The stellate cell, 4. Between the stellate cell and the next principal cell, 5. A principal cell in the main segment as far away as possible from any surrounding stellate cells, and 6. A principal cell in the distal region (See fig. 3.9).

A

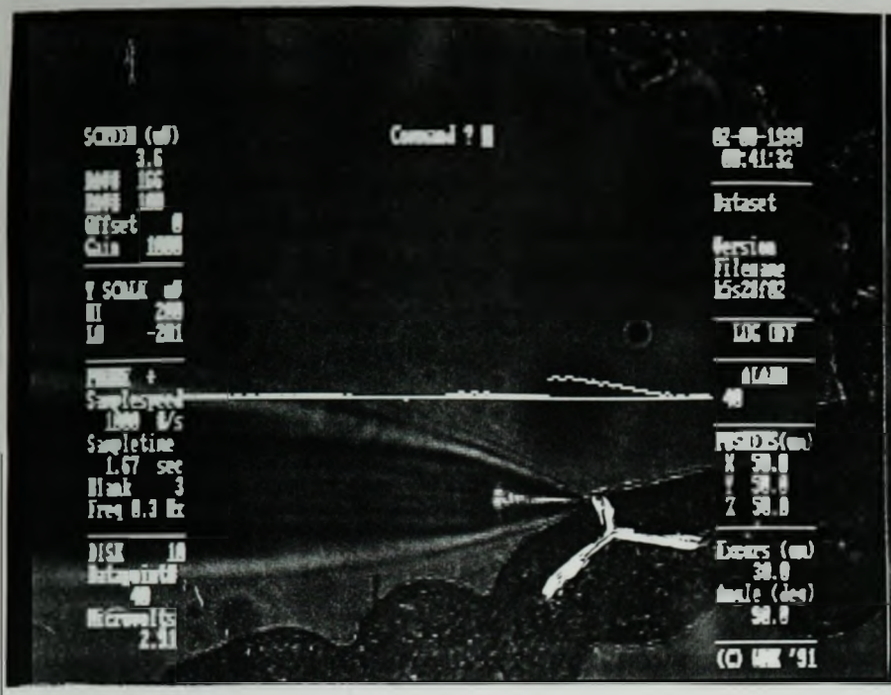
Command ? _
Dataset
LOG OFF
(C) UMK '91

B

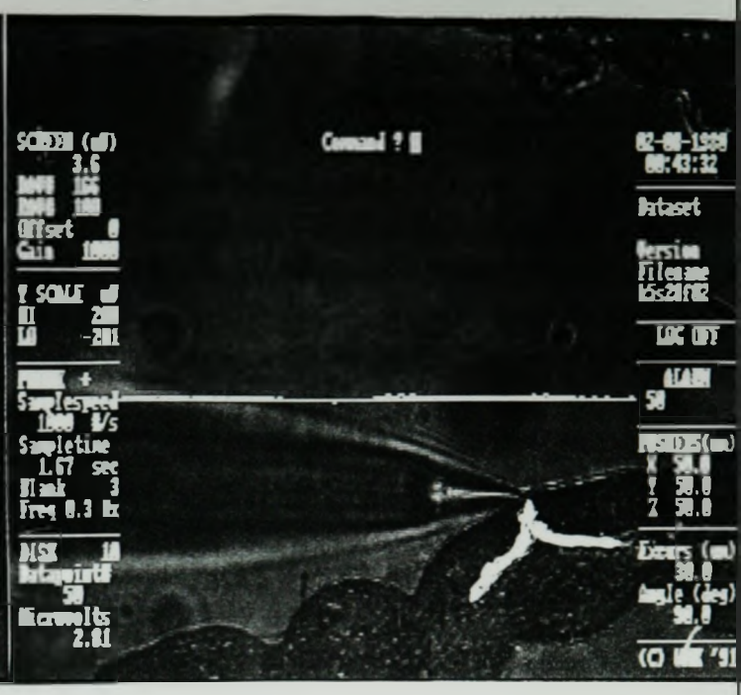
Command ? _
Dataset
LOG OFF
(C) UMK '91

C

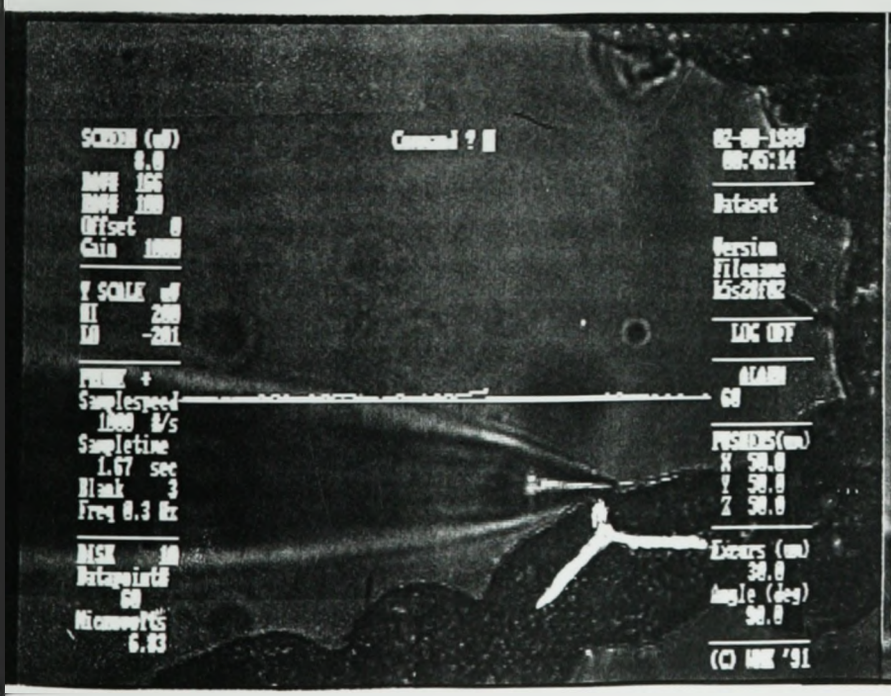
Command ? _
Dataset
LOG OFF
(C) UMK '91

D

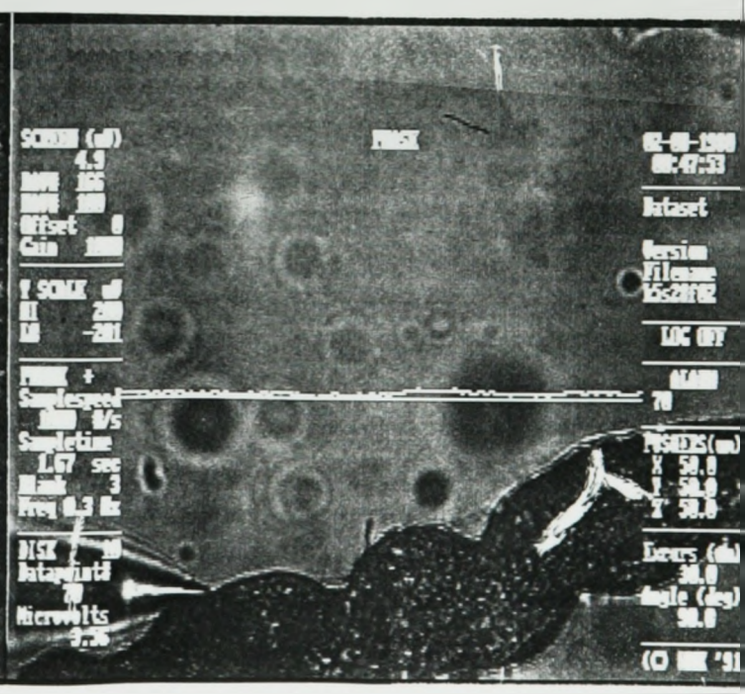
Dataset
LOG OFF

Ion activity was measured before and after stimulation with 10^{-6} - 10^{-3} mol l^{-1} LKI, or 10^{-5} mol l^{-1} Thapsigargin, or the addition of both 10^{-5} mol l^{-1} cAMP and 10^{-6} mol l^{-1} LKI.

Flux rates ranged from -1300 to +3050 $pmol \cdot cm^2 \cdot sec^{-1}$ (data not shown). Positive and negative values normally denote effluxes and influxes respectively, however in regions of the tubule known to function in secretion (thus an influx), effluxes were measured. Likewise, influxes were measured sporatically in regions known to function in reabsorption (i.e. the proximal region). These inconsistencies were apparent in studies of more than 50 tubules. There were no significant changes in response to 10^{-6} - 10^{-3} mol l^{-1} LKI. Possible explanations for these results are discussed below.

DISCUSSION

This chapter demonstrated that both secretion and reabsorption of K^+ by Malpighian tubules from *Drosophila melanogaster* can be assessed both qualitatively and quantitatively by measurement of K^+ concentrations in the USL associated with the basolateral cell surface. Also, the basolateral measurements of ion transport capacity were determined before and after putative stimulants were added to the bathing saline droplets. It would be of interest in the future to see whether ion transport capacity could be measured before and after K^+ and Cl^- channel blockers were added to bathing salines using this technique. Due to the measurable accumulation or decline in K^+ in the USL (depending on region of tubule) it is likely that this technique would be sufficient in accurately measuring the effects of such inhibitors. As with *Rhodnius*, the spatial resolution of this technique is comparable to that of an individual cell. The spatial resolution of this technique however, proved more potent in *Drosophila* tubules as a single arm of a stellate cell may be no more than 40 μm in width.

This technique revealed several features of ion transport in the Malpighian tubule of *Drosophila melanogaster*. The increase in $[K^+]_{USL}$ as the electrode is positioned in the proximal segment is consistent with reabsorption occuring. Also, the decline in $[K^+]_{USL}$ as the electrode is positioned in the main segment is consistent with previous studies which demonstrate that secretion is restricted to the main segment. Moreover, our data reveal two new findings. Firstly, K^+ reabsorption was found not just in the proximal segment, but also in the distal segment. This finding is perplexing as *Drosophila* secrete ions at rapid rates and at a position downstream from the distal region. The source for these K^+ ions is uncertain. One suggestion of a possible ion source could be from the abundant concretion bodies found almost exclusively in the lumen of the distal segment. Alternatively, contractions of the muscles associated with the tubule may provide some mixing of the contents of the lumen of the distal and main segment.

Secondly, secretion within the main segment is not uniform. Specifically K^+ secretion is cell dependent, with areas near the stellate cells transporting more K^+ than neighboring principal cells in the same region. Although TEM studies of stellate cells (data not shown) do not

support an active transport function, the increase in K^+ transport across stellate cells may be due to a local difference in TEP. It is known that LKI stimulation acts through intracellular Ca^{+2} levels which are thought to increase Cl^- permeability through Cl^- channels in stellate cells (O'Donnell *et al*, 1997). If this were the case then the Cl^- transport via stellate cells may create a micro-environment with a less lumen positive TEP. The result would be a more favourable electrochemical gradient for principal cells adjacent Cl^- secreting stellate cells to transport K^+ ions. Similarly, principal cells at a distance from stellate cells would have a more lumen positive TEP, opposing bath to lumen transport of K^+.

Our data also reveal that an apparent uniformity in cell type does not constitute functional uniformity. Principal cells are found in all three regions of the anterior tubule, however there is a discontinuity in principal cell function as one moves along the length of the tubule. The lower most 30% of the tubule (proximal) has principal cells which function very effectively at K^+ reabsorption. The next 40% of the tubule has principal cells in the main segment functioning in K^+ secretion. Lastly, the principal cells in the distal most 30% of the tubule once again function in K^+ reabsorption, however at a

much lower capacity than the proximal region. These results are consistent with Sözen *et al* (1997) who have found that otherwise morphologically indistinguishable cells have distinct subsets of cells with different transcriptional properties and thus different functions. Genetic mapping of tubule cell types by Sözen *et al* (1997), has found at least two distinct subpopulations of principal cells, and a bar-shaped counterpart to stellate cells, called tiny cells.

Results of experiments with Cl^- or Ca^{+2}-SMEs positioned in the USL were not as consistent as experiments using K^+-SMEs. Firstly, measurement of Cl^- always has an inherent problem resulting from high background Cl^- concentrations. Salines contain approximately 150 mmol l^{-1} Cl^-, higher than the 4-20 mmol l^{-1} K^+. For example, a MT secretes ions (K^+ and Cl^-) from the USL such that USL concentrations drop approximately 1 mmol l^{-1} from that of the bath. The change in voltage would be the product of the electrode slope(58 mV)and the logarithm of $[Cl^-]_{USL}/[Cl^-]_{BATH}$. Even in 50% Cl^- replete saline, this change in voltage is less than or equal 0.3 mV. Since the temporal resolution of the static probe falls within the 0.2 - 0.4 mV range, this real signal will be lost in background noise. In an attempt to resolve the signal to noise problem, experiments were performed using the vibrating Cl^- microelectrode.

However, two problems were encountered in experiments with the use of the Cl^--vibrating probe. Firstly, the Schneiders medium was thought to interfere with the ionophore, possibly because some components in the medium acted as a chelator, shuttling ions across the liquid - ionophore interface (J. Kunkel, *personal communication*). Later experiments used only control saline. Tubules are known to function poorly in a saline-only medium when compared to the 1:1 mixture (M. O'Donnell, *personal communication*), and transport capacity declined during the period required for measurements with the vibrating Cl^--microelectrode.

Secondly, the Cl^- ionophore was only 20 times more sensitive to Cl^- than to HCO_3^- (Walker, 1971). Since *Drosophila* tubules are metabolically very active (especially when stimulated), large amounts of HCO_3^- may accumulate from conversion of CO_2 and H^+ in the USL. Measurements with solid-state Cl^--selective microelectrodes, which are insensitive to HCO_3^- (eg. Wright and O'Donnell, 1992), may be able to resolve $[Cl^-]_{USL}$ more effectively.

Attempts to monitor Ca^{+2} transport by measurement of $[Ca^{+2}]_{USL}$ with static Ca^{+2}-microelectrodes were unsuccessful. The static electrodes are very effective at measuring

changes in $[ion]_{USL}$ produced by transepithelial fluxes in the nmol cm^{-2} s^{-1} range, however, previous studies performed with Ca^{+2} suggest *Drosophila* tubules have Ca^{+2} flux rates in the pmol cm^{-2} s^{-1} range (O'Donnell and Maddrell, 1995). The vibrating Ca^{+2} microelectrode has proved to be very effective at measuring Ca^{+2} fluxes in the pmol cm^{-2} s^{-1} range for several cell cultures, and would be a valuable tool in further studies on Ca^{+2} transport by *Drosophila* Malpighian tubules (Smith *et al*, 1994).

In summary, this technique has proven to be effective at characterizing K^{+} ion transport capacity of a single cell in a species which not only has 3 identifiable segments (proximal, main, and distal), but also has heterogenous cell types (principal and stellate).

CHAPTER 4: Analysis of Epithelial Ion Transport By Measurement of Extracellular Ion Concentration Gradients: an Evaluation, With Suggestions For Further Research

Concluding remarks

My results indicate that non-invasive measurement of unstirred layer ion concentrations provides new information on ion transport by insect Malpighian tubules. This technique should also find use with other rapidly transporting epithelia, including insect salivary glands and midgut.

This technique is much less expensive than X-ray microanalysis, flame photometry, and radioisotopes; and requires less training and less preparation of the sample. Previous methods used for analysis of secreted fluid (see introduction) all share the same limitations: temporal resolution and spatial resolution are poor, and too much time is required to gather the appropriate volume of secreted fluid to be analysed.

The temporal resolution of this method is dependent on the ionophore used. Most ISME's with tip diameters >2 µm have a response time of approximately 2-10 secs. This

allows for rapid measurement of ion transport when assessing the effects of pharmacological reagents, and putative diuretic hormones on tubule functions. Also, cost can be cut dramatically by using very small quantities of drugs or peptides which can be applied to the tubule surface by pressure or iontophoresis.

In the past, spatial resolution was limited by the length of the tubule which could be isolated in a bathing droplet of saline. With the use of extracellular ISME's, different segments of a single tubule can be examined non-invasively. This minimizes variability because each tubule acts as its' own control. This study has shown that the influence of even a single cell on ion concentrations in the basolateral USL can be detected by an extracellular ISME. Also, measurement of ion concentrations in the USL permits transport to be assessed without the use of radio-isotopes.

Lastly, this technique allows ion transport to be tracked in real time. Previous studies required typically 5-10 minutes to produce enough fluid for analysis. This study has shown that when a nanoliter volume of a drug is applied to the basolateral surface of MTs, ion transport measurements could be taken within seconds of drug application. The time require for the tissue to respond to a given agonist can be accurately assessed. Such

information is of use in determining how first and second messengers control ion transport.

Further directions for research

Use of a solid-state chloride electrode

- As the results of *Drosophila* $[Cl^-]_{USL}$ from this study were inconclusive, a more selective Cl^- electrode is needed. The solid-state electrode is less sensitive to interference by HCO_3^- than the conventional Cl^--SME, and would therefore be more effective at measuring Cl^- transport.

Use of a vibrating ion-selective microelectrode

- For those systems which transport more slowly, the more sensitive vibrating ion probe technique, involving slow vibration of the ISME and signal averaging, can be used Smith et al, 1994).

Use of a shielded ion-sensitive microelectrode (SIM)

- The SIM is a tool for investigating ion efflux across a defined area of a membrane. It is comprised of an inner electrode filled with an ionophore, which is encased in

an outer empty glass barrel electrode. The SIM limits diffusion of ions to a small compartment, formed by the outer shielding electrode (Danker *et al*, 1996). This method would further improve the signal to noise ratio and would permit otherwise undetected effluxes to be detected.

Effect of changes in diffusion coefficients on USL ion concentration gradients

- It would be of interest to alter the diffusion coefficients for ions by addition of macromolecules (such as high molecular weight Dextrans or agar) to the bathing saline. The resultant reduction of diffusion coefficients will tend to steepen the ion concentration gradient between the USL and the bulk solution. This may provide a means for increasing the spatial resolution for measurement of differences in USL ion concentration.

fin

roken back to tip diameters of approximately 10 µm. Techniques or fabrication of ISMEs and reference electrodes have been escribed previously (Maddrell *et al.* 1993). Ion-selective and eference microelectrodes were connected by chlorided silver ires to high-impedance (>10^{15} Ω) electrometers, which were onnected in turn to a computerized data acquisition and analysis ystem (Axotape, Burlingame, CA, USA).

Although ion-selective electrodes measure ion activity and ot concentration, data can be expressed as concentrations if it s assumed that the activity coefficient is the same in both the alibration solution and the bathing saline. Over the range of onic strengths of fluids encountered in this study 80–180 mmol l^{-1}), errors resulting from this assumption are ess than 5 % (Maddrell *et al.* 1993). Expressing ISME data as oncentrations simplifies comparisons with previous studies in hich ion concentrations were measured by flame photometry.

K^+ and Cl^- concentrations were calculated using the llowing equation:

$$[I]_{USL} \text{ or } [I]_{Bath} = [I]_c \times 10^{(\Delta V/S)}, \quad (1)$$

here $[I]_{USL}$ or $[I]_{Bath}$ is the concentration of K^+ or Cl^- in the JSL or bathing saline, and $[I]_c$ is the corresponding oncentration in the calibration droplet. ΔV is the change in lectrical potential (in mV) between the calibration solution nd the USL or bathing saline, and S is the slope (in mV) easured for a 10-fold change in K^+ or Cl^- concentration. alibration solutions for K^+ and Cl^- electrodes were prepared om mixtures of 150 mmol l^{-1} NaCl and KCl.

Values of pH were calculated using the equation:

$$pH_{USL} \text{ or } pH_{Bath} = pH_c - (\Delta V/S), \quad (2)$$

here pH_{USL} or pH_{Bath} refers to the pH of the USL or bathing aline and pH_c to the pH of a calibration solution. S is the slope n mV) measured for a pH difference of 1 unit. Calibration olutions were prepared from salines adjusted to two pH alues, usually differing by 1 unit.

Ion concentrations or pH were measured at varying distances om the basolateral surface and at several positions along the bule's length. Distances were measured using a calibrated yepiece micrometer in the dissecting microscope. Positions ong the length of the lower tubule are expressed as rcentages of its length (approximately 17 mm for a tubule om a fifth-instar *R. prolixus*), where 0 % corresponds to the npulla and 100 % to the junction of the upper and lower bules. Reference electrodes were positioned at least 5 mm vay from the tubule.

In situ *measurements*

Measurements of $[K^+]_{USL}$ and pH_{USL} were also made on Ts *in situ*. Insects were killed by crushing the head with rceps, the dorsal cuticle of the posterior half of the abdomen as removed, and 100 µl of 4K saline was added to the emocoel. The animal was pinned down by the legs to a ssecting dish lined with Sylgard, and the fat body and heart ere pulled slightly to one side to expose the tubules and the t. Evaporation of the saline was prevented by covering the saline surface with 50 µl of paraffin oil. The preparation was illuminated from the ventral side. Ion-selective and reference electrodes were placed in the saline/haemolymph to measure ion activity. Mean ion concentrations were measured 5 µm from the basolateral surface. The reference electrode was placed at least 5 mm away from the tubules.

Preliminary measurements indicated that $[K^+]_{USL}$ and pH_{USL} did not vary along the length of the UMT, and a mean value was determined for three measurements for three tubules from each animal. For the lower tubule, $[K^+]_{USL}$ and pH_{USL} were calculated as the mean of three measurements at the same site 20–30 % of the distance along the length of each of three tubules in each insect.

Pressure ejection of drugs to localized regions of the basolateral surface of Malpighian tubules

Micropipettes pulled to tip diameters of less than 1 µm were broken back to tip diameters of 3–4 µm. Each pipette was filled with paraffin oil and attached to polyethylene tubing and a 25 ml syringe filled with distilled water. Drugs were dissolved in saline and droplets of known volume were expelled under paraffin oil (see Results). The tip of the micropipette was placed into the droplet containing the dissolved drug, and the entire droplet was taken up into the micropipette by creating a slight negative pressure in the syringe. The micropipette was then placed next to the ion-selective microelectrode in the USL. While observing the saline/oil interface in the micropipette through the microscope, sufficient pressure was applied to the syringe plunger to eject the entire volume of saline within the micropipette.

Data analysis

All experiments were performed at room temperature, 20–25 °C. Values are reported as means ± S.E.M. Significance of differences between means was evaluated by paired or unpaired Student's *t*-tests (two-tailed), using a critical value of $P<0.05$ for significance. Previous studies by Boutilier and Shelton (1980) justify the calculation of mean values and standard errors for pH data, and the pH measurements were not converted, therefore, to $[H^+]$ (mol l^{-1}) before statistical treatment.

Results

Extracellular K^+ and Cl^- concentrations near the basolateral surface of the lower tubule

K^+ concentrations were measured in the USL within 5 µm of the basolateral surface at 10 %, 25 %, 50 %, 75 % and 95 % along the length of the lower tubule (inset, Fig. 2A). This minimum distance was a consequence of the wall thickness of the ISME. For unstimulated tubules, the mean $[K^+]$ in the fluid of the unstirred layer of the basolateral surface of the lower tubule ($[K^+]_{USL}$) did not vary significantly along the length of the tubule (Fig. 2A), and the data were therefore pooled. $[K^+]_{USL}$ of unstimulated tubules (4.49±0.03 mmol l^{-1}; N=30 sites on six tubules) was slightly but significantly ($P<0.05$) above $[K^+]_{Bath}$ (4.33±0.01 mmol l^{-1}, N=6). This small difference may reflect

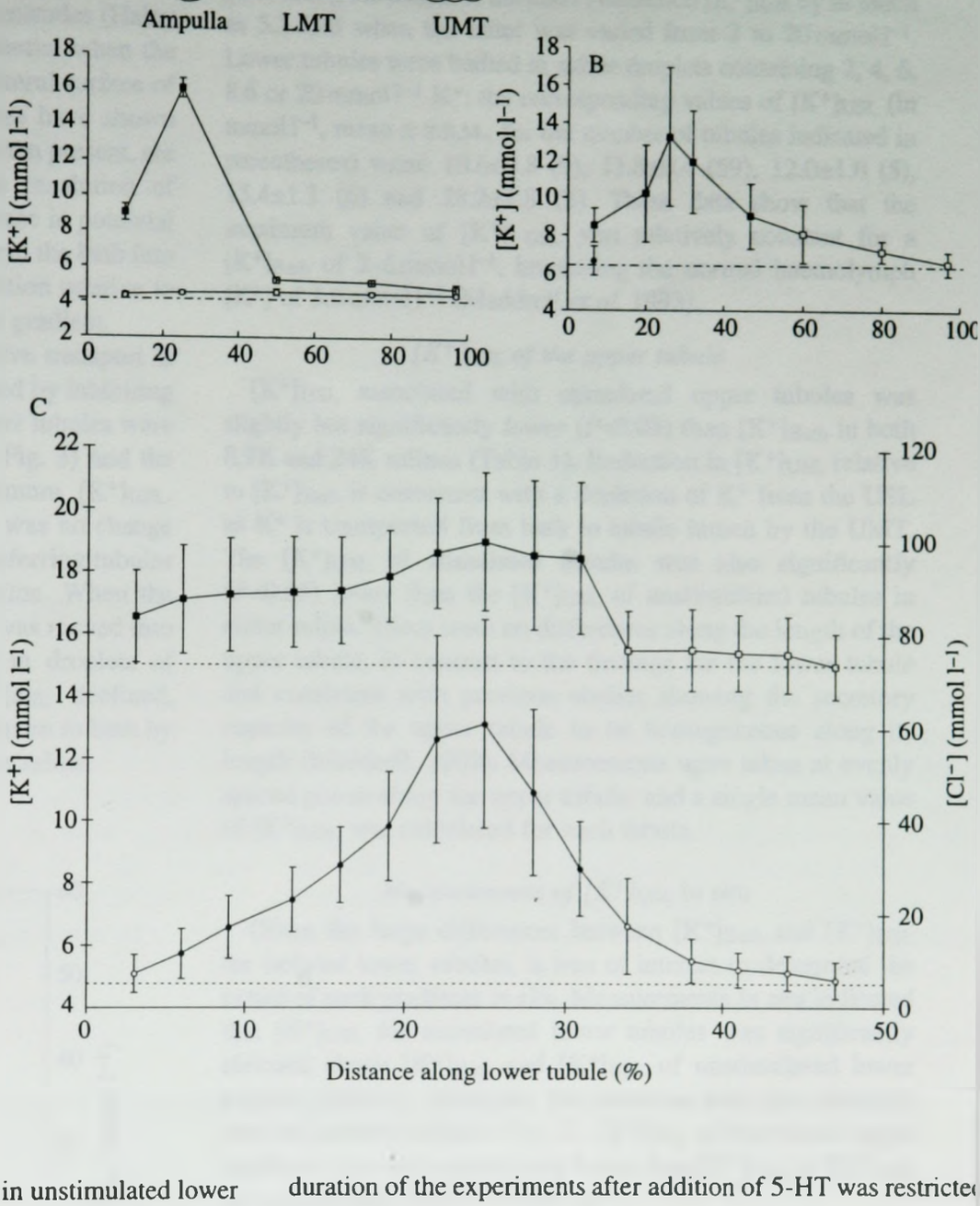

Fig. 2. Effects of 10^{-6} mol l^{-1} 5-hydroxytryptamine (5-HT) on $[K^+]$ and $[Cl^-]$ near the basolateral surface of the lower Malpighian tubule (LMT). (A) Comparisons of $[K^+]_{USL}$ at five different sites along the length of unstimulated (circles) and stimulated (squares) lower tubules (N=4). The dashed lines indicate $[K^+]_{Bath}$ for the LMT at the end of the experiment. Filled squares indicate $[K^+]_{USL}$ significantly greater (P<0.05) than the corresponding value in unstimulated tubules. (B) The pattern of changes in $[K^+]_{USL}$ (squares) was examined in greater detail by scanning tubules at eight positions along the lower tubules length (N=6). Filled squares indicate significant increases above $[K^+]_{Bath}$ (filled circle and dashed line). (C) Simultaneous measurements of $[K^+]_{USL}$ (circles) and $[Cl^-]_{USL}$ (squares) using double-barrelled ion-selective microelectrodes (ISMEs). The ion-selective electrode was positioned in the unstirred layer (USL) within 5 µm of the lower tubule surface and was moved at increments of 500 µm along the length of the lower half of the lower tubule. $[K^+]_{Bath}$ and $[Cl^-]_{Bath}$ in 50 % Cl^--replete saline are indicated by the upper and lower dashed lines, respectively. Points significantly (P<0.05) elevated above corresponding bathing saline concentrations are indicated by filled symbols; N=4 tubules. Values are means ± S.E.M.

passive leakage of K^+ from lumen to bath in unstimulated lower tubules. In stimulated tubules, the concentration of K^+ in the unstirred layer adjacent to the basolateral surface increased, relative to that of the bath, and these differences were most dramatic at 10 % and 25 % along the length of the lower tubules (Fig. 2A). The increase in $[K^+]_{USL}$ relative to $[K^+]_{Bath}$ is consistent with accumulation of K^+ in the USL as K^+ is transported from lumen to bath by the LMT. The pattern of changes in $[K^+]_{USL}$ was examined in greater detail by scanning at eight positions along the length of the lower tubule (Fig. 2B). The lower values of $[K^+]_{USL}$ at distances greater than or less than the peak at 25 % along the length of the lower tubule presumably reflect both the reabsorptive capacity of the epithelium and the luminal concentration of K^+ (see Discussion). The differences in bathing saline $[K^+]$ in Fig. 2A,B reflect the gradual increase in $[K^+]_{Bath}$ with time as K^+ is reabsorbed from lumen to bath in stimulated tubules. For tubules isolated in 200 µl droplets of 4K bathing saline, this increase was less than 2 mmol l^{-1} over a period of 60 min. In all subsequent experiments, therefore, the duration of the experiments after addition of 5-HT was restricte to 50 min.

Previous studies have shown that equal amounts of K^+ an Cl^- are reabsorbed by the lower tubule (Maddrell and Phillips 1975). Measurement of $[Cl^-]_{USL}$ was not feasible in saline containing the control Cl^- concentration (148.1 mmol l^{-1}); a increase of 2 mmol l^{-1} above the bath level, for example, woul result in a voltage change of only 0.3 mV for a Cl^--selectiv microelectrode with a slope of 58 mV per 10-fold change i $[Cl^-]$. For this reason, measurements of $[Cl^-]_{USL}$ near the lowe tubule were made in saline containing 4 mmol l^{-1} K^+ an 74.1 mmol l^{-1} Cl^- (i.e. 50 % of control $[Cl^-]$). Preliminar results showed significant increases in $[Cl^-]_{USL}$ relative t $[Cl^-]_{Bath}$ in the lower half of stimulated but not unstimulate lower tubules (N=5, data not shown).

Simultaneous measurement of $[Cl^-]$ and $[K^+]$ with double barrelled ISMEs showed that USL concentrations of both ion reached maximum values at 15–30 % along the length of th tubule (Fig. 2C). The maximum $[Cl^-]_{USL}$ was nearly 24 mmol l

gher than $[Cl^-]_{Bath}$ in 74.1 mmol l^{-1} Cl^- saline (N=6). omparison of Fig. 2B and Fig. 2C shows that $[K^+]_{USL}$ was not fected by a twofold change in $[Cl^-]$ in the bathing saline.

Measurement with voltage-sensitive microelectrodes (Haley id O'Donnell, 1997) show no change in potential when the icroelectrode is moved adjacent to the basolateral surface of e LMT prior to impalement. Previous studies have shown at extracellular voltage gradients near cells, when present, are pically in the nanovolt range, beyond the resolution of MEs (Kuhtreiber and Jaffe, 1990). The increase in potential hen the K^+ or Cl^- microelectrode is moved from the bath into e USL is due to an increase in ion concentration relative to at in the bath, therefore, and not to a voltage gradient.

The dependence of elevated $[K^+]_{USL}$ on active transport in -HT-stimulated lower tubules was demonstrated by inhibiting etabolism with KCN (Fig. 3). Upper and lower tubules were t up in control conditions under oil (B1 in Fig. 3) and the MT was scanned to find the site of maximum $[K^+]_{USL}$. $K^+]_{USL}$ was quickly re-established, and there was no change [K^+] in the secreted fluid ($[K^+]_{SF}$) after transferring tubules fresh droplets (B2 in Fig. 3) of control saline. When the MT remained in control saline and the LMT was moved into K saline containing 2 mmol l^{-1} KCN, [K^+] in droplets of creted fluid ($[K^+]_{SF}$) increased and $[K^+]_{USL}$ declined, nsistent with an inhibition of K^+ flux from lumen to bath by CN; both changes were reversed in KCN-free saline.

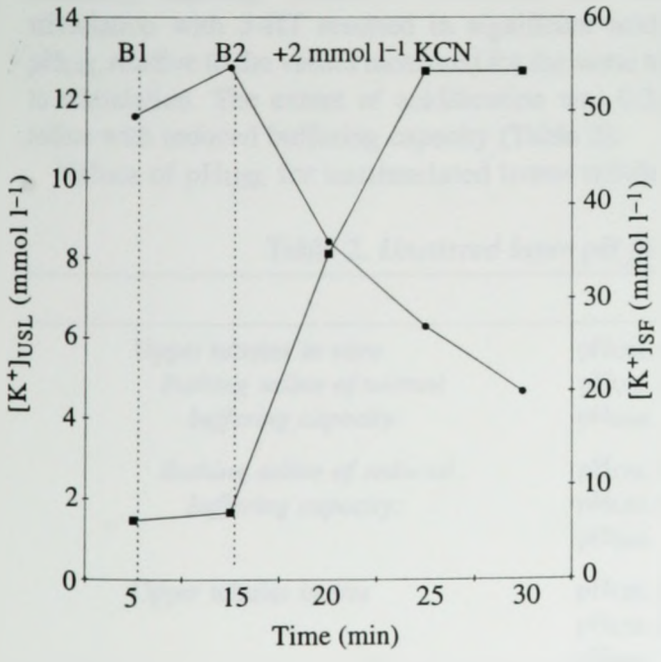

g. 3. The decrease in $[K^+]_{USL}$ and inhibition of K^+ reabsorption after dition of KCN. Upper and lower tubules were bathed in 24K and saline, respectively, and stimulated with 10^{-6} mol l^{-1} 5-HT. $^+]_{USL}$ was measured at 25–30 % along the length of the LMT, and creted fluid was collected after passage through the whole tubule. the UMT and LMT were moved from one pair of bathing saline plets (B1) to a second pair of identical droplets (B2), both $[K^+]_{USL}$ rcles) and $[K^+]_{SF}$ (squares) were maintained. Transfer of the LMT 4K saline containing KCN reduced $[K^+]_{USL}$ and increased $[K^+]_{SF}$. nilar patterns were observed with three other tubules.

Effects of $[K^+]_{Bath}$ on $[K^+]_{USL}$

The maximum $[K^+]_{USL}$ (i.e. that measured between 20 % and 30 % along the length of the LMT) exceeded $[K^+]_{Bath}$ by as much as 5.3-fold when the latter was varied from 2 to 20 mmol l^{-1}. Lower tubules were bathed in saline droplets containing 2, 4, 6, 8.6 or 20 mmol l^{-1} K^+; the corresponding values of $[K^+]_{USL}$ (in mmol l^{-1}, mean ± S.E.M., for the number of tubules indicated in parentheses) were: 10.6±0.8 (9), 11.8±0.4 (59), 12.0±1.0 (5), 15.4±1.3 (6) and 28.2±1.8 (5). These data show that the maximum value of $[K^+]_{USL}$ was relatively constant for a $[K^+]_{Bath}$ of 2–6 mmol l^{-1}, bracketing the normal haemolymph $[K^+]$ of 3.6 mmol l^{-1} (Maddrell *et al.* 1993).

$[K^+]_{USL}$ of the upper tubule

$[K^+]_{USL}$ associated with stimulated upper tubules was slightly but significantly *lower* (P<0.05) than $[K^+]_{Bath}$ in both 8.9K and 24K salines (Table 1). Reduction in $[K^+]_{USL}$ relative to $[K^+]_{Bath}$ is consistent with a depletion of K^+ from the USL as K^+ is transported from bath to tubule lumen by the UMT. The $[K^+]_{USL}$ of stimulated tubules was also significantly (P<0.05) lower than the $[K^+]_{USL}$ of unstimulated tubules in either saline. There were no differences along the length of the upper tubule, in contrast to the findings for the lower tubule and consistent with previous studies showing the secretory capacity of the upper tubule to be homogeneous along its length (Maddrell, 1969). Measurements were taken at evenly spaced points along the upper tubule, and a single mean value of $[K^+]_{USL}$ was calculated for each tubule.

Measurements of $[K^+]_{USL}$ in situ

Given the large differences between $[K^+]_{Bath}$ and $[K^+]_{USL}$ for isolated lower tubules, it was of interest to determine the extent of such gradients *in situ*. Measurements *in situ* indicated that $[K^+]_{USL}$ for stimulated lower tubules was significantly elevated above $[K^+]_{Bath}$ and $[K^+]_{USL}$ of unstimulated lower tubules (Table 1). However, the increases were less dramatic than for isolated tubules (Fig. 2). $[K^+]_{USL}$ of stimulated upper tubules *in situ* was significantly lower than $[K^+]_{Bath}$ or $[K^+]_{USL}$ of unstimulated tubules (Table 1).

One explanation for the difference between *in situ* and isolated tubules is that the saline (or haemolymph) surrounding the tubules *in situ* is mixed by contractions of the hindgut and midgut. These contractions increased in both frequency (from 15.8±0.8 min^{-1} to 37.0±0.9 min^{-1}, N=9 animals) and amplitude in response to 5-HT, and may have minimised the build-up of K^+ in unstirred layers *in situ*, relative to isolated tubules. In addition, the use of 24K saline for isolated upper tubules increases [K^+] of fluid secreted by the upper tubules. More K^+ was reabsorbed by the LMT, therefore, and the difference between $[K^+]_{USL}$ and $[K^+]_{Bath}$ increased.

Acidification of the unstirred layer

pH was measured in the USL within 5 µm of the basolateral surface of upper or lower tubules. Measurements were taken at 10 %, 25 %, 50 %, 75 % and 95 % along the length of upper and lower tubules. Upper tubule measurements taken at these various

Table 1. *Values of $[K^+]$ in the unstirred layer for upper and lower tubules* in vitro *and* in situ

		$[K^+]_{USL}$	*N*	*P*
Upper tubules *in vitro*	$[K^+]_{USL}$ unstimulated	8.97±0.10	15(5)	NS
8.9K bath	$[K^+]_{USL}$ stimulated*	7.48±0.18		<0.05
	$[K^+]_{Bath}$	8.92±0.36		–
24K bath	$[K^+]_{USL}$ unstimulated	24.05±0.14	15(5)	NS
	$[K^+]_{USL}$ stimulated	22.03±0.15		<0.05
	$[K^+]_{Bath}$	23.77±0.07		–
Upper tubules *in situ*	$[K^+]_{USL}$ unstimulated	3.41±0.14	15(5)	NS
	$[K^+]_{USL}$ stimulated	2.78±0.20		<0.005
	$[K^+]_{Bath}$	3.50±0.26		–
Lower tubules *in situ*	$[K^+]_{USL}$ unstimulated	3.44±0.14	15(5)	NS
	$[K^+]_{USL}$ stimulated	4.42±0.22		<0.001
	$[K^+]_{Bath}$	3.50±0.26		–

Values ($mmol\,l^{-1}$) are given as means ± S.E.M.
N, total number of measurement sites for the number of tubules indicated in parentheses.
P values are for paired *t*-tests comparing $[K^+]_{Bath}$ and $[K^+]_{USL}$.
NS, not significant.
*Tubules were stimulated by addition of 10^{-6} mol l^{-1} 5-HT to the bathing saline.

points, whether the tubule was unstimulated or stimulated, showed no minimum pH (i.e. maximum $[H^+]$) at a particular position along its length, and data for each upper tubule were therefore pooled. The pH_{USL} of unstimulated upper tubules was slightly but significantly acidic to pH_{Bath} in saline of reduced buffering capacity (Table 2, $P<0.001$). In both salines, stimulation with 5-HT resulted in significant acidification of pH_{USL} relative to the values measured for the same tubules prior to stimulation. The extent of acidification was 0.3 pH units in saline with reduced buffering capacity (Table 2).

Values of pH_{USL} for unstimulated lower tubules were not significantly acidic relative to pH_{Bath} (Fig. 4). Stimulation of the lower tubule alone, or both upper and lower tubules, resulted in slight but significant ($P<0.05$) reduction of pH_{USL} relative to pH_{Bath} (Fig. 4). As with $[K^+]_{USL}$ and $[Cl^-]_{USL}$, the maximum change was found at a site approximately 25 % of the distance along the length of the tubule, and this site was significantly ($P<0.05$) more acidic than the pH_{USL} at 10 % along the length of the tubule. Acidification is probably a consequence of one (or both) of the following processes: (1) accumulation of metabolic CO_2 generated during active reabsorption of KCl; and (2) transfer of acidic equivalents

Table 2. *Unstirred layer pH for upper and lower Malpighian tubules* in vitro *and* in situ

		pH	*N*	*P*
Upper tubules *in vitro*	pH_{USL} unstimulated	7.18±0.00	21(7)	NS
Bathing saline of normal	pH_{USL} stimulated*	7.13±0.00		<0.001
buffering capacity:	pH_{Bath}	7.19±0.00		–
Bathing saline of reduced	pH_{USL} unstimulated	6.99±0.01	20(4)	<0.001
buffering capacity:	pH_{USL} stimulated	6.69±0.02		<0.001
	pH_{Bath}	7.04±0.01		–
Upper tubules *in situ*	pH_{USL} unstimulated	7.26±0.02	15(5)	NS
	pH_{USL} stimulated	7.14±0.01		<0.001
	pH_{Bath}	7.26±0.01		–
Lower tubules *in situ*	pH_{USL} unstimulated	7.25±0.02	15(5)	NS
	pH_{USL} stimulated	7.07±0.01		<0.001
	pH_{Bath}	7.26±0.01		

Values are means ± S.E.M.
N, total number of measurement sites for the number of tubules indicated in parentheses.
P values are for paired *t*-tests comparing pH_{Bath} and pH_{USL}.
NS, not significant.
*Tubules were stimulated by addition of 10^{-6} mol l^{-1} 5-HT to the bathing saline.

om lumen to bath as the luminal fluid is alkalized during assage through the LMT (Haley and O'Donnell, 1997; see iscussion). Acidification of the USL in non-reabsorptive gions of the LMT (i.e. at 50 % and 75 % of the LMT's ngth, Fig. 4) may reflect accumulation of metabolic CO_2 the fluid secreted by the UMT and subsequent diffusion CO_2 from lumen to bath across the unstimulated lower bule.

Measurements of pH_{USL} in situ

In situ the maximum differences in pH_{USL} of stimulated *rsus* unstimulated tubules bathed in saline of normal uffering capacity were 0.12 and 0.18 pH units for UMTs and MTs, respectively (Table 2). For isolated tubules bathed in aline of normal buffering capacity, the corresponding fference was 0.05 pH units for both UMTs (Table 2) and MTs (Fig. 4). The bases for these differences are discussed elow.

K^+ flux in the lower tubule

Fluxes were calculated from $[K^+]_{USL}$ measured at eight sites 0 %, 20 %, 25 %, 30 %, 50 %, 60 %, 80 % and 100 %) along the wer tubule's length. At each site, the $[K^+]$ was measured at stances of 5, 47, 84, 168, 210, 315 and 550 µm perpendicular the long axis of the basolateral surface of the tubule ig. 5A–D). Fluxes were calculated using the Fick equation:

$$J = -D(\Delta C/\Delta r), \quad (3)$$

here J is the flux in mol cm^{-2} s^{-1}, D is the diffusion coefficient for K^+ (1.96×10^{-5} cm^2 s^{-1}), $\Delta r = r_2 - r_1$ and $\Delta C = C_2 - C_1$. Values of r_2 and r_1 were 4.7×10^{-3} cm and 5×10^{-4} cm from the tubule surface, respectively, and C_2 and C_1 are the corresponding K^+ concentrations (in mol cm^{-3}) measured at these two distances. The flattening of the $[K^+]_{USL}$ curves at distances greater than 200–400 µm results from periodic movement of the K^+ microelectrode for measurement of $[K^+]_{Bath}$ at a distance 5 mm away from the tubule surface. This large-scale movement caused some convective mixing, so that K^+ close to the tubule surface was swept outwards. Fluxes were therefore calculated using $[K^+]_{USL}$ measurements at the two positions closest to the tubule surface. The flattening was not apparent in other tubules where the K^+ microelectrode was moved in stages towards a single site on the tubule surface.

Fig. 6 shows measured fluxes and those estimated at increments of 5 % of tubule length by interpolation (hatched bars). For example, the K^+ flux at 40 % was calculated as the mean of the fluxes at 30 % and 50 %, and the flux at 35 % was calculated from the mean of the fluxes at 30 % and 40 %. Separate experiments indicated that fluxes in the upper half of the lower tubule (i.e. 50–100 % along the tubule length) were negligible. The flux of 2.03 nmol cm^{-2} s^{-1} across the whole lower tubule was then calculated by summing the fluxes measured in each of the bins (where each bin equals 5 % of the LMT's length) and dividing by the number of bins. This value is within 5 % of the flux calculated from the change in $[K^+]_{SF}$ after passage through the LMT and the surface area of the LMT, as follows. For the tubule in Fig. 5, the change in $[K^+]$ during passage through the lower tubule was 82.6 mmol l^{-1}, and fluid was secreted at 73.2 nl min^{-1}. The surface area of the tubules was estimated to be 0.048 cm^2, calculated from πdL, where d is the tubule diameter (90 µm) and L is its length (17 mm). The K^+ secretion rate of 0.101 nmol s^{-1} [$=(73.2\times10^{-9}$ l min$^{-1})(82.6\times10^{-3}$ mol l$^{-1})(1/60)$] then corresponds to an area-specific flux of 2.10 nmol cm^{-2} s^{-1} [$=(0.101$ nmol s^{-1}/0.048 cm^2)].

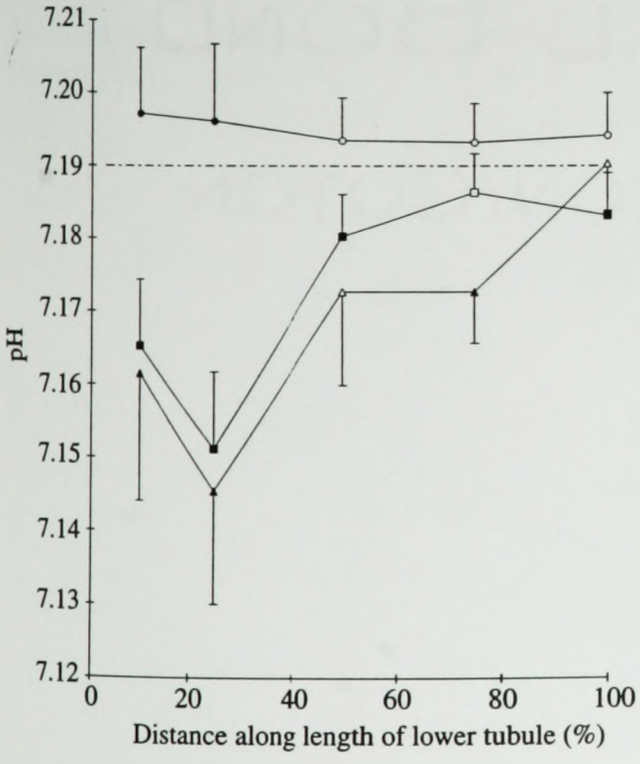

. 4. Acidification of the lower tubule unstirred layer (USL). pH_{USL} s measured in unstimulated tubules (circles) and after addition of ^{6} mol l^{-1} 5-HT to the lower tubule bathing saline (squares), or to h the upper and lower tubule bathing salines (triangles). pH_{Bath} is icated by the dashed line. Filled symbols denote significant erences ($P<0.05$) from pH_{Bath}. $N=7$ tubules. Values are means ± M.

Effects of furosemide and bumetanide on $[K^+]_{USL}$ in upper tubules

Measurements of changes in $[K^+]_{USL}$ of the upper tubule could also be used as an assay for drugs known to inhibit MT fluid secretion, and the changes in $[K^+]_{USL}$ could be correlated with a decrease in K^+ flux. For example, the presence of a basolateral $Na^+/K^+/2Cl^-$ cotransporter in the Malpighian tubules of *R. prolixus* (O'Donnell and Maddrell, 1984), *Aedes aegypti* (Hegarty *et al.* 1991) and *Formica polyctena* (Leyssens *et al.* 1994) has been proposed on the basis of inhibition of fluid secretion by 10^{-5} to 10^{-4} mol l^{-1} bumetanide or 10^{-4} mol l^{-1} furosemide. Fluid secretion by the upper Malpighian tubules of *R. prolixus* is reduced by 79–80 % by 10^{-4} mol l^{-1} furosemide or 10^{-5} mol l^{-1} bumetanide (O'Donnell and Maddrell, 1984).

Fig. 7 shows that bumetanide (4×10^{-5} mol l^{-1}) significantly ($P<0.05$) increased $[K^+]_{USL}$, consistent with less depletion of K^+ from the USL (i.e. a decrease in K^+ influx). The increase in $[K^+]_{USL}$ was reversible upon returning the tubules to

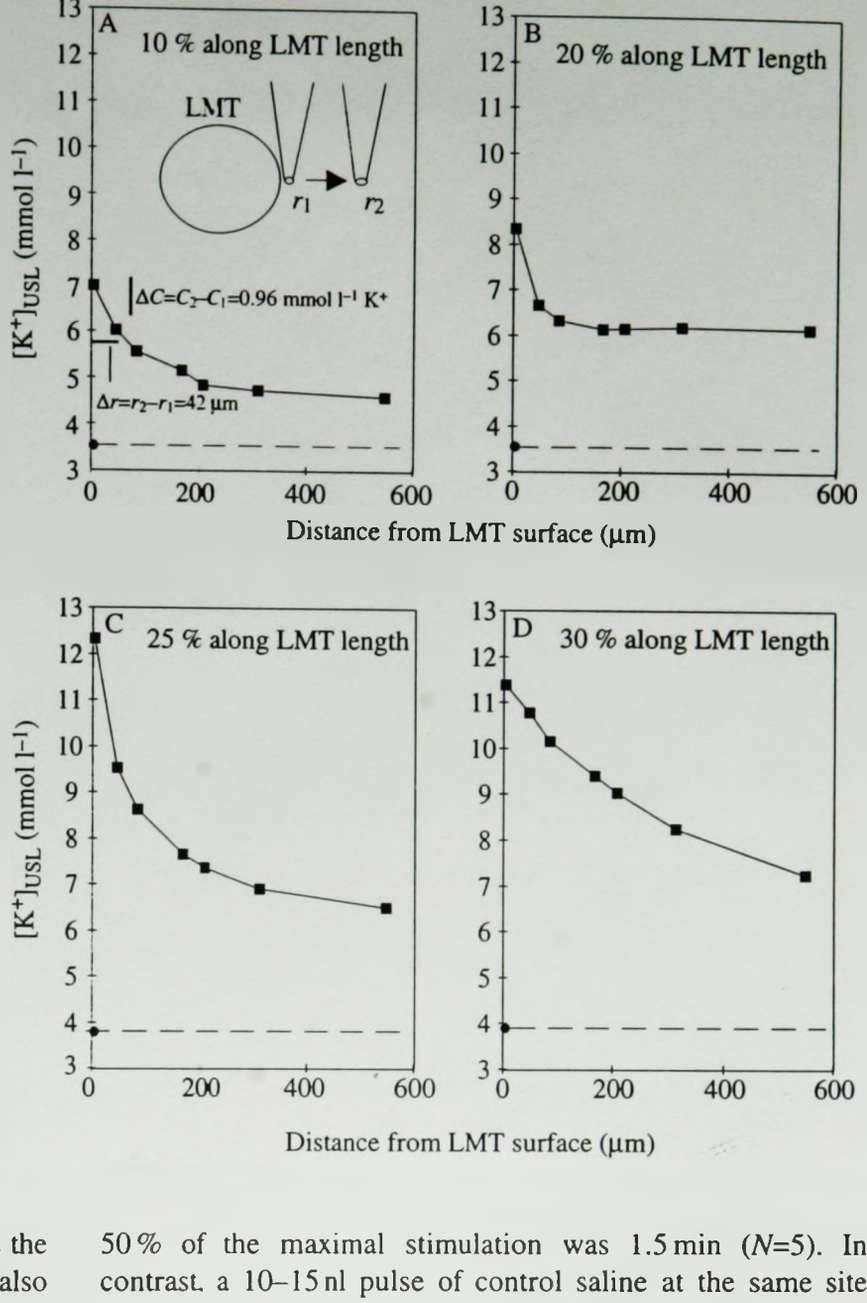

Fig. 5. $[K^+]_{USL}$ measured at increasing distances from the basolateral surface. Separate plots are presented for measurements at 10 % to 30 % along the length of the same LMT (A–D). The vertical and horizontal bars in A indicate the points used to calculate ΔC and Δr for determination of K^+ flux (see text). The inset diagram shows the relative positions of the K^+ microelectrode tip and the basolateral surface of the LMT. The tip was positioned at the equator of the tubule, as viewed in cross section, so that the side of the barrel touched the basolateral surface. The minimum distance (r_1) at which $[K^+]_{USL}$ could be measured was determined by the wall thickness of the microelectrode near its tip. Calculation of K^+ flux required measurements at a second distance (r_2) from the tubule surface (see text). $[K^+]_{Bath}$ is indicated by the filled circle and dashed line in each panel. Similar patterns were observed in 3 other tubules.

bumetanide-free saline. Upper tubule K^+ flux, calculated as the product of secretion rate (nl min^{-1}) and $[K^+]_{SF}$ (mmol l^{-1}), also declined by more than 65 % within 10 min of addition of 4×10^{-5} mol l^{-1} bumetanide to the bathing saline. The effects of 10^{-4} mol l^{-1} furosemide on $[K^+]_{USL}$ and K^+ flux were similar (N=6, data not shown). These findings suggest that measurement of USL ion concentrations can provide useful information on the effects of drugs that inhibit specific ion transporters.

Measurement of speed of response to 5-HT by measurement of $[K^+]_{USL}$

It was of interest to determine how rapidly changes in $[K^+]_{USL}$ occurred in response to stimulation of KCl reabsorption with 5-HT. A pulled micropipette (tip diameter approximately 3–4 µm) containing 10–15 nl of 10^{-7} to 10^{-4} mol l^{-1} 5-HT was positioned adjacent to the ISME in the USL. Tubules were set up in control conditions, with only the UMT stimulated with 10^{-6} mol l^{-1} 5-HT. 5-HT (1–1000 fmol) was then ejected from the micropipette into the USL at 25 % along the length of the LMT. A volume of 10–15 nl was sufficient to envelop 2–3 LMT cells.

$[K^+]_{USL}$ increased over 10 min following localized application of 5-HT (Fig. 8A). The mean time taken to produce 50 % of the maximal stimulation was 1.5 min (N=5). In contrast, a 10–15 nl pulse of control saline at the same site caused no sustained increase in $[K^+]_{USL}$ over 3 min (Fig. 8A). The maximum $[K^+]_{USL}$ and the duration of the rise in $[K^+]_{USL}$ increased with higher doses of 5-HT (Fig. 8B). $[K^+]_{USL}$ subsequently declined as 5-HT diffused into the 200 µl droplet of bathing saline, reducing the concentration of 5-HT to less than 5 nmol l^{-1}, which is below the threshold for stimulation of KCl reabsorption (Maddrell *et al.* 1993).

Extracellular $[K^+]$ near the basolateral membrane of single upper tubule cells

The results demonstrate that information about ion transport by isolated or *in situ* tubules can be inferred from analysis of USL ion concentrations measured using ISMEs. Importantly, we have found that it is feasible to measure the effects of ion transport by a single cell on USL ion concentrations. These measurements exploited the finding that, near the junction of the upper and lower Malpighian tubule, one or more UMT cells may be isolated from the rest of the UMT and surrounded by LMT cells (Fig. 9, inset). As noted above, the LMT cells near the junction of the LMT and UMT do not reabsorb K^+ (Fig. 2). Isolated UMT cells are found in about 10 % of tubules (Maddrell

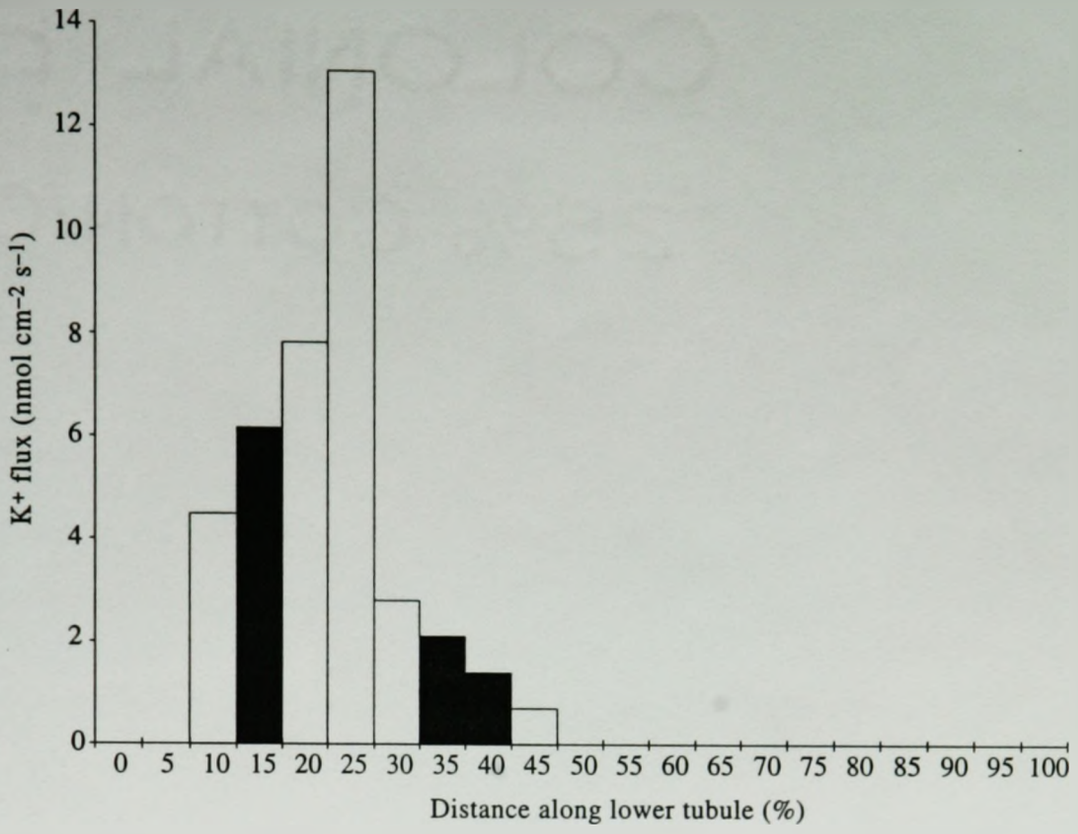

g. 6. K^+ flux along the length of a lower bule (the same tubule as Fig. 5). Open bars note fluxes calculated directly from easurements of $[K^+]_{USL}$, and hatched bars note fluxes estimated by interpolation (see xt). $[K^+]_{USL}$ could not be measured at stances between 0% and 10% along the MT's length. Fluxes measured at 50%,)%, 80% and 100% along the lower bule length were negligible.

id Overton, 1985) and have been shown to transport Na^+ and ganic acids in the same manner as UMT cells found in the per tubule proper (Maddrell and Overton, 1985).

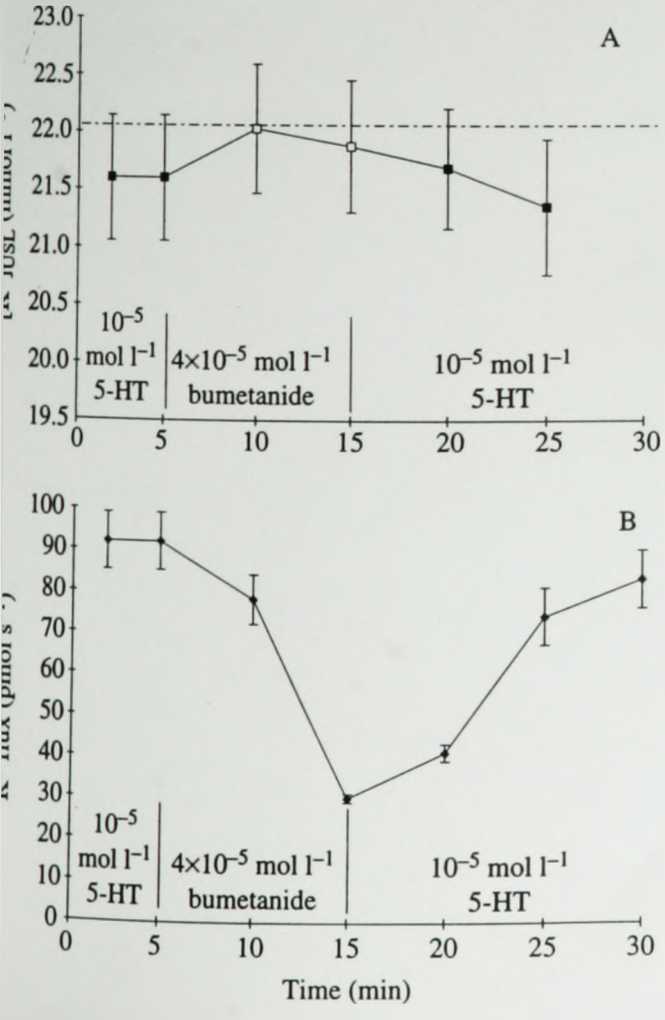

$[K^+]_{USL}$ was measured near isolated UMT cells and neighbouring LMT cells. Significant decreases in $[K^+]_{USL}$ for isolated UMT cells relative to that for neighbouring LMT cells were apparent after, but not before, 5-HT stimulation (Fig. 9). Measurement of $[K^+]_{USL}$ can thus provide information on MT ion transport with a spatial resolution comparable to that of the dimensions of an individual cell (100 μm).

Discussion

This study demonstrates that both secretion and reabsorption of ions by Malpighian tubules from *R. prolixus* can be assessed both qualitatively and quantitatively by ISME measurement of ion concentrations in the USL associated with the basolateral cell surface. This technique can be used to measure anions or cations, provided that there is an appropriately selective ionophore. Also, basolateral measurements of ion transport capacity can be determined before and after putative stimulants or inhibitors are added to the bathing saline droplets. Very small differences in electrical potential (approximately 0.1–0.2 mV) can be consistently resolved with a temporal resolution of approximately 2–10 s. The spatial resolution of this technique is comparable to that of an individual cell (100 μm). Importantly, the techniques described in this paper can be used for Malpighian tubules *in situ* as well as *in vitro*.

Fig. 7. Bumetanide increases $[K^+]_{USL}$ and decreases K^+ influx into 5-HT-stimulated upper tubules. Values are means ± S.E.M. (N=9). (A) $[K^+]_{USL}$. $[K^+]_{Bath}$ is indicated by the dashed line. Significant decreases in $[K^+]_{USL}$ relative to $[K^+]_{Bath}$ are indicated by filled squares. (B) K^+ influx.

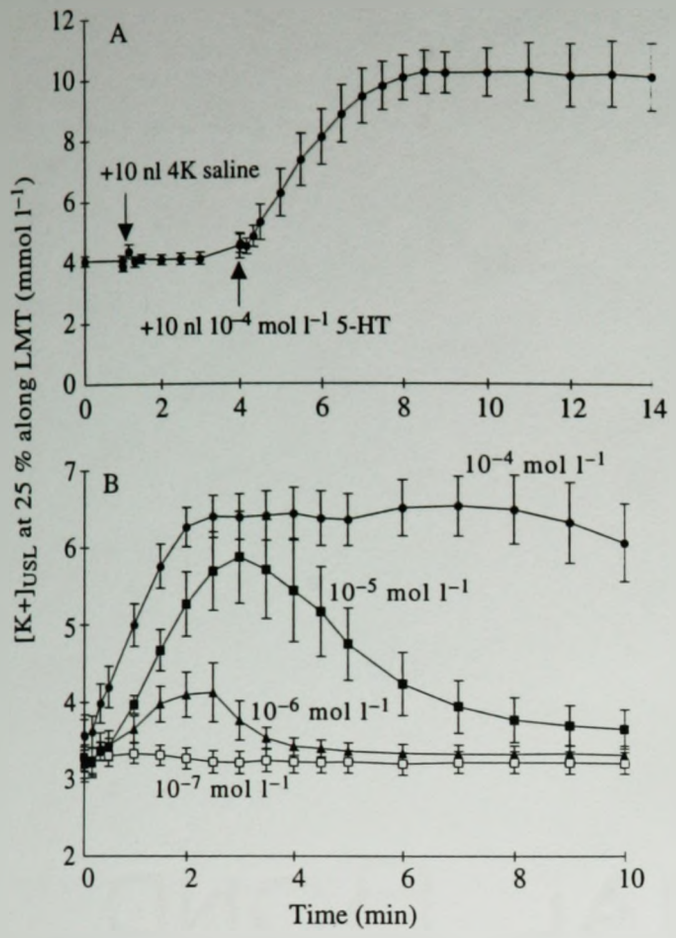

Fig. 8. Time course of changes in $[K^+]_{USL}$ after localized application of 5-HT. (A) A 10 nl pulse of saline applied between 20 % and 30 % along the length of the LMT had no sustained effect on $[K^+]_{USL}$. A 10 nl pulse of 10^{-4} mol l^{-1} 5-HT (1 pmol) applied between 20 % and 30 % along the length of the LMT rapidly increased $[K^+]_{USL}$. (B) The size and duration of the change in $[K^+]_{USL}$ increased with the concentration of 5-HT. In each case, the mean volume of solution ejected was 10–15 nl (N=6 tubules).

This technique revealed several new features of ion transport in a well-characterized transporting epithelium, the Malpighian tubule of *R. prolixus*. The effects of 5-HT and KCN indicate that elevation of $[K^+]$ and $[Cl^-]$ within the USL is a direct consequence of 5-HT stimulation of metabolically dependent KCl reabsorption by the lower tubule. The decline in $[K^+]_{USL}$ as the electrode is moved from 30 % to 50 % of the LMT's length is consistent with previous studies which demonstrate that KCl reabsorption is restricted to the lower third of the lower tubule (Maddrell, 1978). Moreover, our data reveal a new finding: K^+ reabsorption within the lower third of the tubule is not constant. K^+ flux between 20 and 30 % of the LMT's length is higher than flux calculated from $[K^+]_{USL}$ measurements closer to the ampulla. The decline in $[K^+]_{USL}$ closer to the ampulla may reflect a decline in $[K^+]$ as fluid in the tubule lumen passes through the lower third of the LMT. K^+ reabsorption becomes progressively more difficult and both $[K^+]_{USL}$ and K^+ flux decline. Double-barrelled ISME measurements confirm that both K^+ and Cl^- are reabsorbed across the same regions of the lower tubule.

The $[K^+]$ in the USL of the lower tubule may be more than five times greater than that in the bathing saline when $[K^+]_{Bath}$ is in the range 2–6 mmol l^{-1}, bracketing the normal haemolymph $[K^+]$ of 3.6 mmol l^{-1}. These findings are of relevance for the development of models of ion transport by rapidly transporting epithelia such as Malpighian tubules. Such models often involve calculations of electrochemical gradients for ion movements across epithelia, and it is usually assumed that the concentration of an ion in contact with the apical or basolateral surface is equal to the concentration in the bulk solution at a distance from the surface. Our results indicate that this assumption would lead to errors in calculated electrochemical gradients; estimates of electrochemical gradients should be made, therefore, using tubules which are superfused so as to minimize USL effects.

Measurements of $[K^+]_{USL}$ surrounding the basolateral membrane of the upper tubule confirm findings from previous studies regarding the homogeneous secretory capacity of the UMT along its length (Maddrell, 1969). Experiments with bumetanide and furosemide indicate that the effects of these drugs can be detected not just through changes in fluid secretion rates (O'Donnell and Maddrell, 1984) and K^+ flux (this paper) but also through the decline in the K^+ concentration gradient between the USL and the bathing saline.

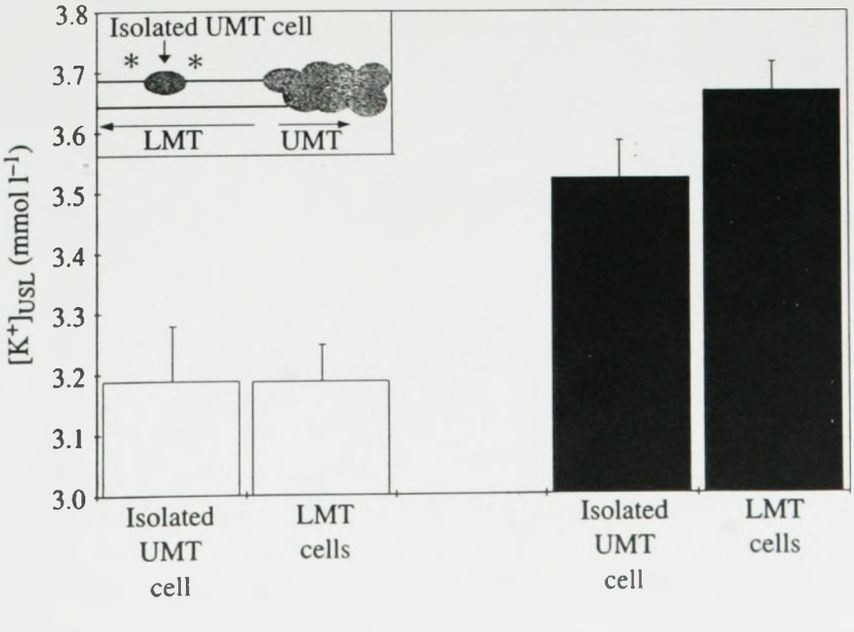

Fig. 9. Comparison between the $[K^+]_{USL}$ of an isolated upper tubule cell and that of the neighbouring lower tubule cells. The inset shows the sites for measurement of $[K^+]_{USL}$ over the isolated UMT cell (arrow) and the neighbouring LMT cells (asterisks). Whole tubules were set up under control conditions, and therefore the isolated UMT cells were bathed in 3.2K to 3.5K saline with the rest of the LMT, and not in 24K saline as were the UMT cells forming the upper tubule proper. Measurements before (open bars) and after (filled bars) stimulation with 10^{-6} mol l^{-1} 5-HT were made on eight tubules. The elevation of $[K^+]_{Bath}$ from 3.2 to 3.5 mmol l^{-1} for stimulated tubules resulted from K^+ reabsorption by the LMT. $[K^+]_{USL}$ for 5-HT-stimulated isolated UMT cells was significantly less (P<0.001) than that of neighbouring LMT cells. Values are means + S.E.M.

Acidification of the USL of upper and lower tubules esumably reflects the transfer of acid–base equivalents into out of the USL, and also accumulation of metabolic CO_2 d its subsequent hydration to form HCO_3^- and H^+. The crease in USL acidification *in situ* may be related to higher tes of ion transport of *in situ* relative to isolated tubules laddrell, 1991). Experiments with microelectrodes which easure pH and P_{CO_2} simultaneously (Bomsztyk and Calalb, 986) will be of use in determining the contributions of various ocesses to USL acidification. During KCl reabsorption, the MT alkalizes the fluid produced by the UMT by 1.2 pH units, d the secreted fluid is 1.4 pH units alkaline to the bath after ssage through the LMT (Haley and O'Donnell, 1997). idification of the basolateral USL may be a consequence, in rt, therefore of luminal alkalization; if base is transported to the lumen, then maintenance of cytoplasmic pH will quire an equivalent transfer of acidic equivalents into the thing saline or haemolymph. Acidification of the USL in stimulated upper tubules may reflect metabolism associated th secretion of KCl at slow rates, and with homeostatic and cretory processes. The UMT secretes fluid of nearly neutral I, and this is unaffected when pH_{Bath} is varied between 6.9 d 8.1 (Maddrell and O'Donnell, 1992). When pH_{Bath} is 7. erefore, there does not appear to be a requirement for transfer acid–base equivalents from lumen to bath. Reductions in per tubule pH_{USL} relative to pH_{Bath} are more likely. erefore, to reflect diffusion of CO_2 into the USL or acid–base change across the basolateral cell membrane.

Conversion of CO_2 to H^+ and HCO_3^- may introduce a small or into our measurements of $[Cl^-]_{USL}$, because the Cl^--ective liquid ion exchanger microelectrodes used here are ly 20 times more sensitive to Cl^- than to HCO_3^- (Walker, 71). The electrode may therefore overestimate the extent of accumulation in the USL if HCO_3^- concentrations rise matically above those of the bath (10.2 mmol l^{-1}). asurements with solid-state Cl^--selective microelectrodes, ich are insensitive to HCO_3^- (e.g. Wright and O'Donnell, 92), could resolve the extent of this error.

Previous studies have shown that a bathing saline $[K^+]$ ve 30 mmol l^{-1} inhibits KCl reabsorption (Maddrell and llips, 1977), consistent with blockade of passive efflux from to bath through basolateral K^+ channels (Haley and Donnell, 1997). Our data indicate that the effective centration of K^+ at the basolateral surface of the tubule will, act, be much higher than this value because of accumulation K^+ in the USL. Our *in situ* measurements suggest that the vective mixing of the haemolymph by 5-HT-stimulated tractions of the midgut and hindgut minimizes the build-up K^+ within the USL. This decrease in the boundary layer centrations of $[K^+]$ *in situ* was detected in both upper and er tubules. These findings raise the possibility that, in intact nals, the contractions of the hindgut are stimulated by the mones released at diuresis and that this increase in traction frequency serves to minimize the establishment of differences in $[K^+]$ between the haemolymph and the . The build-up of Cl^- in the USL will be much less inhibitory since the levels of Cl^- in the bathing fluid are high (148 mmol l^{-1} in 4K saline) and the proportionate change in $[Cl^-]_{USL}$ relative to $[Cl^-]_{Bath}$ will be much smaller.

Flux measurements determined from measurements of $[K^+]_{USL}$ are in good agreement with those determined from measurements of fluid secretion rates and secreted fluid $[K^+]$. The technique described in this paper may, therefore, be useful in characterizing Malpighian tubules of other species. This may be of particular interest for species such as the hemipteran *Cenocorixa bifida* (Cooper *et al.* 1989), in which MTs have several identifiable segments, each of which may have different transport functions, or for species having Malpighian tubules composed of heterogeneous cell types, such as the Malpighian tubules of *Drosophila melanogaster*, which contain stellate cells and principal cells (e.g. O'Donnell *et al.* 1996). Our preliminary results (K. A. Collier and M. J. O'Donnell, unpublished observations) indicate that K^+ gradients near secretory and reabsorptive segments of *D. melanogaster* can be detected. This technique should also find use with other rapidly transporting epithelia, including insect salivary glands and midgut.

This study has shown that the influence of even a single cell on ion concentrations in the basolateral USL can be detected by an extracellular ISME. The technique is also useful for assessing the effects of pharmacological reagents and putative diuretic hormones on tubule functions, since small quantities of material can be applied by pressure or ionophoresis onto the tubule surface. Measurement of ion concentrations in the USL permits transport to be assessed without the use of radio-isotopes. For systems which transport more slowly, the more sensitive vibrating ion probe technique, involving slow vibration of the ISME and signal averaging, can be used (Smith *et al.* 1994).

We are grateful to Dr Jon Harrison for his comments on a draft of the manuscript and Dr John Machin for his suggestions regarding flux calculations.

References

BOMSZTYK, K. AND CALALB, M. B. (1986). A new microelectrode method for simultaneous measurement of pH and P_{CO_2}. *Am. J. Physiol.* **251**, F933–F937.

BOUTILIER, R. G. AND SHELTON, G. (1980). The statistical treatment of H^+ concentration and pH. *J. exp. Biol.* **84**, 335–339.

COOPER, P. D., SCUDDER, G. G. E. AND QUAMME, G. A. (1989). Segmental differences in secretion by the Malpighian tubules of the fresh water dwelling corixid, *Cenocorixa blaisdelli* (Hung.) (Corixidae, Hemiptera). *J. Insect Physiol.* **35**, 531–536.

HALEY, C. A. AND O'DONNELL, M. J. (1997). Potassium reabsorption by the lower Malpighian tubule of *Rhodnius prolixus*: inhibition by Ba^{2+} and blockers of H^+/K^+-ATPases. *J. exp. Biol.* **200**, 139–147.

HEGARTY, J. L., ZANG, B., PANNABECKER, T. L., PETZEL, D. H., BAUSTIAN, M. D. AND BEYENBACH, K. W. (1991). Dibutyryl cyclic AMP activates bumetanide-sensitive electrolyte transport in Malpighian tubules. *Am. J. Physiol.* **261**, C521–C529.

KUHTREIBER, W. M. AND JAFFE, L. F. (1990). Detection of

extracellular calcium gradients with a calcium-specific vibrating electrode. *J. Cell Biol.* **110**, 1565–1573.

LEYSSENS, A., DIJKSTRA, S., VAN KERKHOVE, E. AND STEELS, P. (1994). Mechanisms of K^+ uptake across the basal membrane of Malpighian tubules of *Formica polyctena*: the effects of ions and inhibitors. *J. exp. Biol.* **195**, 123–145.

MADDRELL, S. H. P. (1969). Secretion by the Malpighian tubules of *Rhodnius*. The movements of ions and water. *J. exp. Biol.* **51**, 71–97.

MADDRELL, S. H. P. (1978). Physiological discontinuity in an epithelium with an apparently uniform structure. *J. exp. Biol.* **75**, 133–145.

MADDRELL, S. H. P. (1991). The fastest fluid-secreting cell known: The upper Malpighian tubule cell of *Rhodnius*. *BioEssays* **13**, 357–362.

MADDRELL, S. H. P. AND O'DONNELL, M. J. (1992). Insect Malpighian tubules: V-ATPase action in ion and fluid transport. *J. exp. Biol.* **172**, 417–429.

MADDRELL, S. H. P., O'DONNELL, M. J. AND CAFFREY, R. (1993). The regulation of haemolymph potassium activity during initiation and maintenance of diuresis in fed *Rhodnius prolixus*. *J. exp. Biol.* **177**, 273–285.

MADDRELL, S. H. P. AND OVERTON, J. A. (1985). Maintenance of function in single epithelial cells spatially isolated from similar cells. *J. Embryol. exp. Morph.* **90**, 409–414.

MADDRELL, S. H. P. AND PHILLIPS, J. E. (1975). Secretion of hypo-osmotic fluid by the lower Malpighian tubules of *Rhodnius prolixus*. *J. exp. Biol.* **62**, 671–683.

MADDRELL, S. H. P. AND PHILLIPS, J. E. (1977). Regulation of absorption in insect excretory systems. In *Comparative Physiology* (ed. K. Schmidt-Nielsen, L. Bolis and S. H. P. Maddrell), pp. 179–185. Cambridge: Cambridge University Press.

O'DONNELL, M. J., ALDIS, G. K. AND MADDRELL, S. H. P. (1982). Measurements of osmotic permeability in the Malpighian tubules of an insect, *Rhodnius prolixus* Stal. *Proc. R. Soc. Lond. B* **216**, 267–277.

O'DONNELL, M. J., DOW, J. A. T., HUESMANN, G. R., TUBLITZ, N. J. AND MADDRELL, S. H. P. (1996). Separate control of anion and cation transport in Malpighian tubules of *Drosophila melanogaster*. *J. exp. Biol.* **199**, 1163–1175.

O'DONNELL, M. J. AND MADDRELL, S. H. P. (1984). Secretion by the Malpighian tubules of *Rhodnius prolixus* Stal: Electrical events. *J. exp. Biol.* **110**, 275–290.

RAMSAY, J. A. (1952). The excretion of sodium and potassium by the Malpighian tubules of *Rhodnius*. *J. exp. Biol.* **29**, 110–126.

SMITH, P. J. S., SANGER, R. H. AND JAFFE, L. F. (1994). The vibrating Ca^{2+} electrode: A new technique for detecting plasma membrane regions of Ca^{2+} influx and efflux. *Methods Cell Biol.* **40**, 115–134.

WALKER, J. L. (1971). Ion-specific liquid ion exchanger microelectrodes. *Analyt. Chem.* **43**, 89A–93A.

WIGGLESWORTH, V. B. (1931). The physiology of excretion in a blood-sucking insect, *Rhodnius prolixus* (Hemiptera, Reduviidae). II. Anatomy and histology of the excretory system. *J. exp. Biol.* **8**, 428–442.

WIGGLESWORTH, V. B. AND SALPETER, M. M. (1962). Histology of the Malpighian tubules in *Rhodnius prolixus* (Hemiptera). *J. Insect Physiol.* **8**, 299–307.

WRIGHT, J. C. AND O'DONNELL, M. J. (1992). Osmolality and electrolyte composition of pleon fluid in *Porcellio scaber* (Crustacea, Isopoda, Oniscidea): implications for water vapour absorption. *J. exp. Biol.* **164**, 189–203.

APPENDIX B

Figure B1 -- Micrograph of an unstimulated stellate cell (SC) between two principal cells (PC). Note the small nucleus (Nuc) in the central region of the stellate cell. The brush border (bb) in the stellate cell is shorter than in the principal cells, and also lacks mitochondria. The basal infoldings (arrowheads) are less extensive in the stellate cell, than in the principal cells. Lumen (LU).

Scale bar = 1 μm.

Nuc
gb
LU

REFERENCES

Aldis G.K. (1988). The unstirred layer during osmotic flow into a tubule. *Bull. Math. Biol.* **50**, 531-545.

Alkassis W., and Schoeller-Raccaud J. (1984). Ultrastructure of the Malpighian tubules of blow fly larva, Calliphora erythrocephala meigen (Diptera: Calliphoridae). *Int. J. Insect Morphol. and Embryol.* **13**:215-231.

Ammann D. (1986). Ion-selective microelectrodes: principles, design, and application. Springer-Verlag, Berlin.

Ashburner M. (1989). *Drosophila:* a laboratory manual. Cold Spring Harbour Laboratory Press.

Aston R.J., and White A.F. (1974). Isolation and purification of the diuretic hormone from *Rhodnius prolixus. J. Insect Physiol.* **20**, 1673-1682.

Barnes R.B., Richardson D., Berry J.W., and Hood R.L. (1945). Flame photometry: a rapid analytical procedure. *Ind. Eng. Chem. Anal. Ed.* **17(10)**, 605-611.

Bertram G. (1991). Intracellular pH regulation in Malpighian tubules of *Drosophila hydei* affected by metabolic inhibitors and bafilomycin. *Verb. Dtsch. Zool. Ges.* **84**, 495-496.

Bertram G., Schleithoff L., Zimmermann P., and Wessing A. (1991). Bafilomycin A_1 is a potent inhibitor of urine formation by Malpighian tubules of *Drosophila hydei*: is a vacuolar-type ATPase involved in ion and fluid secretion? *J. Insect Physiol.* **37**:201-209.

Bertram G., Schleithoff L., Zimmermann P., and Wessing A. (1991). Bafilomycin A_1 as a potent inhibitor of urine formation by Malpighian tubules of *Drosophila hydei*: is a vacuolar-type ATPase involved in ion and fluid secretion? *J. Insect. Physiol.* **37**, 201-209.

Bomsztyk, K. and Calalb, M.B. (1986). A new microelectrode method for simultaneous measurement of pH and P_{CO2}. *Am. J. Physiol.* **251**, F933-F937.

Boutilier, R.G. and Shelton, G. (1980). The statistical treatment of H^+ concentration and pH. *J. exp. Biol.* **84**, 335-339.

Bowman E.J., Siebers A., and Altendorf K. (1988). Bafilomycins: a calss of inhibitors of membrane ATPases from microorganisms, animal cells, and plant cells. Proc. *Natn. Acad. Sci. USA* **85**, 7972-7976.

Chandler J.A. (1977). X-ray mocroanalysis in the electron microscope: practical methods in electron microscopy. North-Holland Publishing Co., Amsterdam.

Cooper, P.D., Scudder, G.G.E. and Quamme, G.A. (1989). Segmental differences in secretion by the Malpighian tubules of the fresh water dwelling corixid, *Cenocorixa blaisdelli* (Hung.) (Corixidae, Hemiptera). *J. Insect Physiol.* **35**, 531-536.

Danker T., Gabner B., Oberleithner H., and Schwab A. (1996). Extracellular detection of K+ release during migration of transformed Madin-Darby canine kidney cells. *Pflugers Arch-Eur J. Physiol.* **433**, 71-76.

Davies S.A., Huesmann G.R., Maddrell S.H.P., O'Donnell M.J., Dow J.A., and Tubulitz N.J. (1995). CAP_{2b} a cardioacceleratory peptide is present in *Drosophila* and stimulates fluid secretion by Malpighian tubules *via* cyclic GMP. *Am. J. Physiol.* **269**, R1321-R1326.

Deyhimi F., and Coles J.A. (1982). Rapid silyation of a glass surface: choice of reagent and effect of experimental parameters on hydrophobicity. *Helv. Chim. Acta.* **65**, 1752-1759.

Dow J.A.T., Kelly D.C., Davies S.A., Maddrell S.H.P., and Brown D. (1995). A member of the major intrinsic protein family in *Drosophila* tubules. *J. Physiol.,Lond.* **489**, 110P.

Dow J.A.T., Maddrell S.H.P., Davies S.A., Skaer N.J.V., and Kaiser K. (1994a). A novel role for the nitric oxide/cyclic GMP signalling pathway: the control of fluid secretion in *Drosophila*. *Am. J. Physiol.* **266**, R1716-R1719.

Dow J.A.T., Maddrell S.H.P., Gortz A., Skaer N.J.V., Brogan S., and Kaiser K. (1994b). The Malpighian tubules of *Drosophila melanogaster*: a novel phenotype for studies of fluid secretion and its control. *J. exp Biol.* **197**, 421 - 428.

Forgac M. (1989). Structure and function of vacuolar class of ATP-driven proton pumps. *Physiol. Rev.* **69**, 765-796.

Gee J.D. (1975). The control of diuresis in the tsetse fly *Glossina auteni*: a preliminary investigation of the diuretic hormone. *J. Exp. Biol.* 63, 391-401.

Gimblet E.G., Marney A.F., and Bonsnes R.W. (1967). Determination of Calcium and Magnesium in serum, urine, diet, and stool by atomic absorption spectrophotometry. *Clin. Chem.* **13(3)**, 204-214.

Haley C.A., Fletcher M., and O'Donnell M.J. (1997). KCl reabsorption by the lower Malpighian tubule of *Rhodnius prolixus*: Inhibition by Cl^- channel blockers and acetazolamide. *J. Insect Physiol. In press.*

Haley, C.A. and O'Donnell, M.J. (1997). Potassium reabsorption by the lower Malpighian tubules of *Rhodnius prolixus*: Inhibition by Ba^{+2} and blockers of H^+/K^+-ATPases. *J. exp. Biol.* **200**, 139-147.

Harvey W.R., and Wieczorek H. (1997). Animal plasma membrane energization by chemiosmotic H^+ V-ATPases. *J. Exp. Biol.* **200**, 203-216.

Hayat M.A. (1980). X-ray microanalysis in biology. University Park Press, Baltimore.

Hegarty, J.L., Zang, B., Pannabecker, T.L., Petzel, D.H., Baustian, M.D., and Beyenbach, K.W. (1991). Dibutyryl cAMP activates bumetanide-sensitive electrolyte transport in Malpighian tubules. *Am. J. Physiol.* **261**, C521 - C529.

Klein, Löffelmann U.G., and Wieczorek H.(1991). The midgut as a model system for insect K^+-transporting epithelia: immunocytochemical localization of vacuolar-type H^+ pump. *J. Exp. Biol.* **161**, 61-75.

Kuhtreiber, W. M. and Jaffe, L.F. (1990). Detection of extracellular calcium gradients with a calcium-specific vibrating electrode. *J. Cell Biol.* **110**, 1565-1573.

Lange A. B., Orchard I., and Barrett F. M. (1989). Changes in haemolymph serotonin levels associated with feeding in the blood-sucking bug, *Rhodnius prolixus*. *J. Insect. Physiol.* **35**, 393-399.

Leyssens, A., Dijkstra, S., Van Kerkhove, E., and Steels, P. (1994). Mechanisms of K^+ uptake across the basal membrane of Malpighian tubules of *Formica polyctena*: The effects of ions and inhibitors. *J. exp. Biol.* **195**, 123 - 145.

Maddrell S.H.P. (1981). The functional design of the insect excretory system. *J. exp. Biol.* **90**, 1-15.

Maddrell S.H.P. (1991). The fastest fluid-secreting cell known: the upper Malpighian tubule cell of *Rhodnius*. *BioEssays* **13**, 357-377.

Maddrell S.H.P., and Gardiner B.O.C.(1976). Excretion of alkaloids by Malpighian tubules of insects. *J. Exp. Biol.* **64**, 267-281.

Maddrell S.H.P., and O'Donnell M.J. (1992). Insect Malpighian tubules: V-ATPase action in ion and fluid transport. *J. exp. Biol.* **172**, :417-429.

Maddrell S.H.P., and Phillips J.E. (1976). Regulation of absorption in insect excretory systems. *Pers. Exp. Biol. Zool.* **1**, 179-185.

Maddrell S.H.P., Pilcher D.E.M., and Gardiner B.O.C. (1971). Pharmacology of the Malpighian tubules of *Rhodnius* and *Carausius:* the structure-activity relationship of tryptamine analogues and the role of cyclic AMP. *J. exp. Biol.* **54**, 779-804.

Maddrell, S. H. P. and O'Donnell M. J. (1992) Insect Malpighian tubules: V-ATPase action in ion and fluid transport. *J. exp. Biol.* **172**, 417-429.

Maddrell, S.H.P. (1978). Physiological discontinuity in an epithelium with an apparently uniform structure. *J. exp. Biol.* **75**, 133 - 145.

Maddrell, S.H.P. (1963). Excretion in the blood sucking bug, *Rhodnius prolixus* Stal. I. The control of diuresis. *J. exp. Biol.* **40**, 247 - 256.

Maddrell, S.H.P. (1969). Secretion by the Malpighian tubules of *Rhodnius*. The movements of ions and water. *J. exp. Biol.* **51**, 71 - 97.

Maddrell, S.H.P. (1991) The fastest fluid-secreting cell known: The upper Malpighian tubule cell of *Rhodnius*. *Bioessays* **13**, 357-362.

Maddrell, S.H.P., and Overton, J.A. (1985). Maintenance of function in single epithelial cells spatially isolated from similar cells. *J. Embryol. Exp. Morph.* **90**, 409 - 414.

Maddrell, S.H.P., and Phillips, J.E. (1975). Secretion of hypo-osmotic fluid by the lower Malpighian tubules of *Rhodnius prolixus*. *J. exp. Biol.* **62**, 671 - 683.

Maddrell, S.H.P., and Phillips, J.E. (1977). Regulation of absorption in insect excretory systems. In *Comparative Physiology* (ed. K. Schmidt-Nielsen, L. Bolis and S.H.P. Maddrell), pp. 179-185. Cambridge University Press.

Maddrell, S.H.P., Herman, W.S., Farndale, R.W., and Riegel, J.A. (1993). Synergism of hormones controlling epithelial fluid transport in an insect. *J. exp. Biol.* **174**, 65 - 80.

Maddrell, S.H.P., Herman, W.S., Mooney, R.L., and Overton, J.A. (1991). 5-Hydroxytryptamine: a second diuretic hormone in *Rhodnius prolixus*. *J. exp. Biol.* **156**, 557 - 566.

Maddrell, S.H.P., O'Donnell, M.J.O., and Caffrey, R. (1993b). The regulation of haemolymph potassium activity during initiation and maintenance of diuresis in fed *Rhodnius prolixus*. *J. exp. Biol.* **177**, 273 - 285.

Morel F., and Roinel N. (1969). Application do la microsonde electronique a l'analyse elementaire quantitative d'echantillons liquids d'un volume inferieur a 10^{-9} l. **146**, 1084-1091.

Morgan A.J. (1985). X-ray microanalysis in electron microscopy for biologists. Royal Microscopical Society. Oxford University Press, New York.

Munoz J.L., Deyhimi F., and Coles J.A. (1983). Silanization of glass in the making of ion-sensitive microelectrodes. *J. Neurosc. Meth.* **8**, 231-247.

Nicolson, S.W. (1993). The ionic basis of fluid secretion in Insect Malpighian tubules: Advances in the last 10 years. *J. Insect Physiol.* **39**, 451 - 458.

O'Donnell M. J., and Maddrell S.H.P.. (1984). Secretion by the Malpighian tubules of *Rhodnius prolixus* stal: electrical events. *J. Exp. Biol.* **110**, 275-290.

O'Donnell M.J., and Maddrell S.H.P. (1983). Paracellular and transcellular routes for water and solute movements across insect epithelia. *J. exp. Biol.* **106**, 231-253.

O'Donnell, M.J. (1997). Mechanisms of excretion and ion transport in invertebrates, In: Comparative physiology. Section 13, volume 2. (ed. Dantzler W.H.). Oxford University Press. New York. Pp 1207-1291.

O'Donnell, M.J., Aldis, G.K., and Maddrell, S.H.P. (1982). Measurements of osmotic permeability in the Malpighian tubules of an insect, *Rhodnius prolixus* Stal. *Proc. R. soc. Lond.* **B216**, 267 - 277.

O'Donnell M.J., and Maddrell S.H.P. (1995). Fluid reabsorption and ion transport by the lower Malpighian tubules of adult female *Drosophila*. J.exp.Biol. **198**, 1647-1653

O'Donnell, M. J., Dow J.A.T,. Huesmann, G.R., Tublitz, N.J. and S.H.P. Maddrell.(1996) Separate control of anion and cation transport in Malpighian tubules of *Drosophila melanogaster J. exp. Biol.* **199**: 1163-1175.

Orchard I. (1989). Serotonergic neurohaemal tissue in *Rhodnius prolixus*: synthesis, release and uptake of serotonin. *J. Insect Physiol.* **35**, 943-947.

Orchard I., Lange A. B., and Barrett F. M.. (1988). Serotonergic supply ot the epidermis of *Rhodnius prolixus*: evidence for serotonin as the plasticising factor. *J. Insect Physiol.* **34**, 873-879.

Pannabecker T.L., Hayes T.K., and Beyenbach K.W.. (1993). Regulation of epithelial shunt conductance by the peptide leucokinin. *J. Membrane Biol.* **132**, :63-76.

Pannabecker, T. (1995). Physiology of the Malpighian tubule. *Ann. Rev. Ent.* **40**, 493 - 510.

Quinton P. (1979). Energy-dispersive X-ray analysis of biological microdroplets. In: Microbeam analysis in Biology, pp 327-345. Academic Press, New York.

Ramirez-Munoz J. (1968). Atomic absorption spectroscopy and analysis by atomic absorption flame photometry. Elsevier Publishing Co. Amsterdam.

Ramsay J.A. (1950). The determination of sodium in small volumes of fluid by flame photometry. *J. Exp. Biol.* **27**, 407-419.

Ramsay J.A. (1953). Active transport of potassium by the Malpighian tubules of insects. *J. Exp. Biol.* **30**, 358-369.

Ramsay J.A., Brown R.H.J., and Croghan P.C. (1955). Electrometric titration of chloride in small volumes. *J. Exp. Biol.* **32**, 822-829.

Ramsay J.A., Brown R.H.J., and Falloon S.W.H.W. (1953). Simultaneous determination of sodium and potassium in small volumes of fluid by flame photometry. *J. Exp. Biol.* **30**, 1-16.

Ramsay, J.A. (1952). The excretion of sodium and potassium by the Malpighian tubules of *Rhodnius*. *J. exp. Biol.* **29**, 110 - 126.

Roinel N. (1975). Electron microprobe quantitative analysis of lyophilised 10^{-10} l volume samples. *J. microsc. Biol. Cell.* **22**, 261-268.

Sanderson P.H. (1952). Potentiometric determination of chloride in biological fluids. *Biochem. J.* **52**, 502-505.

Satmary W.M., andBradley T.J. (1984). The distribution of cell types in the Malpighian tubules of *Aedes tainiorhynchus* (wiedemann) (Diptera: *culicidae*). Int. *J. Insect Morphol. & Embryol.* **13**, :209-214.

Saunders J.H., and Brown H. M. (1977). Liquid and solid-state Cl^- micro-electrodes: characteristics and application to intracellular Cl^- activity in *Balanus* photreceptors. *J. gen. Physiol.* **70**, 507-530.

Shaw J. (1955). A simple procedure for the study of ionic regulation in small animals. *J. Exp. Biol.* **32**, 321-329.

Smith, P. J. S., Sanger R.H., and Jaffe L.F. (1994). The vibrating Ca^{2+} electrode: A new technique for detecting plasma membrane regions of Ca^{2+} influx and efflux. *Methods in Cell Biol.* **40**, 115-134.

Sözen M.A., Armstrong J.D., Yang M., Kaiser K., and Dow J.A.T. (1997). Functional domains are specified to single-cell resolution in a *Drosophila* epithelium. *Proc. Natl. Acad. Sci. USA.* **94**, 5207-5212.

Spring K., Wright F.S., Chan Y.L., and Fein H. (1975). Electrometric titration of nanoliter volumes of chloride. *Technical newslettter*, WPI.

Thomas R.C. (1978). Ion-selective intracellular microelectrodes: how to make and use them. Academic Press, London.

Van Eekelen C.A.G., Boekestein A., Stols A.L., and Stadhouders A. M. (1980). X-ray microanalysis of picoliter microdroplets: improvement of the method for quantitative X-ray microanalysis of samples of biological fluids. *Micron* **11**, 137-145.

Van Kerkhove E., Weltens R., Roinel N., and DeDecker N. (1989). Haemolymph composition in *formica* and urine formation by the short isolated Malpighian tubules: electrochemical gradients for ion transport. *J. Insect Physiol*. **35**, 991-1003.

Walker, J. L. (1971). Ion-specific liquid ion exchanger microelectrodes. *Analyt. Chem*. **43**, 89A-93A.

Wessing A., and Eichelberg D.. (1978). Malpighian tubules, rectal papilla and excretion. In The Genetics and Biology of *Drosophila* (Eds Ashburner M, and T.R.F. Wright), Vol. 2, pp 148-172. Academic Press, London.

Wessing A., and Zierold K. (1993). Heterogenous distribution of elements in the larval Malpighian tubules of *Drosophila hydei*: X-ray microanalysis of freeze-dried cryosections. *Cell Tissue Res.* **272**, 491-497.

Wessing A., Bertram G., and Zierold K. (1993). Effects of bafilomycin A_1 and amiloride on the apical potassium and proton gradients in *Drosophila* Malpighian tubules studied by X-ray microanalysis and microelectrode measurements. *J. Comp. Physiol.* **B163**, 452-462.

Whittembury G., Biondi A.C., Paz-Aliaga A., Linares H., Parthe V., and N. Linares. (1986). Transcellular and paracellular flow of water during secretion in the upper segment of the Malpigian tubule of *Rhodnius prolixus*: Solvent drag of molecules of graded size. *J. exp. Biol.* **123**, 71-92.

Wigglesworth, V.B. (1931). The physiology of excretion in a blood-sucking insect, *Rhodnius prolixus* (Hemiptera, Reduviidae). II. Anatomy and histology of the excretory system. *J. exp. Biol.* **8**, 428 - 442.

Wigglesworth, V.B., and Salpeter, M.M. (1962). Histology of the Malpighian tubules in *Rhodnius prolixus* (Hemiptera). *J. Insect Physiol.* **8**, 299 - 307.

Williams and Beyenbach K. (1984). Differential effects of secretogues on the electrophysiology of the Malpighian tubules of the yellow fever mosquito. *J.Comp. Physiol.* **154**, 301-309.

Willis J.B. (1960). The determination of metals in blood serum by atomic absorption spectroscopy. I. Calcium. *Spectrochem. Acta.* **16**, 259.

Wright, J. C. and O'Donnell, M.J. (1992). Osmolality and electrolyte composition of pleon fluid in *Porcellio scaber* (Crustacea, Isopoda, Oniscidea); Implications for water vapour absorption. *J. exp. Biol.* **164**, 189-203.

Zhang S., Leyssens A., Van Kerkhove E., Weltens R., Van Driessche W., and Steels P. (1994). Electrophysiological evidence for the presence of an apical H+-ATPase in Malpighian tubules of *Formica polyctena*: intracellular and luminal pH measurements. *Pflugers Arch.* **426**, 288-295.